

DOT/FAA/AR-09/13

Air Traffic Organization
NextGen & Operations Planning
Office of Research and
Technology Development
Washington, DC 20591

Technical Compendium From Meetings of the Engine Harmonization Working Group

April 2009

Final Report

This document is available to the U.S. public
through the National Technical Information
Services (NTIS), Springfield, Virginia 22161.



U.S. Department of Transportation
Federal Aviation Administration

NOTICE

This document is disseminated under the sponsorship of the U.S. Department of Transportation in the interest of information exchange. The United States Government assumes no liability for the contents or use thereof. The United States Government does not endorse products or manufacturers. Trade or manufacturer's names appear herein solely because they are considered essential to the objective of this report. This document does not constitute FAA certification policy. Consult your local FAA aircraft certification office as to its use.

This report is available at the Federal Aviation Administration William J. Hughes Technical Center's Full-Text Technical Reports page: actlibrary.act.faa.gov in Adobe Acrobat portable document format (PDF).

1. Report No. DOT/FAA/AR-09/13		2. Government Accession No.		3. Recipient's Catalog No.	
4. Title and Subtitle TECHNICAL COMPENDIUM FROM MEETINGS OF THE ENGINE HARMONIZATION WORKING GROUP				5. Report Date April 2009	
				6. Performing Organization Code	
7. Author(s) Robert S. Mazzawy				8. Performing Organization Report No. TSI-FAATC-06-001	
9. Performing Organization Name and Address Trebor Systems, Inc. 572 Coldbrook Road South Glastonbury, CT 06073-2706				10. Work Unit No. (TRAIS)	
				11. Contract or Grant No. DTFACT-05-P-00144	
12. Sponsoring Agency Name and Address U.S. Department of Transportation Federal Aviation Administration Air Traffic Organization NextGen & Operations Planning Office of Research and Technology Development Washington, DC 20591				13. Type of Report and Period Covered Final Report	
				14. Sponsoring Agency Code ANE-100	
15. Supplementary Notes The Federal Aviation Administration Airport and Aircraft Safety R&D Division COTR was Jim Riley.					
16. Abstract This document is a compendium of the key technical information considered by the joint Engine Harmonization Working Group/Power Plant Installation Harmonization Working Group that pertains to the effects of supercooled large drops and mixed-phase/glaciated icing conditions on commercial transport power plants. The effort spanned the period from early in 2003 through mid-2005. During these sessions, recommendations were proposed for new power plant icing certification rules as well as for accompanying advisory material.					
17. Key Words Engine Harmonization Working Group, Supercooled large drops, Mixed-phase icing, Glaciated icing, Aircraft engine icing			18. Distribution Statement This document is available to the U.S. public through the National Technical Information Service (NTIS), Springfield, Virginia 22161.		
19. Security Classif. (of this report) Unclassified		20. Security Classif. (of this page) Unclassified		21. No. of Pages 80	22. Price

TABLE OF CONTENTS

	Page
EXECUTIVE SUMMARY	xi
1. BACKGROUND	1
2. DATABASE	1
2.1 Process	2
2.2 Nomenclature	2
2.3 Classification of Events by Icing Environment	3
2.4 Ambient Temperature of Events	4
2.5 Classification of Events by Engine Symptoms	5
2.6 Rollback/Flameout/Stall Events	6
2.7 Core Damage Events	8
2.8 Fan Damage Events	9
2.9 Other Engine Damage Events	11
2.10 Summary Charts	12
2.11 Summary	14
3. TECHNICAL MATERIAL RELATING TO PROPOSED CHANGES TO 14 CFR 33.68	14
3.1 Comparison of EASA Test Points and Current AC 20-147 Test Points	14
3.2 Freezing Rain Threshold	17
3.3 Freezing Fog	17
3.4 Ground Operation in Snow	17
4. PROPOSED APPENDIX D TO 14 CFR PART 33	19
4.1 Background	19
4.2 Previous Guidelines and Measurements	20
4.3 Tracing Past Guidelines	23
4.4 The Cloud Horizontal Extent Factor	24
4.5 Estimates of Maximum TWC From Adiabatic Parcel Calculations	25
4.6 An Interim Guidance for Maximum TWC in Proposed Appendix D Conditions	27
4.7 Comparisons Between Old and New Table 2 TWC Guidelines	29
4.8 Ice Particle Characteristic Size	30

4.9	The TAT Anomaly Data	31
5.	ICE CRYSTAL TEST FACILITIES	32
5.1	Ice Crystal Size	32
5.2	Ice Crystal Velocity	32
5.3	Total Water Content Requirements	33
5.4	Compensation for Higher Approach Air Speeds	36
6.	TECHNICAL DATA AND INFORMATION RELATING TO PROPOSED CHANGES TO 14 CFR 33.77	36
6.1	Ice Slab Legacy Testing Results	36
6.2	Ice Impact Kinetic Energy	38
6.3	Ice Slab Breakup	39
7.	TECHNICAL DATA AND INFORMATION RELATING TO 14 CFR 25.1093	40
7.1	Equivalence of Aircraft-Sourced Ice to 14 CFR 33.77 Ice Slab	40
7.2	Airframe Ice Trajectory Acceleration	41
	7.2.1 Calculation Procedure	41
	7.2.2 Drag Coefficients of Various Slab Shapes	42
	7.2.3 Effect of Ice Slab Tumbling	44
	7.2.4 Comparison of Calculation Results	45
7.3	Ice Slab Reynolds Number	50
7.4	Summary	52
8.	TECHNICAL DATA AND INFORMATION RELATING TO PROPOSED CHANGES TO AC 20-147	52
8.1	Inlet Scoop Factor	52
	8.1.1 Inlet Scoop Effects	52
	8.1.2 Test Evaluation of Scoop Factor	53
	8.1.3 Required Velocity Ratio Range	54
	8.1.4 Illustration of Sea Level Test and Flight Scoop Factors	57
8.2	Summary	58
9.	REFERENCES	58

APPENDIX A—PROPOSED NEW RULES

LIST OF FIGURES

Figure		Page
1	Distribution of All Icing Events vs Environmental Discriminator	3
2	Subset of High Bypass Ratio Turbofan Events vs Environmental Discriminator	4
3	Ambient Temperature of Icing Events	5
4	Distribution of High Bypass Ratio Turbofan Events vs Engine Symptoms Discriminator	6
5	Rollback/Flameout/Stall Events vs Environmental Conditions Discriminator	7
6	Altitude Distribution of Rollback/Flameout/Stall Events	7
7	Altitude of Mixed-Phase/Glaciaded Rollback/Flameout/Stall Events	8
8	Core Damage Events vs Environmental Conditions Discriminator	8
9	Altitude Distribution of Core Damage Events (Confirmed Mixed-Phase Events Noted)	9
10	Fan Damage Events vs Environmental Conditions Discriminator	10
11	Altitude Distribution of Fan Damage Events	10
12	Other Damage Events vs Environmental Conditions Discriminator	11
13	Altitude Distribution of Other Damage Events	12
14	Distribution of Engine Symptoms for SLD and Mixed-Phase/Glaciaded Conditions	13
15	Summary Chart for Rollback/Flameout/Stall and Core Damage	13
16	Summary Chart for Fan Damage	14
17	Comparison of Stator Ice Accretion	16
18	Reference 4 Data on Snow Concentration	18
19	Database Events Compared With 14 CFR Part 25 Appendix C	19
20	Convective Cloud Ice Crystal Envelope	20
21	McNaughtan Dataset in Proposed Appendix D Envelope	24
22	The EHWG Recalculation of Average TWC as a Function of Distance Scale, and Comparison to Table 2 Guidelines	25

23	Adiabatic Profiles of TWC for Eight Different Surface Temperatures Between 0°C and 35°C.	26
24	Reduction in TWC With Distance Normalized to 17.4 nmi	27
25	Exposure Length Influence on TWC	28
26	Total Water Content	29
27	Distance From Onset of TAT Anomaly to Engine Event vs Database Event Number	31
28	Total Airplane Exposure to TAT Anomaly From Engine Event Cloud Encounter vs Database Event Number	32
29	Potential Ice Crystal Velocity Difference From Flight Environment	33
30	Total Water Content for “Free Jet” Test Setup	34
31	Total Water Content for “Direct Connect” Test Setup	35
32	Water Flow Rate Requirements	36
33	Slab Thickness for Range of Engine Inlet Size	37
34	Slab Length With Historic Engine Data	37
35	Normal Component of Kinetic Energy of Ice Slab	38
36	Ice Slab Orientation Effects	39
37	Available Data on Ice Slab Breakup	40
38	Sample of Ice Slab Kinetic Energy Analysis Worksheet	41
39	Drag Coefficient vs Reynolds Number	42
40	Drag Coefficient for Rectangles	43
41	Drag Coefficient at Reynolds Number = 10^5 for Annular Rings	43
42	Drag Coefficient for Caps of Various Height Ratio	44
43	Normal Force Coefficient at Varying Approach Angles	44
44	Ice Slab Velocity Comparison at 11,750 Feet and 0.41 Mn	46
45	Ice Slab Acceleration Load at 11,750 Feet and 0.41 Mn	46
46	Ice Slab Velocity Relative to Engine at 11,750 Feet and 0.41 Mn	47

47	Comparison of Simple Ice Mass-Based Impact Kinetic Energy at 11,750 Feet and 0.41 Mn	48
48	Sensitivity of Kinetic Energy Comparison to Drag Coefficient	49
49	Influence of Fan Wheel Speed on Ice Slab Energy	49
50	Ice Slab Reynolds Number for the Example Calculation	51
51	Background Data on Scoop Factor	54
52	The NACA Test Results in Terms of Modified Inertia Parameter	55
53	Required Range of Modified Inertia Parameter	56
54	Splitter Modified Inertia Parameter at Sea Level	56
55	Splitter Modified Inertia Parameter at 20K 0.6 Mn	57
56	Illustration of Overall Scoop Factor for Two Icing Environments	58

LIST OF TABLES

Table		Page
1	The AC 20-147 Table Points Compared With EASA Requirements	15
2	Ice Crystal Concentration Standards	22
3	Comparisons Between Old and New TWC Guidelines	29
4	Comparison of Flight Conditions With Test Facility Requirements	34
5	The Proposed 14 CFR 33.77 Ice Slab Dimension Requirements	50
6	Reynolds Numbers for Different Inlet Highlite Areas for Specified Conditions	51

LIST OF ACRONYMS

AC	Advisory Circular
ARAC	Aviation Rulemaking Advisory Committee
CFR	Code of Federal Regulations
CPA	Critical Point Analysis
CRI	Certification Review Item
EASA	European Airworthiness Standards Authority
EHWG	Engine Harmonization Working Group
FAA	Federal Aviation Administration
FTHWG	Flight Test Harmonization Working Group
IPHWG	Ice Protection Harmonization Working Group
IWC	Ice water content
LCT	Large commercial transport
LWC	Liquid water content
Mn	Mach number
MOC	Method of compliance
NACA	National Advisory Committee for Aerodynamics
OAP	Optical array probe
PPIHWG	Power Plant Installation Harmonization Working Group
SLD	Supercooled large drops
T _{amb}	Ambient temperature
TAT	Total air temperature
TWC	Total water content

EXECUTIVE SUMMARY

This document is a compendium of key technical information considered by the combined Engine Harmonization Working Group/Power Plant Installation Harmonization Working Group that pertains to the effects of supercooled large drops (SLD) and mixed-phase/glaciated icing conditions on commercial transport power plants. The effort spanned the period from early 2003 through mid-2005. During these sessions, recommendations were proposed for new power plant icing certification rules as well as for accompanying advisory material.

The effort began with an assessment of the extent of engine problems in SLD or mixed-phase/glaciated environments. Icing events from the engine manufacturers' records were compiled into a database that was analyzed and discussed in detail by the combined working group. The combined working group concluded that mixed-phase/glaciated conditions were a significant threat to engine operation, with rollback, flameout, stall and core damage symptomatic of some events. Freezing rain and drizzle (SLD) events were confined primarily to ground events with fan damage at a few airports.

These conclusions resulted in a working group effort to define a mixed-phase/glaciated icing environment, resulting in the proposed Title 14 Code of Federal Regulations (CFR) Part 33 Appendix D.

The report also provides technical background for proposed changes to 14 CFR 33.68, 33.77, and 25.1093.

1. BACKGROUND.

In response to National Transportation Safety Board recommendations A-96-54, A-96-56, and A-96-58, the joint Engine Harmonization Working Group (EHWG) and Power Plant Installation Harmonization Working Group (PPIHWG) was assembled by the Ice Protection Harmonization Working Group (IPHWG) for the purpose of reviewing requirements for engine and engine installation certification under supercooled large drops (SLD) and mixed-phase/glaciated icing conditions. The IPHWG is itself a working group of the Aviation Rulemaking Advisory Committee (ARAC). For the purpose of this report, the combined EHWG and PPIHWG will simply be referred to as the EHWG.

The EHWG was tasked to review all icing-related engine service difficulty experience and flight test icing-related difficulty experience that may be related to SLD or mixed-phase icing and to determine possible SLD and mixed-phase threats to engine operation. As part of this activity, the EHWG reviewed the proposed Appendix X SLD environment to determine possible engine design vulnerabilities to both SLD and mixed-phase conditions. Additionally, the EHWG reviewed current Appendix C methods of compliance (MOC) to determine if they were sufficient or if additional MOCs needed to be added. Advisory material in Advisory Circular (AC) 20-147 was also examined and modifications proposed as required for applicability to both SLD and mixed-phase ice. A summary report to the co-chairs of the IPHWG summarized the Engine Subgroup's recommendations for possible rulemaking and advisory material modification suggestions.

Members of the EHWG researched various issues and performed analyses for the combined working group to develop proposed rule changes and related advisory material. The results of this research and analysis were presented at meetings and teleconferences of the combined working group. Under the rules of ARAC, this information was not public information during the development period. However, now that the IPHWG has submitted to the Transport Aircraft Engines Issues Group, the proposed rule changes, advisory material, and information from the meetings can be made public (subject to the approval of the participating companies). The purpose of this report is to provide a compendium of key technical information underlying the proposed rules and advisory material.

2. DATABASE.

The EHWG initially assessed the extent of engine problems in SLD or mixed-phase/glaciated environments based upon service history provided by the manufacturers participating in the EHWG. Information on engine icing events were compiled into a database with events categorized according to a number of variables, including the nature of problems encountered.

This section presents various summary plots based upon the database that was considered by the EHWG, which includes engine events from 1989 through the end of 2003.

Note that flight condition information, such as altitude and ambient temperature was not available for all events. Consequently, some summary charts that are presented in this section represent only part of the total event history.

Using service history, the purpose was to determine the need for new certification regulations for engines and engine installations pertaining to the proposed Title 14 Code of Federal Regulations (CFR) Part 25 Appendix X for SLD and/or mixed-phase/glaciated icing conditions.

2.1 PROCESS.

The data were collected from the engine manufacturers and assembled by a neutral party. The engine manufacturer identification was removed, and the following sorting process was performed to facilitate the analysis of the data and the conclusion process.

The events were categorized with respect to thrust as follows:

- High bypass ratio (HBPR) engines:
 - H3—more than 40,000 lb takeoff thrust
 - H2—between 20,000 lb and 40,000 lb takeoff thrust
 - H1—less than 20,000 lb takeoff thrust
- Other:
 - Low bypass ratio (LBPR)
 - Propeller driven (PROP)

The events were further categorized with respect to the following:

- Inference of conditions from pilot reports and other circumstantial evidence (e.g., Appendix C, proposed Appendix X, mixed-phase/glaciated)
- Sorting by symptoms (damage, stall, etc.)
- Sorting by power setting

2.2 NOMENCLATURE.

Standards for identifying the environmental conditions for the events were established by the EHWG to discern Appendix C (AC) events from proposed Appendix X (AX) and mixed-phase/glaciated (MP) events. A question mark (?) was used when it could not be conclusively categorized, but some evidence supported the classification. The following listing of environmental discriminators defines the basis used for categorization.

UNC—Unclassified due to lack of details in records

AC—Appendix C icing incidents (These were quite limited given that the current certification standards focus on this icing envelope. As such, they only included a known nose cone Pt2 probe icing problem on one particular engine model and any event identified as freezing fog.)

AX—Proposed Appendix X conditions identified as either freezing rain or freezing drizzle

AX?—Possible proposed Appendix X conditions if attributable to ice shed from fuselage into aft fuselage mounted engines

Not AX AC—Above 22,000 ft or below 30°C (limits of the envelopes)

MP—Mixed-phase/glaciated when there was indication of the Rosemount total air temperature (TAT) probe icing (a known characteristic of this probe) or if snow was reported

MP?—Possible mixed-phase/glaciated (or at least in convective clouds) inferred from core engine issues (rollback/flameout/stall (rfs) or damage) normally due to high water content and/or greater rearward penetration of ice accretion sites into the engine, particularly at higher engine power settings.

2.3 CLASSIFICATION OF EVENTS BY ICING ENVIRONMENT.

Figure 1 shows the results of this categorization for all events, and a subset of events limited to the high bypass ratio engines are shown in figure 2. Note that some events involved multiple engines. The environmental discriminator labels correspond to the icing condition categorization as discussed above.

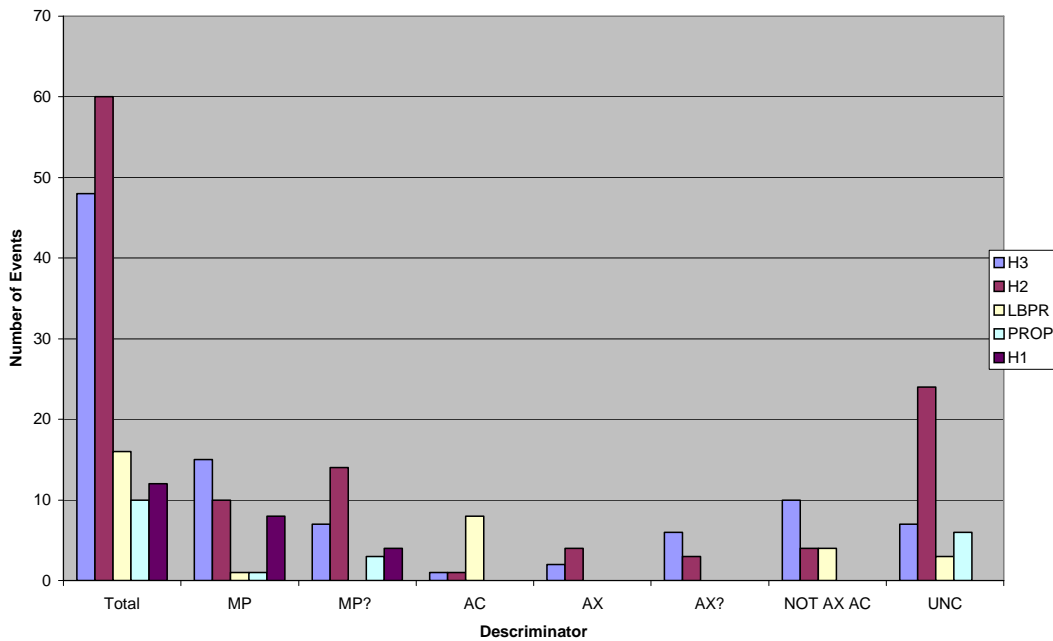


Figure 1. Distribution of All Icing Events vs Environmental Discriminator

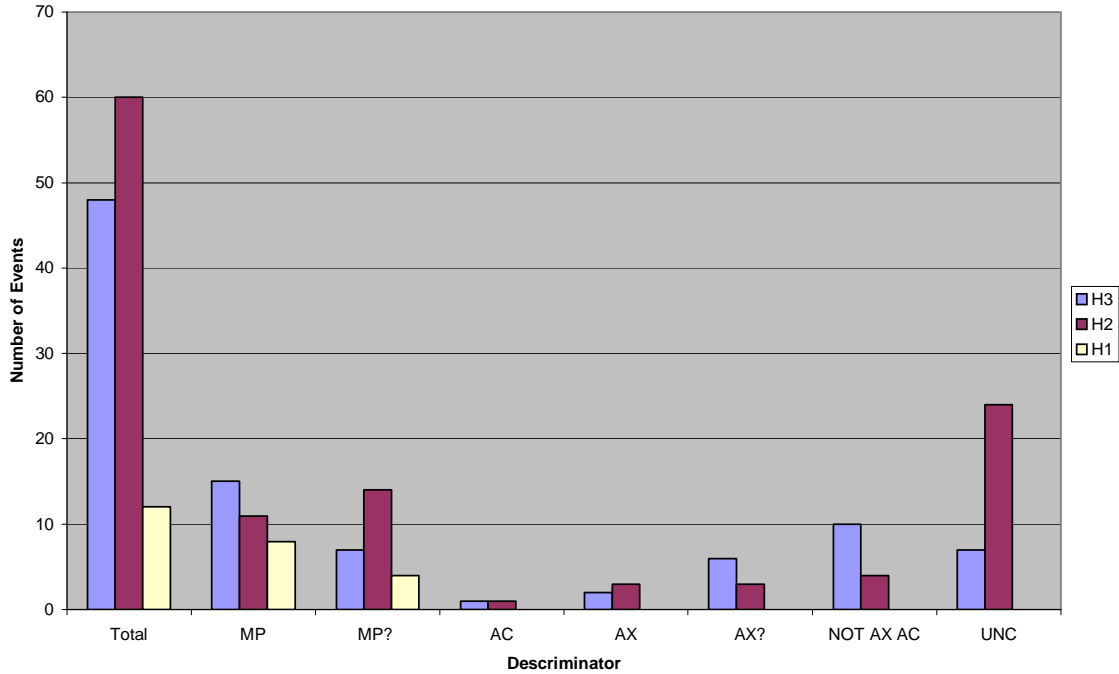


Figure 2. Subset of High Bypass Ratio Turbofan Events vs Environmental Discriminator

2.4 AMBIENT TEMPERATURE OF EVENTS.

In some records, ambient temperature (T_{amb}) was recorded and provided insight into the nature of conditions. Figure 3 shows temperature data as compared to the standard atmosphere temperature lapse with altitude. Conclusions drawn from this information can be summarized as follows:

- As expected, icing conditions at low altitude occur below standard day temperatures.
- At high altitude, temperatures above standard day are consistent with operation in convective clouds.

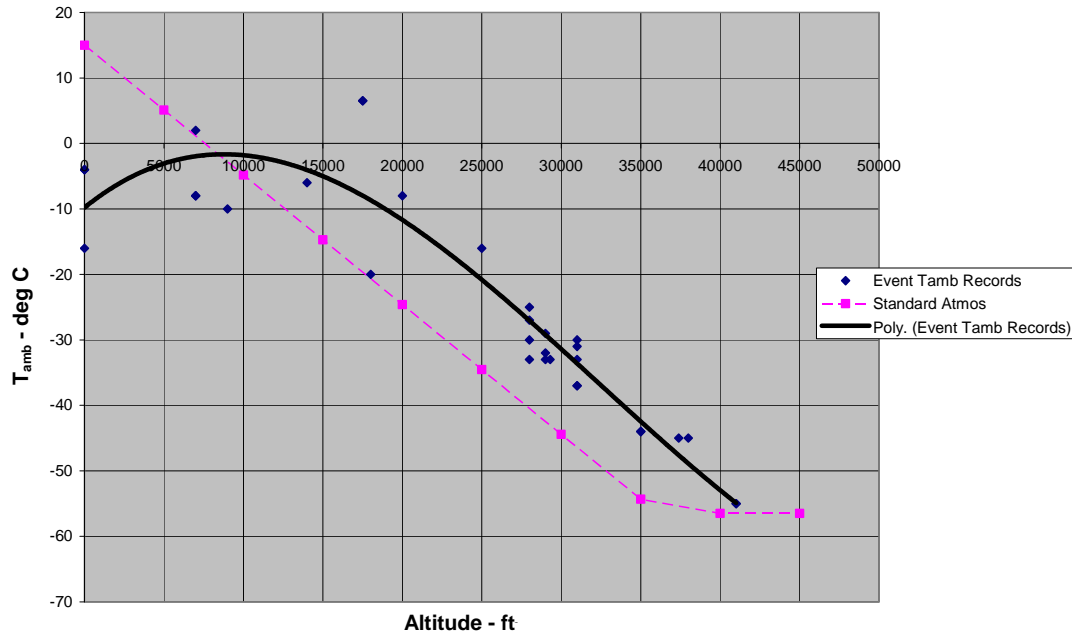


Figure 3. Ambient Temperature of Icing Events

2.5 CLASSIFICATION OF EVENTS BY ENGINE SYMPTOMS.

The symptoms of the events were categorized per the following procedure.

- Focused on high-, mid-, and low-thrust turbofan categories
- Engine symptom discriminators were defined to categorize events by the following categories:
 - Fan Damage (fd)
 - Core Damage (cd)
 - Other Damage (e.g., acoustic liners) (ed)
 - Rollback/Flameout /Stall
 - Vibration (most event symptoms include vibration—this category applied to events listing only vibration) (vib only)
- Some engines had multiple symptoms (other than vibration) and were included in tally of each.

The results are shown in figure 4 and include the total number of engines for the events, reflecting the fact that some events involved multiple engines. For in-flight events, only a single aircraft was involved. However, for ground events, several aircraft might have been involved,

all with at least one engine affected by the meteorological conditions (e.g., sustained freezing drizzle) at the airport. As an example, there were only a few proposed Appendix X ground events in freezing rain or drizzle, but in some cases, they effected the ground operations of several aircraft at a particular airport, resulting in fan damage for numerous engines.

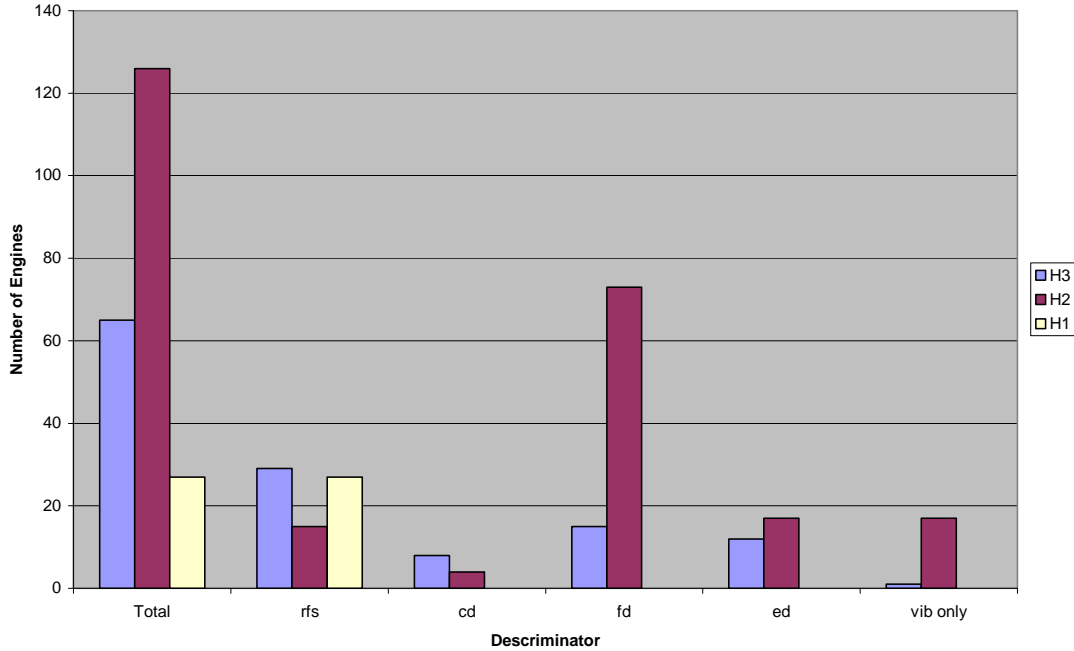


Figure 4. Distribution of High Bypass Ratio Turbofan Events vs Engine Symptoms Discriminator

After separating the events by the individual discriminators of the environmental conditions and the engine symptoms, it was desirable to determine which engine symptoms were most prevalent within a particular environmental condition. The next series of results serve to illustrate the association of the icing environment with resultant engine symptoms.

2.6 ROLLBACK/FLAMEOUT/STALL EVENTS.

The events that resulted in engine rollback, flameout, or stall were delineated by discriminator of environmental conditions for the three ranges of high bypass ratio engine thrust size shown in figure 5. Additionally, the distribution of these events by low engine power including minimum idle and/or approach idle during descent (MI/AI/Descent) and high engine power settings of takeoff, climb, and cruise (TO/CL/CR) is provided in this figure. Figure 6 shows the delineation, which provided insight into the altitude distribution for the number of events in each engine size category.

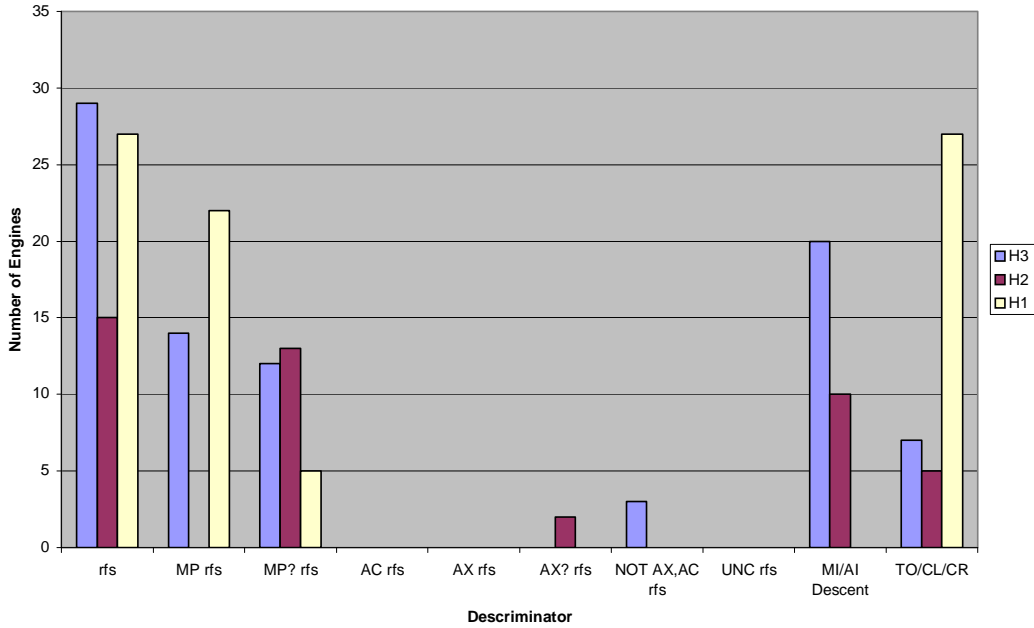


Figure 5. Rollback/Flameout/Stall Events vs Environmental Conditions Discriminator

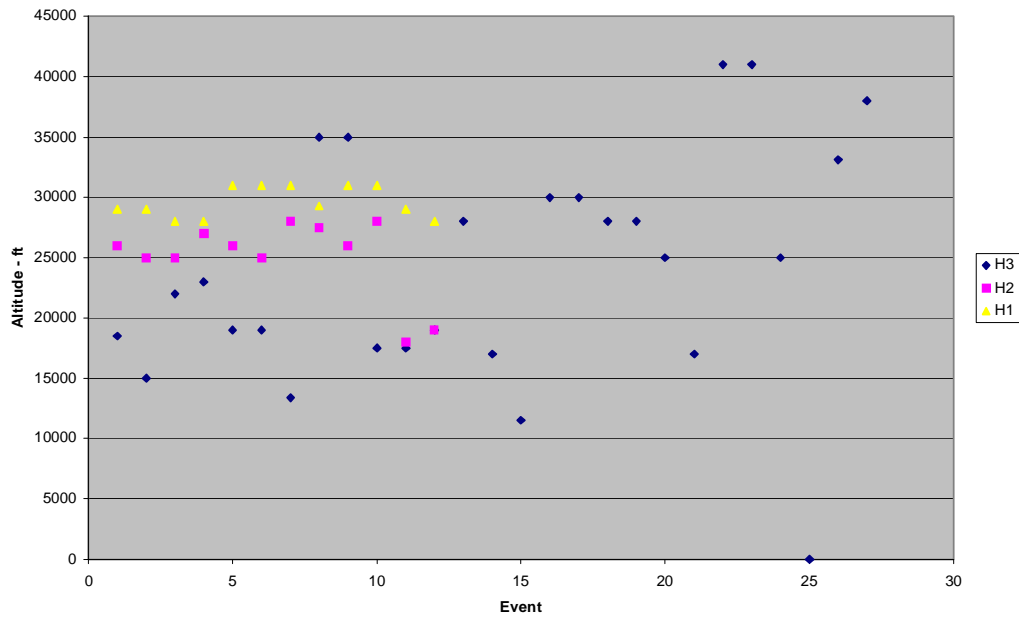


Figure 6. Altitude Distribution of Rollback/Flameout/Stall Events

Since the majority of Rollback/Flameout/Stall events were associated with mixed-phase/glaciated conditions, the altitude distribution was further defined for just these events in figure 7.

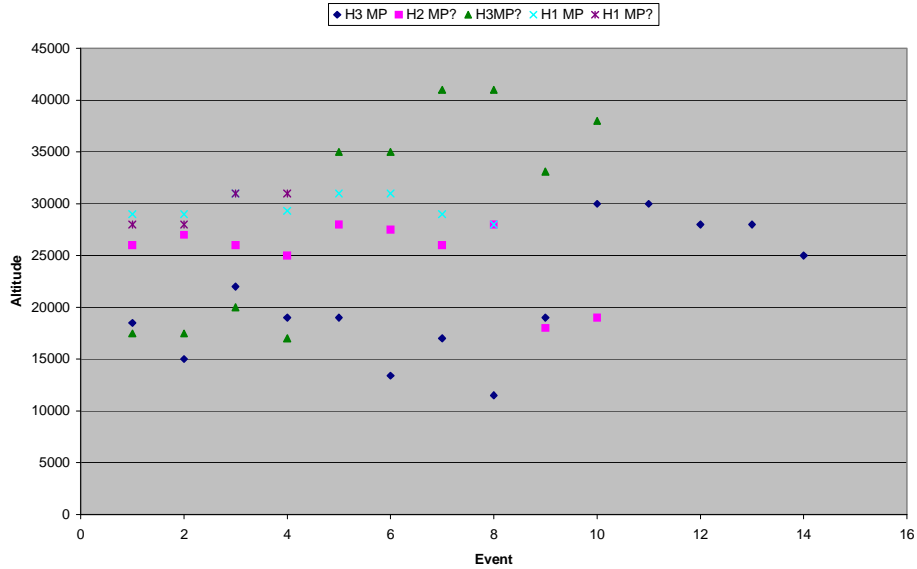


Figure 7. Altitude of Mixed-Phase/Glaciated Rollback/Flameout/Stall Events

2.7 CORE DAMAGE EVENTS.

Events that resulted in damage to the core are shown delineated by environmental condition discriminators in figure 8. The altitude range for the events is shown in figure 9. Figure 9 also notes two particular events where mixed-phase/glaciated conditions were confirmed by freezing of the aircraft TAT probe.

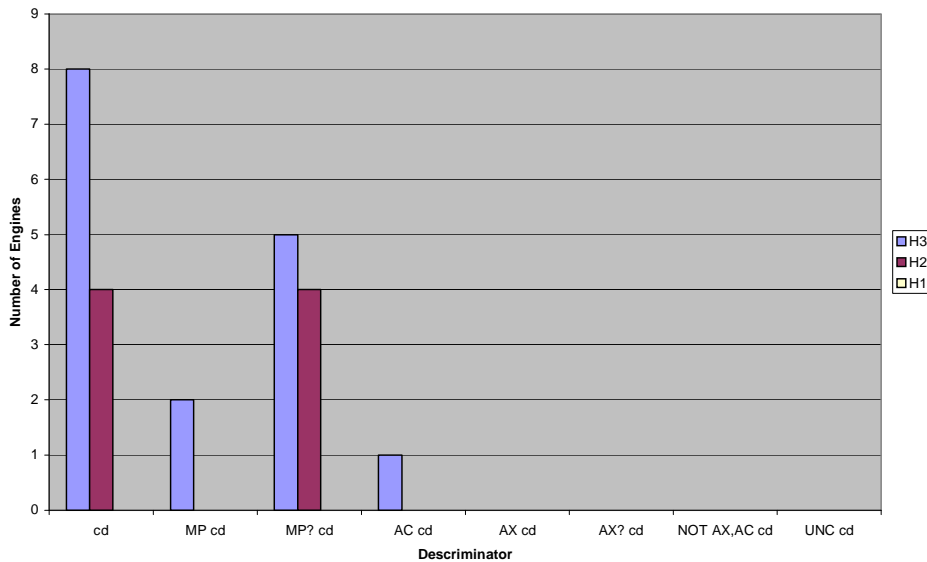


Figure 8. Core Damage Events vs Environmental Conditions Discriminator

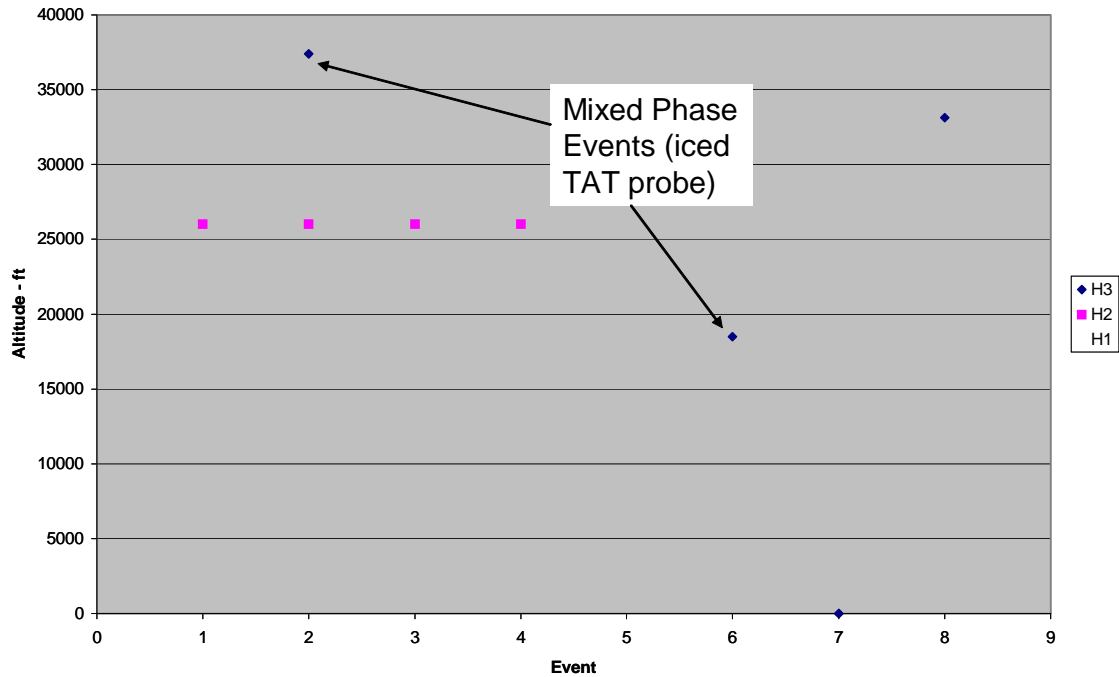


Figure 9. Altitude Distribution of Core Damage Events
(Confirmed mixed-phase events noted)

Based on the event classification, it became apparent that mixed-phase/glaciated conditions were predominately responsible for the engine core icing symptoms of engine rollback, flameout or stall, and core damage. These symptoms were considered to have a high potential for serious consequences and prompted the EHWG to notify the IPHWG that there was a clear need for further work on the icing environment with regard to engines.

2.8 FAN DAMAGE EVENTS.

Unlike the core-related symptoms, fan damage events were primarily associated with the SLD icing environment defined in proposed 14 CFR Part 25 Appendix X, as shown in figure 10. Further, as figure 11 shows, these events were concentrated on the ground at several airport locations that were prone to these conditions. The other events that occurred during flight, shown in figure 11, were not considered to be within proposed Appendix X. The maximum altitude for proposed Appendix X is also shown for reference.

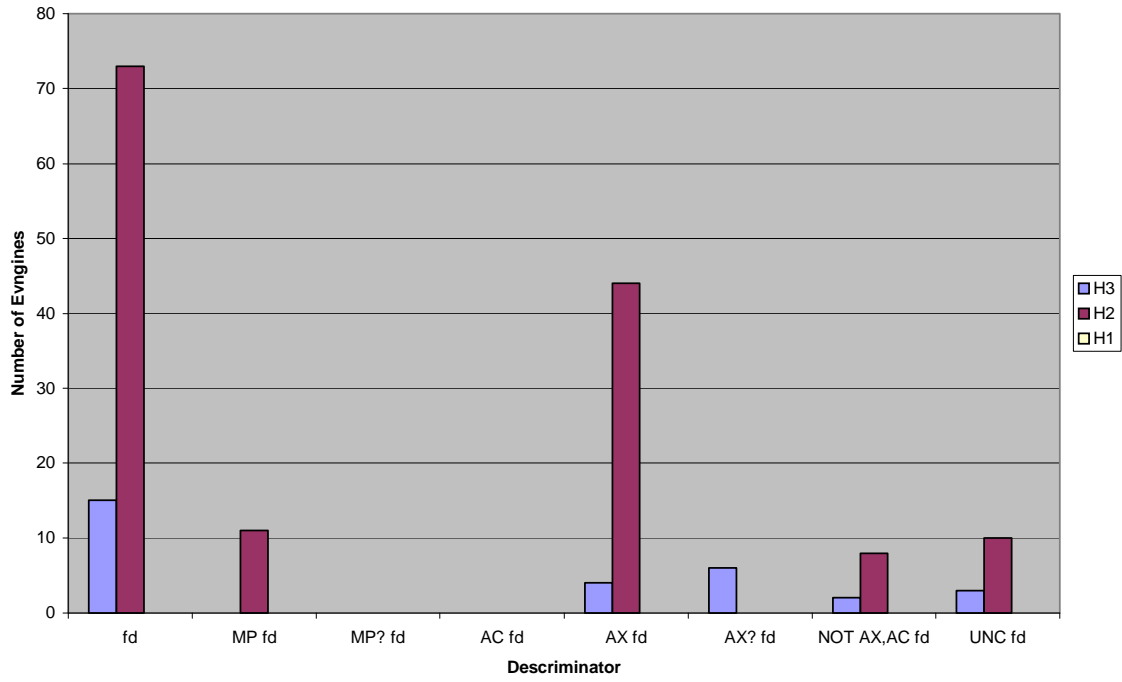


Figure 10. Fan Damage Events vs Environmental Conditions Discriminator

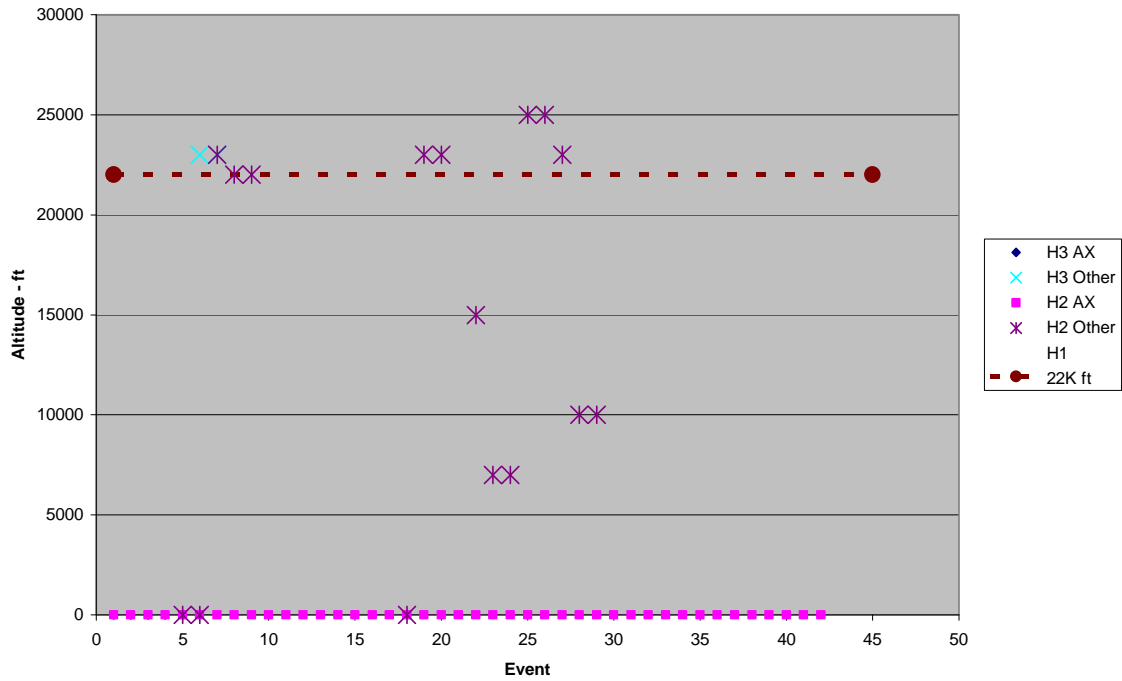


Figure 11. Altitude Distribution of Fan Damage Events

2.9 OTHER ENGINE DAMAGE EVENTS.

This category collected events where some damage was noted in the records, but no details exist on the nature of the damage. Fortunately, this situation applied to a relatively small fraction of the total events. It is noteworthy that this damage category was primarily associated with mixed-phase/glaciated icing conditions. This would seem to imply that the unspecified damage was more likely associated with the core than with the fan. The distribution of environmental conditions and altitude range are shown in figures 12 and 13.

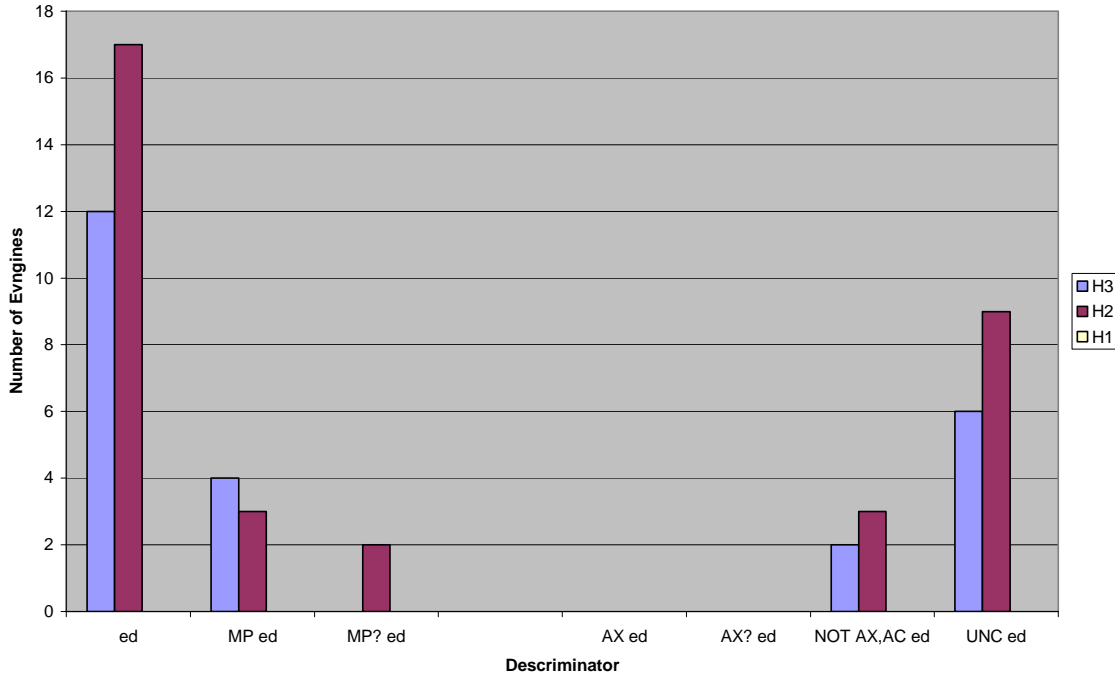


Figure 12. Other Damage Events vs Environmental Conditions Discriminator

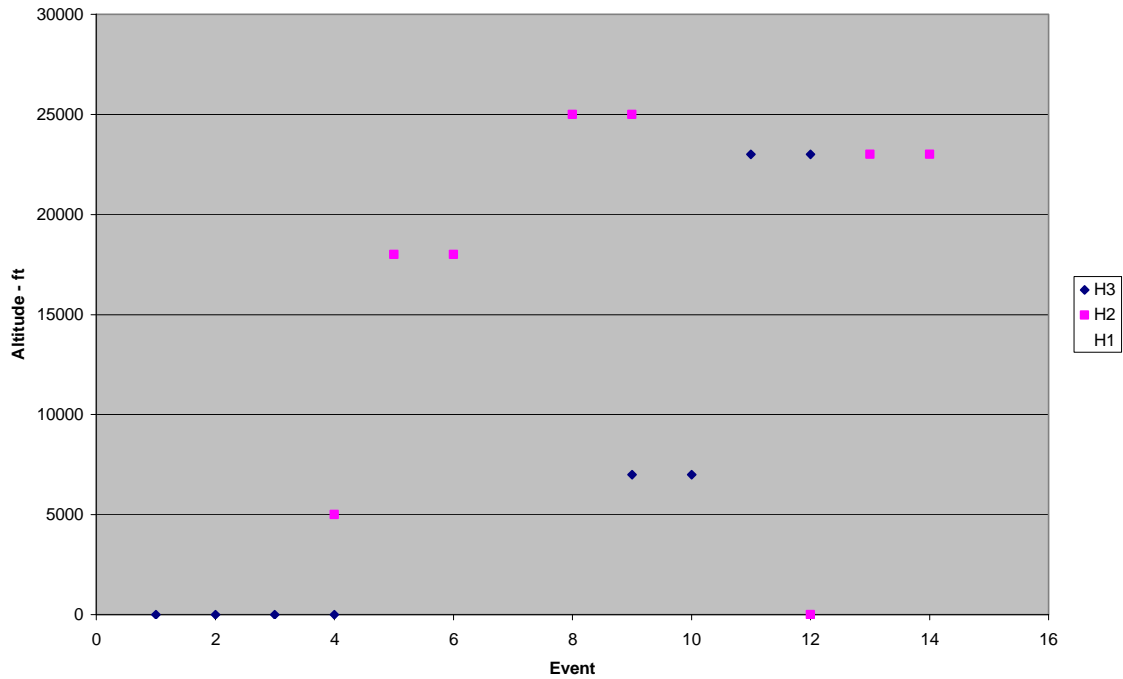


Figure 13. Altitude Distribution of Other Damage Events

The database events have led to the following general conclusions.

- Rollback/Flameout/Stall—Many mixed phase or suspected mixed phase (or convective clouds)
- Core Damage—Many mixed phase or suspected mixed phase (or convective clouds)
- Fan Damage—Primarily on ground and most likely symptom of proposed Appendix X conditions
- Other Damage—Many mixed phase or suspected mixed phase (or convective clouds)

2.10 SUMMARY CHARTS.

Figures 14, 15, and 16 show summary charts for the two primary categories of Rollback/Stall/Flameout associated with mixed-phase/glaciated conditions and fan damage associated with SLD.

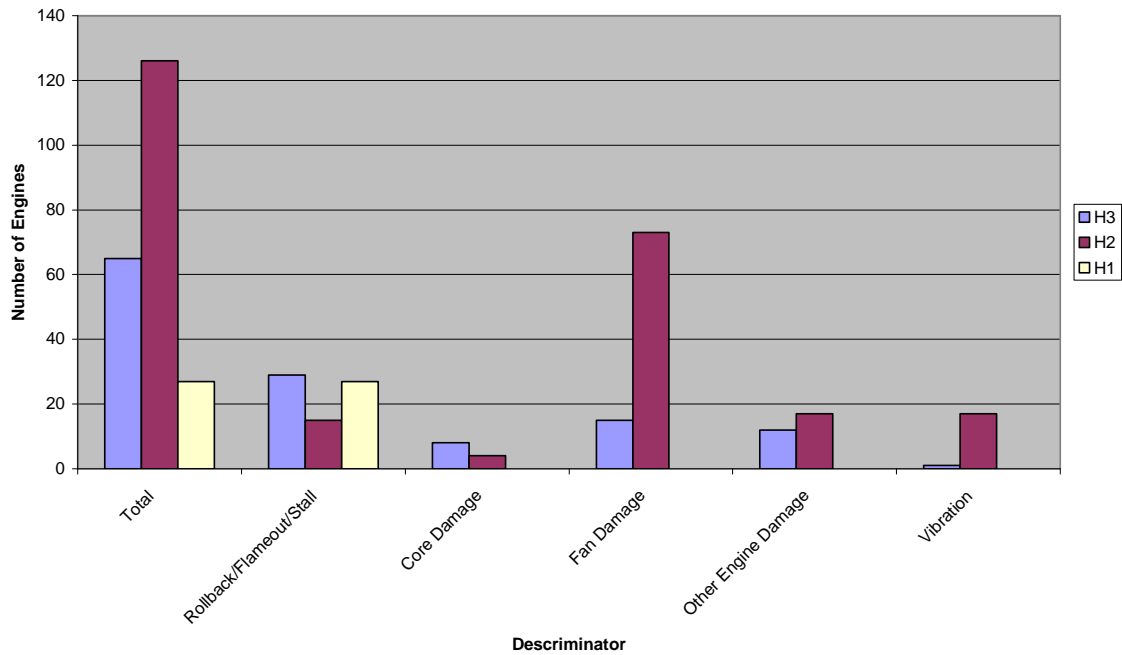


Figure 14. Distribution of Engine Symptoms for SLD and Mixed-Phase/Glaciated Conditions

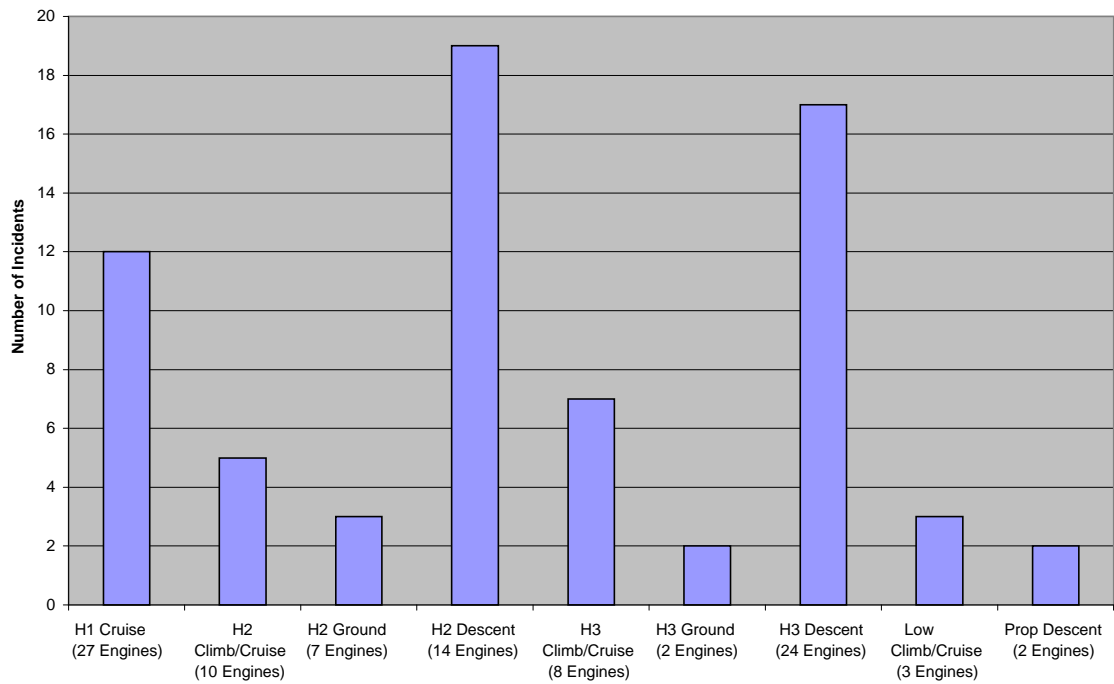


Figure 15. Summary Chart for Rollback/Flameout/Stall and Core Damage

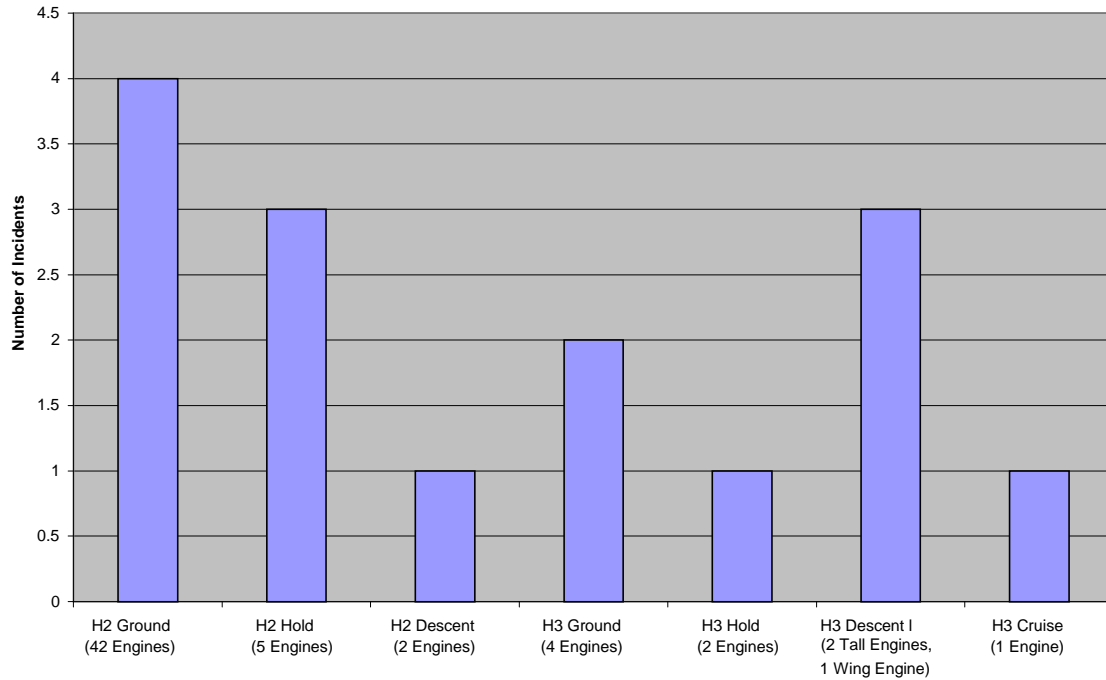


Figure 16. Summary Chart for Fan Damage

2.11 SUMMARY.

In summary, the following conclusions were drawn from the event data.

Of the icing conditions for which data was available, mixed-phase/glaciated conditions posed the greatest threat to in-flight operation of engines equipped with current ice protection systems. Rollback, flameout, stall, and core damage were symptomatic of events in these conditions.

Freezing rain and drizzle were responsible for a few ground events, primarily at Oslo, Norway and Denver, Colorado. Fan damage was the most common symptom of these events.

These conclusions were the primary drivers for the subsequent effort to define the mixed-phase/glaciated icing environment. This effort has resulted in the proposed 14 CFR Part 33 Appendix D material and the technology plan for follow-on work.

3. TECHNICAL MATERIAL RELATING TO PROPOSED CHANGES TO 14 CFR 33.68.

3.1 COMPARISON OF EASA TEST POINTS AND CURRENT AC 20-147 TEST POINTS.

Current AC 20-147 includes a table that specifies recommended icing test points covering the full range of engine power. The Federal Aviation Administration (FAA) indicated that testing successfully at these conditions has resulted in good field experience. If these test points are the reason the industry has good experience, then these points should be contained in the rule, not just in advisory material. The engine manufacturer's position for 14 CFR 33.68 was that the critical point analysis should drive the testing, not the AC 20-147 table points. The basis for this

position was that the table points can be shown by critical point analysis not necessarily to be the worst case conditions for all engines. A study comparing the European Airworthiness Standards Authority (EASA) icing certification standard and the legacy AC 20-147 table points was performed, which indicated similar ice accretion levels for either standard. Knowing that critical point assessment will lead to test conditions that are equal to or more rigorous than either standard, the EHWG proposed a new draft regulation requiring a critical point analysis, where the legacy AC 20-147 table points would only need to be tested if they were shown to be more critical. Table 1 summarizes the AC 20-147 table points compared with the EASA requirements denoted in red. Primarily, EASA requirements are geared toward testing in an altitude icing wind tunnel, but some specifications are made for testing in a sea level engine test facility.

Table 1. The AC 20-147 Table Points Compared With EASA Requirements

Point	Power Setting	LWC	TAT (°F)	Altitude/ Mach No.	Duration (minutes)	EASA Ground Test?
1	Min idle	0.3/ [0.3]	26/[28]	SL/[SL]	30/[30]	Comparable
2	Flt idle	2.0/ [0.3]	23/[17.6]	[15K/0.5- 6K/0.45]	10/[10]	Comparable with LWC Increase for scoop factor
3	50% MC	2.0	23		10	Possibly covered by Hold
4	75% MC	2.0	23		10	N/A
5	Takeoff	2.0	23		5	N/A
6/7	Holding	1.7/0.3 .25 [2.2/0.6] [1.7/0.3] [1.0/0.2]	14 -4 [29] [14.5] [0]	[17K/0.4] [0K/0.45] [25K/0.5]	45 45 [30] [30] [30]	Comparable Range (Any requirement to adjust for “antiscoop” effect at SL likely covered by 45 vs 30 minutes.
8	Flt idle	1.0	-4		10	Not specifically covered
9	50% MC	1.0	-4		10	Possibly covered by Hold
10	75% MC [Max power core ice]	1.0 [1.0/.2]	-4 [0]	[25K/.5]	10 [30]	Comparable
11	Takeoff	1.0	-4		5	N/A

Flt = Flight idle

LWC = Liquid water content

MC = Maximum cruise

N/A = Not applicable

SL = Sea level

A comparison of the EASA requirements with AC 20-147 for the minimum flight idle power setting during idle descent operation was of great interest within the EHWG. Different manufacturers have followed different practices for certifying engines in this phase of flight operation, and the EHWG strived to achieve some measure of harmonization. Consequently, a comparison was made using thermodynamic ice accretion analysis [1] for a hypothetical modern large transport engine at the AC 20-147 table point, tested both at sea level and in an altitude engine test facility, versus the EASA test in an engine altitude icing wind tunnel facility. The focus of the comparison was ice accumulation on the first stator of the low pressure compressor or booster. Ice blockage on this stator can affect engine airflow and can potentially cause

rollback. Ice shedding into core from this stage can also precipitate surge or burner blowout and can possibly cause airfoil damage.

A comparison of the stator ice accumulation for different test options is provided in figure 17. The difference in low rotor speed between FAA (25% N1) and EASA (30% N1) is consistent with the FAA practice of requiring the minimum flight idle setting and the EASA practice of requiring the nominal flight idle setting for the flight condition. The AC test condition run in an altitude facility (second column) with the engine directly connected results in slightly more ice accumulation than the ground test at sea level (first column) with a free jet. This is due to the facility setup differences. (A more complete discussion of facility setup differences can be found in section 5.) Both result in less ice accumulation than the EASA test condition (third column in figure), due primarily to the lower inlet total temperature for the EASA test point (17.6°F vs 23°F). This temperature effect is evident from the re-evaluation of the EASA point at the same inlet total temperature (fourth column in figure). The EASA test condition run as a ground test with an increase in liquid water content (LWC) to compensate for the lack of inlet scoop factor is shown for completeness (fifth column in figure).

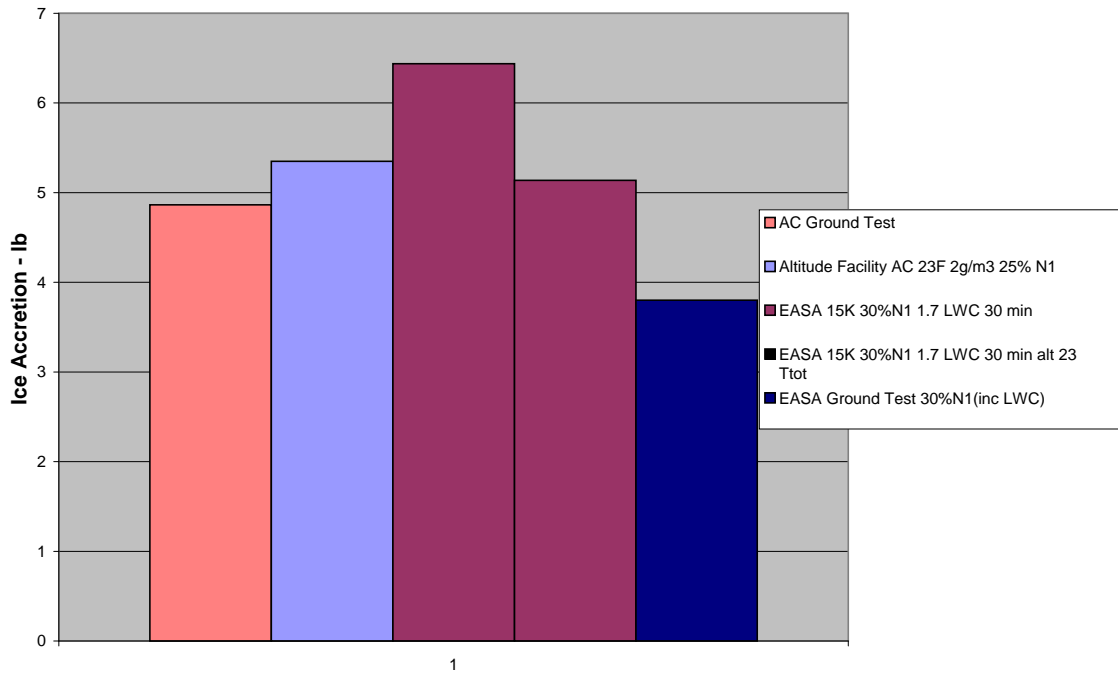


Figure 17. Comparison of Stator Ice Accretion

The conclusion from this analytical study was that the FAA test history using the AC test requirements resulted in an ice accretion level on the critical engine component that is comparable to the EASA test that best simulates actual flight conditions. This result was influential in assuring the FAA that new certification rules based on a critical point analysis (CPA) would not compromise flight safety in icing conditions relative to the legacy testing based on the AC.

3.2 FREEZING RAIN THRESHOLD.

Environment Canada representatives on the EHWG expressed a concern about the proposed 14 CFR 33.68 certification level of liquid water content (LWC) for freezing rain. Keeping any proposal for 14 CFR 33.68 in line with the proposed Appendix X would dictate a LWC no greater than 0.3 g/m^3 . However, Environmental Canada cited that moderate freezing rain is defined to have a precipitation rate between 2.5 and 7.5 mm/hr. Using conventional precipitation rate to mass conversions like that proposed by Marshall and Palmer [2], 7.5 mm/hr translates to 0.42 g/m^3 . It was also noted, however, that a statistical analysis of freezing precipitation rates performed by Transport Canada using a network of stations in Quebec, Canada, for 10,800 minutes of measured freezing precipitation rates, the 99.9% value was 6 mm/hr [3]. Thus, 7.5 mm/hr represents an extreme precipitation rate. The proposed Appendix X defines the extreme value (99%) of LWC in freezing precipitation for median volume diameters greater than $40 \text{ }\mu\text{m}$ as 0.26 g/m^3 for freezing drizzle and 0.29 g/m^3 for freezing rain. To be consistent with the proposed Appendix X, a value of 0.3 g/m^3 was selected to represent a reasonable value of freezing precipitation water content for ground testing. These considerations underlie the recommended value of 0.3 g/m^3 for Condition 4 in proposed Tables 33.68-2 for 14 CFR 33.68 and 25.1093-1 for 14 CFR 25.1093.

3.3 FREEZING FOG.

14 CFR 33.68 has currently required a demonstration of the engine in freezing fog conditions for 30 minutes with an LWC of 0.3 gm/m^3 , nominally in the temperature range of 26°F to 29°F (-3°C to -1.5°C). Joint Airworthiness Regulations (JAR) E 780 required a similar test specified at -2°C . However, the range of temperature for freezing fog icing conditions was extended to lower temperature levels (-9°C (15.8°F) or less) in response to Certification Review Item (CRI) No. T-1 issued by EASA on February 18, 2004 following a freezing fog icing incident that resulted in multiple engine damage. Consequently, the EHWG included recommendations for a change to 14 CFR 33.68 that includes lower temperatures for the freezing fog demonstration. These considerations underlie the recommended rime and glaze icing temperature ranges for Conditions 1 and 2 in proposed Tables 33.68-2 for 14 CFR 33.68 and 25.1093-1 for proposed 14 CFR 25.1093.

3.4 GROUND OPERATION IN SNOW.

The EHWG discussed the basis for snow concentration level for ground taxi operation certification in proposed 14 CFR 33.68 changes. The current 14 CFR 33.68 regulations specify 0.3 g/m^3 LWC for ground taxi operation, but do not specifically address snow. The current 14 CFR 25.1093 requires safe operation in “falling and blowing snow,” but is not specific about snow concentration level. FAA membership stated that snow concentration requirements have

been based on visibility correlations [4]. These correlations specify 1/4 statute mile as the boundary between moderate and heavy snowfall. The correlation specifically is:

$$C = 2100 * V^{1.29}$$

where: C = concentration in gm/m^3
 V = visibility in meters

Substituting $V = 1/4$ mile into the equation yields a concentration $C = 0.91 gm/m^3$. Figure 18 is a reproduction of Figure 12 from reference 4. It includes two curves indicating cumulative probability of snow concentrations calculated from two data sets of observed visibility observations. Curve A is based on the same data set used to derive the correlation, and indicates that the probability is about 94% that snow concentration will not exceed $0.91 gm/m^3$. Curve B is based on a larger multiyear data set, and indicates that the probability is greater than 99% that snow concentration will exceed $0.91 gm/m^3$.

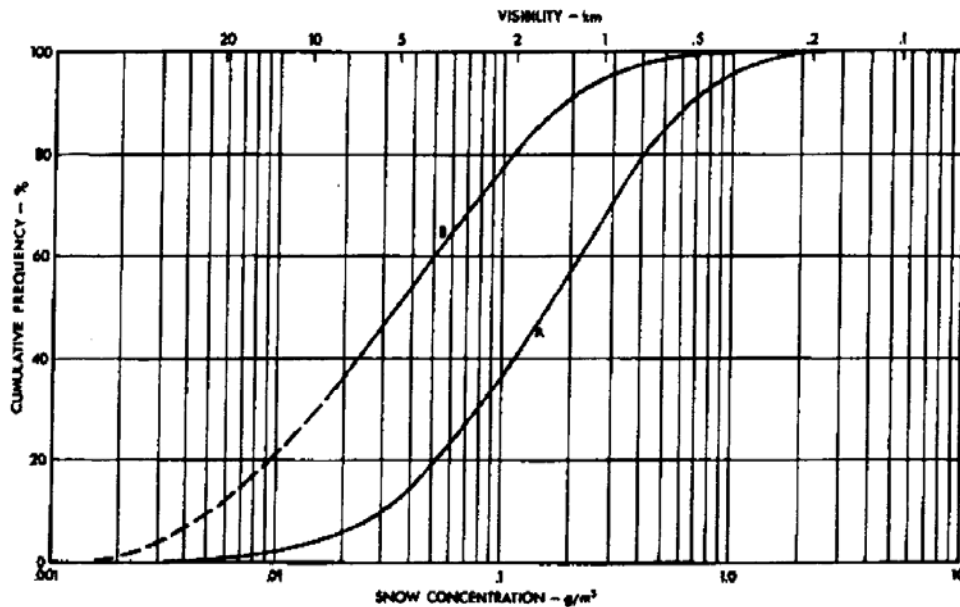


FIG. 12 CUMULATIVE FREQUENCY OF SNOW CONCENTRATION FOR OTTAWA
CURVE A: From N.R.C. Snow Concentration Measurements
CURVE B: As derived from Diurnal Frequencies of Reported Visibility in Combination with Snow for the 20-Year Period 1956-74 at Ottawa International Airport, using the Relation $C = 2100 V^{1.29}$

Figure 18. Reference 4 Data on Snow Concentration

Environment Canada membership offered concern that visibility has been shown by Rasmussen, et al. [5] to be a poor indicator of precipitation rate. To check the above numbers, the following calculation was performed. The maximum precipitation rate for moderate snow is 2.5 mm/hr water equivalent. From a Transport Canada data set of 338,000 minutes of snowfall data, the 95% and 99% values were 2 and 4 mm/hr, respectively, showing that a 2.5 mm/hr threshold provides an extreme value. It was also noted that holdover time tables for anti-icing fluids are

only sanctioned by the FAA for use in light or moderate snow conditions. The upper threshold for moderate snow is 2.5 mm/hr, or corresponding to a visibility of 1/4 statute mile according to the Federal Meteorological Handbook.

Using a rate 2.5 mm/hr and a typical fall speed for snow of 0.8 m/s, this translates into a snow concentration of 0.9 g/m³ water equivalent. The EHWG concluded that the two estimates are similar, and consequently, 0.9 g/m³ became the recommended level for testing at ground idle in snow. These considerations underlie the recommended value of 0.9 g/m³ for Condition 3 in proposed Tables 33.68-2 for 14 CFR 33.68 and for 14 CFR 25.1093-1.

4. PROPOSED APPENDIX D TO 14 CFR PART 33.

4.1 BACKGROUND.

A consequence of the EHWG activity was the creation of a new proposed Appendix D to 14 CFR Part 33 to define the icing envelope for mixed-phase/glaciated conditions. This section documents the process that led to the standards defined in that appendix.

The database of commercial service engine icing events detailed in section 2 in the mixed-phase/glaciated environment established that the current 14 CFR Part 25 Appendix C icing envelope with supercooled large drops does not cover the range of altitude and ambient temperature established by these events. This is evident in figure 19, based upon the limited number of service events having records of ambient temperature.

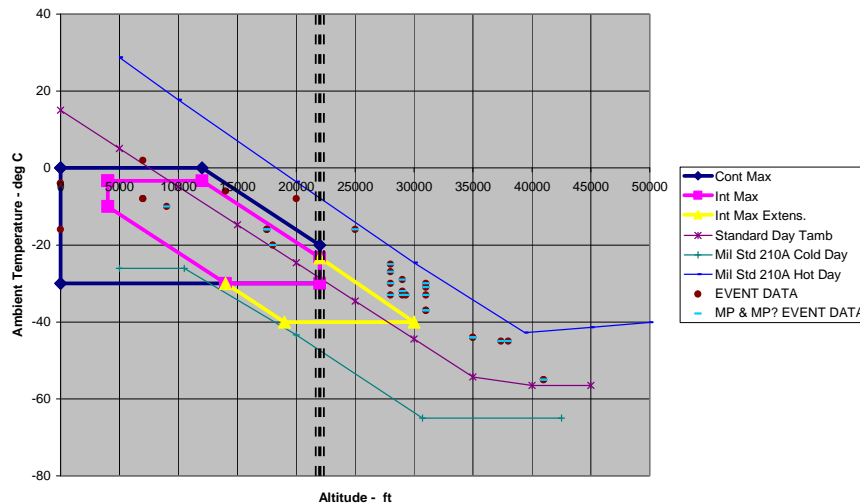


Figure 19. Database Events Compared With 14 CFR Part 25 Appendix C

The database events that were either confirmed as mixed-phase/glaciated or inferred to be mixed-phase/glaciated due to similar characteristics and/or meteorologist input are delineated by the light blue line through the data point. As noted, they are predominately outside 14 CFR Part 25 Appendix C, but appear to be bound by MIL STD 210A Hot Day temperature limits. For this reason it was decided to increase the range of the proposed 14 CFR Part 33 Appendix D beyond

14 CFR Part 25 Appendix C envelope to the MIL STD 210A Hot Day temperature limits, as shown in figure 20, which is identical to figure D-1 in the proposed 14 CFR Part 33 Appendix D.

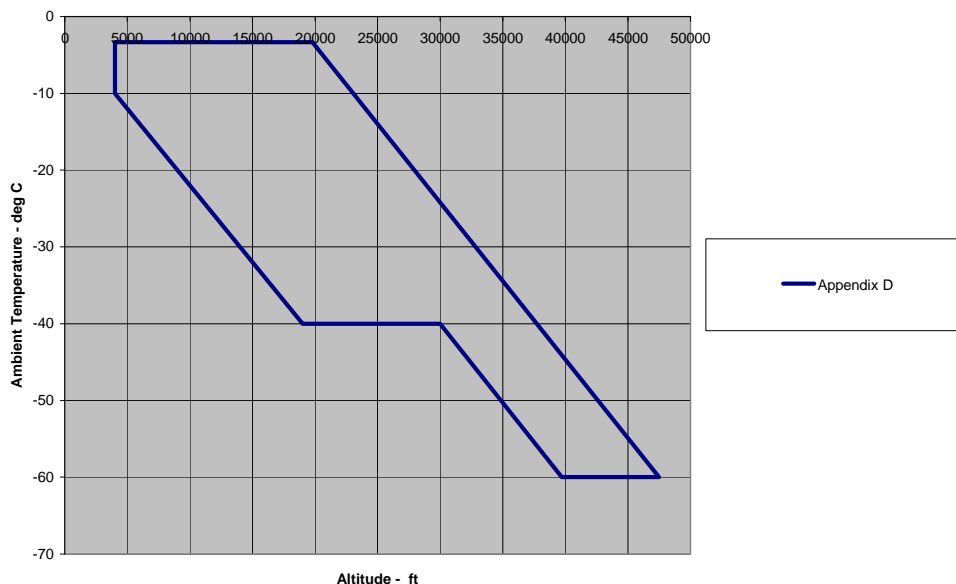


Figure 20. Convective Cloud Ice Crystal Envelope

A common characteristic in most of these events was the proximity to deep convective/tropical storm cloud formations; thus, Appendix D is being proposed primarily as a deep-convective-cloud extension to the Appendix C envelope. The working hypothesis, based on the often rapid onset of engine events, the lack of airframe icing, some observations of strong moisture on the windscreen (e.g., rain reported but suspected to be melting ice crystals), and the proximity to such cloud formations, is that the aircraft are likely encountering an area of high ice water content (IWC). The observations of low or no reflectivity on the pilot's radar are consistent with flight through ice particles, possibly concentrated at small sizes. Further discussion of this hypothesis can be found in AIAA-2006-0206 [6].

4.2 PREVIOUS GUIDELINES AND MEASUREMENTS.

The 1998 FAA review of mixed-phase icing conditions [7] includes a discussion of the published guidelines on the characteristics of such clouds. In the 1950s, it was recognized that conditions in a mixed-phase cloud could be conducive to engine inlet, Pitot tube, and other instrument icing in turbine engine aircraft [8]. It was also recognized that the worst conditions were most likely in deep convective clouds and thick layer clouds in the intertropical convergence zone, and that the cloud hydrometeor mass was most likely dominated by ice particles. (The intertropical convergence zone is a very large scale circulation pattern that leads to enhanced convection in the tropics in the summer time. The thick layer clouds may be due to remnants of cluttered convection.) A series of airborne measurements of cloud total water content (TWC) was conducted between December 1956 and March 1958 in three tropical locations, resulting in an extensive set of 101 cloud measurement flights with 44.5 hours of in-cloud data [9]. These data will hereafter be referred to as the McNaughtan data set. It is speculated that from these

measurements, and perhaps from other unreported measurements, a table was assembled in a Joint Airworthiness Committee Leaflet [8] as a guideline for the expected maximum conditions for flight in mixed-phase clouds. It was further suggested as a note to the table that “below -20°C, all the water present may be assumed to be in the form of ice crystals,” and “of the total free water shown in the 0 to -20°C range, not more than 1 gm⁻³ should be taken as water, and the remainder as ice crystals, except where the total water content is shown as 1 gm⁻³, half should be taken as liquid water, and half as ice crystals.” This table appears in similar form, with the above liquid cloud information added, in the FAA Technical Report ADS-4 [10], where it is claimed to have been supplied by the National Research Council of Canada, but it is clear, by similarity, that the original source of the data is the British leaflet in reference 8. The same table appears in reference 11, with altitudes and distance converted to metric units. The 1998 FAA review of mixed-phase icing conditions [7] includes a version of the table, and it is replicated here as table 2.

Most of the more recent data on the properties of mixed-phase clouds has been collected by the atmospheric research community, but these studies were not focused on measuring maximum TWC areas of deep convective storms, as in the case of the McNaughtan data. A good summary of these measurements up to the mid-1990s was provided by the FAA [12], and an analysis of a limited set of data collected near thunderstorms is provided in reference 13. In the 1990s, focused convective cloud measurements were conducted by industry partners over continental United States [14] and near Costa Rica, but again, the data set is small compared to that of the McNaughtan data set. Although the more recent studies reveal some important information about the microphysical properties of these clouds, they do not provide the volume of information required to provide guidance on maximum expected TWC as a function of distance. The McNaughtan data set still represents the most extensive available for assessing the maximum TWC in mixed-phased clouds, particularly for the deep tropical clouds that likely constitute most of the engine event database cases.

The TWC measurement method employed by McNaughtan [15] was unable to discriminate the liquid and ice fractions, and is reported as “total free water content,” equivalent to TWC. However, the leaflet [8] that proposes the guidelines of table 2, possibly based on the McNaughtan data set, suggests that the major fraction of hydrometeor mass in such clouds was in the form of ice. The reasoning behind this conclusion is not stated, although it is assumed here that other supporting data, such as observations of airframe icing, must have been considered. Similarly, the estimates of the liquid fraction of cloud proposed in reference 8 and accompanying table 2 are presumed to be based on judgment rather than measurement due to the lack of phase discrimination capability in the instrumentation of the time. However, more recent studies also indicate that the ice component greatly dominates the hydrometeor composition above the freezing level in continental thunderstorms [14], and tropical storms and hurricanes [16 and 17]. Observations of high LWC in deep convective cloud tend to be limited to specific areas of the thunderstorm. Supporting measurements by the Rosemount Ice Detector in the engine event database, when available, also indicate that significant airframe icing is not present in the events, again supporting the contention that the major threat to engines in deep convection is from high TWCs dominated by ice particles.

Table 2. Ice Crystal Concentration Standards
(Supplied by the National Research Council of Canada)

Ambient Temperature (°C)	Altitude (1000 ft)	Maximum Total Concentration (Ice crystals plus LWC) (gm ⁻³)	Maximum Concentration in Liquid Form (gm ⁻³)	Extent Statute Mile
0 to -20	10 to 30	8	1	0.5
		5	1	3
		2	1	50
		1	0.5	Indef
-20 to -40	15 to 40	5	0	3
		2	0	10
		1	0	50
		0.5	0	Indef
-40 to -60	20 to 45	2	0	3
		1	0	10
		0.25	0	Indef
-60 to -80	30 to 60	1	0	3
		0.5	0	10
		0.1	0	Indef

Notes:

1. Presently it is not possible to say how much of the “total free water contents” tabulated exist in the form of water and how much as ice crystals, because supercooled water has been shown to exist at temperatures down to -40°C. Furthermore, the percentage of ice crystals and water may vary considerably in any one cloud.
2. From present information, it appears that the worst condition for engine and intake icing in mixed water/ice crystals occurs when there is a small quantity of water present.
3. The following assumptions may reasonably be made for design purposes:
 - a. Below -20°C, all the water present may be assumed to be in the form of ice crystals.
 - b. Of the total free water shown in the 0 to -20°C range, not more than 1 gm/m³ should be taken as water and the remainder as ice crystals, except where the total water content is shown as 1 gm/m³, when half should be considered as water and half ice crystals.
 - c. When the extent of the condition is shown as “indefinite,” it is acceptable to show that the airplane functions satisfactorily during 30 minutes continuous exposure to the conditions.

From ADS-4: Thirty minutes exposure is considered for the “indefinite” extent. However, per FAA Policy, 45 minutes exposure is considered for the “indefinite” extent.

The accuracy of the TWC measurements in all of the above studies is questionable. In the case of the McNaughtan data, bulk measurements of TWC were made by weighing a sample of cloud hydrometeors collected through a nonisokinetic inlet for a measured period of time [15]. Several correction factors were applied to account for nonisokinetic sampling, and nonuniformity of hydrometeor concentrations near the skin of the aircraft. There is simply not enough information 50 years later to establish the traceability and accuracy of this method. Some of the more recent studies noted above used data from optical array probes (OAP), but this technique is estimated to provide an accuracy of no better than a factor of two, due to uncertainty in conversion of two-dimensional particle image data to mass and the inaccuracy of OAPs at particle sizes below about 100 μm . In recent thunderstorm and tropical storm microphysical measurements, there was some indication that significant mass may be concentrated at sizes smaller than 100 μm [15 and 17]. In the most recent studies, TWC has been estimated by bulk sampling with hot-wires. Although this technique provides promise as an accurate and simple measurement technique, wind tunnel comparisons of different wire geometries and high-resolution visualization of particle impacts imply that hydrometeors are not being efficiently collected and evaporated, and the differences in excess of a factor of 2 are observed for different wire geometries [18]. It was therefore concluded that the accuracy of all of the data collected to date is inadequate to provide acceptable guidance, and that further measurements should be made once the technology of TWC measurement has been sufficiently improved and calibrated.

4.3 TRACING PAST GUIDELINES.

The EHWG examined the guidelines of table 2 to determine if the values could be traced in the material that originally reported them. The original report describing the 1956-1959 McNaughtan data set [9] on the tropical cloud measurements contains a series of figures and tables describing the data set, and an appendix summarizing the 1-minute average TWCs for all flights performed in the study. The original 1958 leaflet that is the source for table 2 [8] states that the data are from “measurements in cumulonimbus and heavy layer cloud in the intertropical convergence zone,” a clear reference to the McNaughtan data set. However, the McNaughtan report actually cites reference 8, and briefly compares the data to the guidelines, possibly indicating that the guidelines were formed independently. In another reference containing a variation of table 2 [11], the source of the information is explicitly stated as the McNaughtan report [9]. Regardless of this confusion, it is evident that some information in table 2 is outside the range of measurements in the McNaughtan data set. Figure 21 displays the McNaughtan data set in the proposed Appendix D envelope, with one point for each flight. Note that temperature and altitude generally did not show a great deal of variation during most flights, as most flights were conducted at a fairly constant altitude. The data do not extend past about -26°C and 28,000', even though table 2 proposes guidelines in different temperature categories down to -80°C and 60,000'. Furthermore, the minimum time scale for the McNaughtan data set was 30 seconds, or about 2.6 nmi, at the typical TAS of 315 knots, and yet guidelines are quoted for distance scales down to 0.5 smi. It is therefore assumed that other unreported factors were considered in addition to the possible use of the McNaughtan data set when table 2 was compiled.

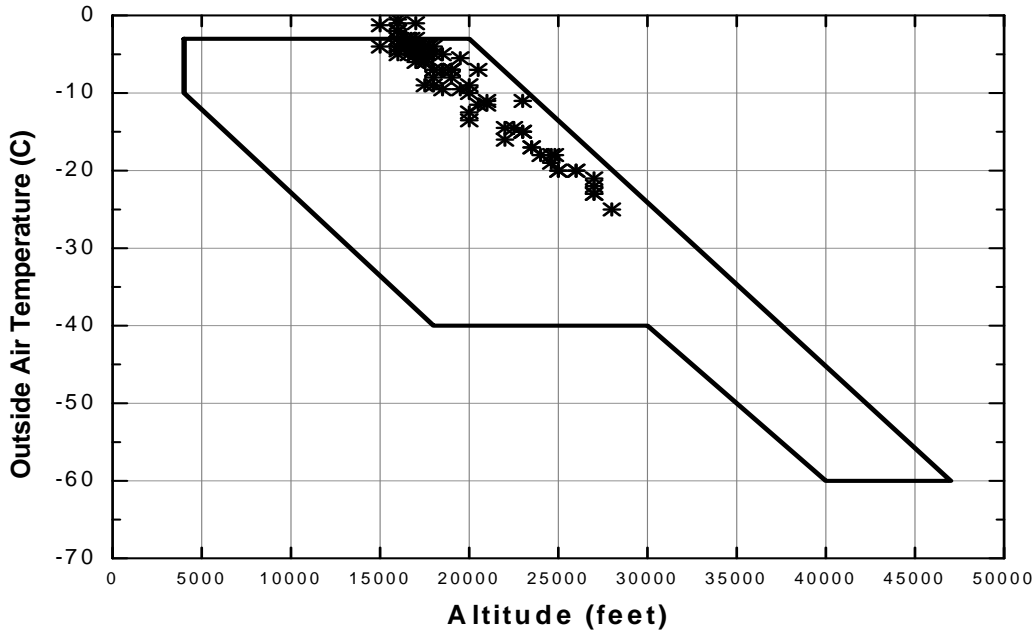


Figure 21. McNoughtan Dataset [9] in the Proposed Appendix D Envelope

4.4 THE CLOUD HORIZONTAL EXTENT FACTOR.

The reduction in the table 2 guideline TWC with increasing distance does not agree with calculations performed by the EHWG using the McNoughtan data set [9]. In the EHWG calculations, all flights were connected back-to-back as a first approximation, and the frequency distribution of TWC values was calculated for a variety of distance-averaging intervals from the minimum of about 4.6 nmi to a maximum of 260 nmi. The results of the 99 and 99.9 percentile TWC values are shown in figure 22, along with the past guidance from table 2. Note that the present calculations show a more gradual TWC reduction with distance. A best fit of the 99% statistics in figure 22 was normalized to the 17.4 nmi value and replotted in figure 24, along with the table 2 mixed phase and the Appendix C guidelines for intermittent and continuous maxima. Based on the similarity of the table 2 and 14 CFR 25 Appendix C continuous maximum distance factors, one can speculate that the originators of table 2 may have adopted from inspection of the data a representative maximum TWC of 5 gm^{-3} for 2.6 nmi, the minimum distance scale for the McNoughtan data set, and then used a distance reduction factor based on the National Advisory Committee for Aerodynamics (NACA) report used to develop the Appendix C continuous icing distance factor. The remaining point of 8 gm^{-3} at 0.44 nmi may have been chosen by extrapolation of the line.

The new calculations of the EHWG/PPIHWG may be biased by the data collection method. A typical type of flight track used in the McNoughtan study (displayed in figure 8 of reference 9) is not simply a straight track, but rather includes diversions intended to keep the aircraft near intense storm cores where the regions of higher TWC are found. The average TWC would tend to decline with distance if the aircraft just flew a straight track; but any decline will certainly tend to be less pronounced when the aircraft is intentionally diverted to stay near the storm core. However, the EHWG concluded that the new calculations of figure 22 are more defensible than

the guidelines of table 2, and acknowledged that they may represent a conservative distance scale guideline. In section 4.6, the rate of reduction shown in figure 22 will be combined with calculated estimates of maximum TWC to form the basis of a new guideline.

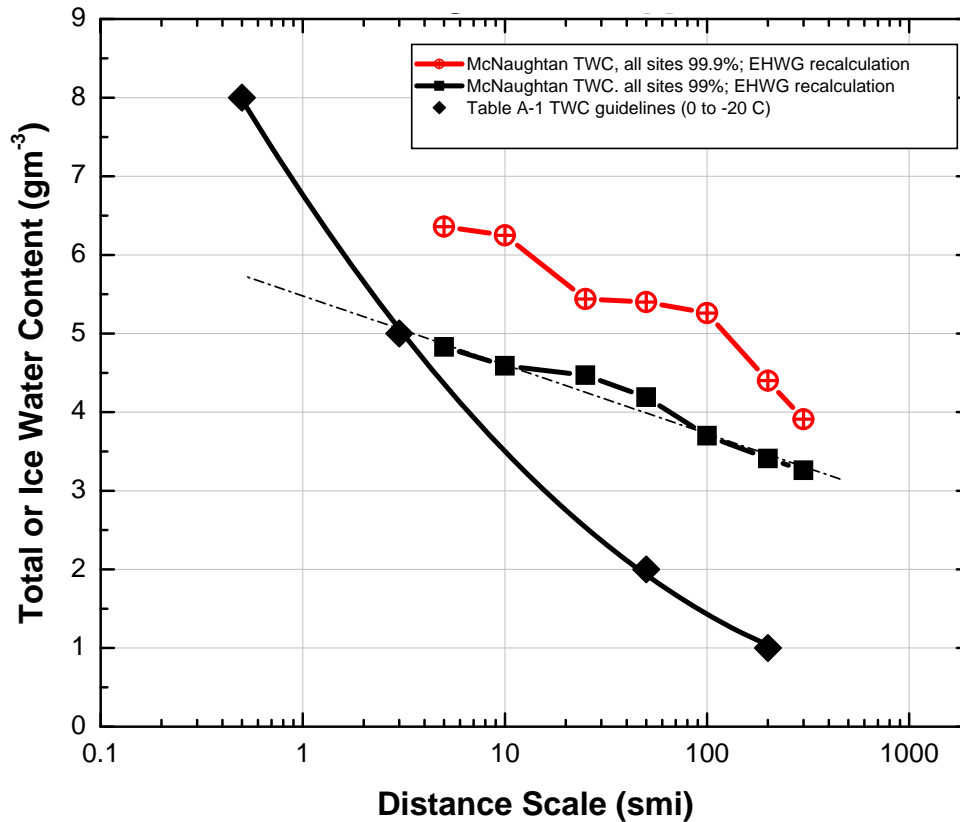


Figure 22. The EHWG Recalculation of Average TWC as a Function of Distance Scale and Comparison to Table 2 Guidelines

4.5 ESTIMATES OF MAXIMUM TWC FROM ADIABATIC PARCEL CALCULATIONS.

The working hypothesis formed by inspection of the engine event database is that the aircraft may have entered a region of high IWC in the vicinity of a deep convective cloud. Such a region of high IWC may be found in major updrafts, and a first approximation of the maximum TWC of such an updraft can be calculated for parcel lift from simple thermodynamics. In an undiluted rising air parcel, the TWC and temperature of the parcel are directly calculable from the appropriate equations. As an air parcel rises from below the cloud base, the parcel cools and expands, eventually reaching saturation. It then continually condenses water as the parcel rises, at a rate dependent on the change in temperature. The actual TWC for such an air parcel tends to be lower in nature due to mixing with outside unsaturated air. It can also be lowered or raised by redistribution of cloud water by precipitation, although augmentation has not been documented and is merely a prediction in some cases from computer models. Nevertheless, adiabatic or near-adiabatic LWC levels have been observed in developing convective clouds, and the adiabatic TWC estimates calculated here provide a first approximation of the maximum TWC that might be expected in deep convective updrafts. Adiabatic TWC estimates provide the means to

estimate maximum TWC as a function of temperature and altitude, an important benefit for guidance material.

The analysis performed for this report calculated the TWC for undiluted air parcel rise from a series of initial surface conditions varying from 0°C to 35°C. A relative humidity of 90% was arbitrarily assumed at the surface in all cases in an attempt to maximize the TWC while maintaining a realistic surface boundary condition. TWC would be augmented by only a small amount if 100% had been assumed. The condensate was assumed to deposit directly to ice particles at temperatures below freezing, due to the usual dominance of the ice phase above the freezing level in tropical convective storms and hurricanes as noted above, and due to the implication from the incident database that the clouds encountered were most likely glaciated or dominated by the ice phase. A summary of the results is shown in figure 23. Only points above the freezing level are plotted. In all profiles, the TWC reached a maximum in gm^{-3} in the 15,000'-25,000' range, depending on the initial temperature. The maximum adiabatic TWC value is about 9 gm^{-3} , and corresponds to the warmest atmosphere likely to be observed in nature.

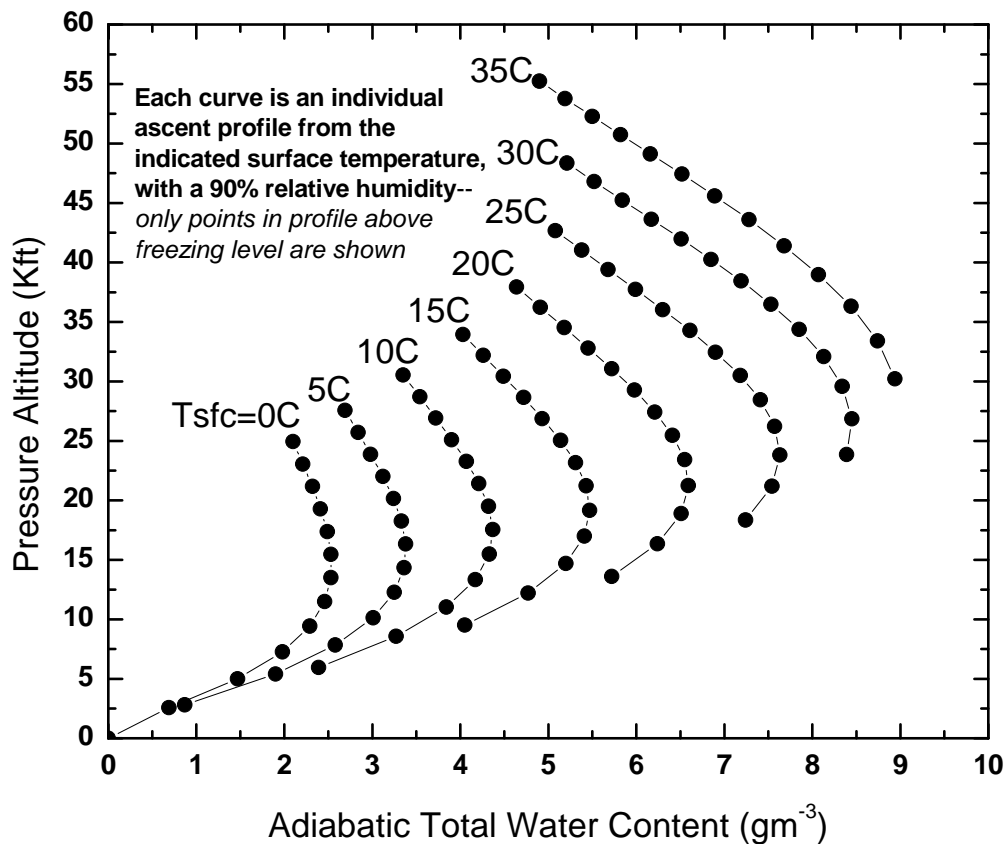


Figure 23. Adiabatic Profiles of TWC for Eight Different Surface Temperatures Between 0°C and 35°C

4.6 AN INTERIM GUIDANCE FOR MAXIMUM TWC IN PROPOSED APPENDIX D CONDITIONS.

Due to the difficulties in tracing the source of some of the past mixed-phase guidelines contained in table 2, the lack of superior measurements since the compilation of table 2, and the general lack of confidence in the accuracy of the TWC estimates from all past studies, the EHWG has recommended that a new effort be conducted to collect a database of deep convective cloud measurements using modern instrumentation with accurate TWC measurement capability. As an interim improvement to the past guidelines, the committee further recommended the use of a new procedure to estimate proposed Appendix D conditions, as detailed in the following paragraphs.

The new procedure adopts the general slope of the TWC reduction with distance scale calculated by the EHWG from the McNaughtan data set (see figure 4) for the 99% TWC, as shown in figure 24. A standard distance scale of 17.4 nmi was chosen as a normalization point, the same as that for 14 CFR 25 Appendix C continuous maximum conditions. This scale also roughly represents a typical onset time for an engine event after the recognition of a TAT anomaly and an indicator of the presence of high TWC. The short distance limit of 4.6 nmi is the lowest that could be deduced from the McNaughtan data set [9]. It was the opinion of the EHWG that this was adequate given the information in the event database and current technical knowledge of onset time for the engine problem. Hence, the distance factor provided in figure 25 is proposed for new engine certification. Figure 25 is identical to Figure D-3 in the proposed 14 CFR Part 33 Appendix D.

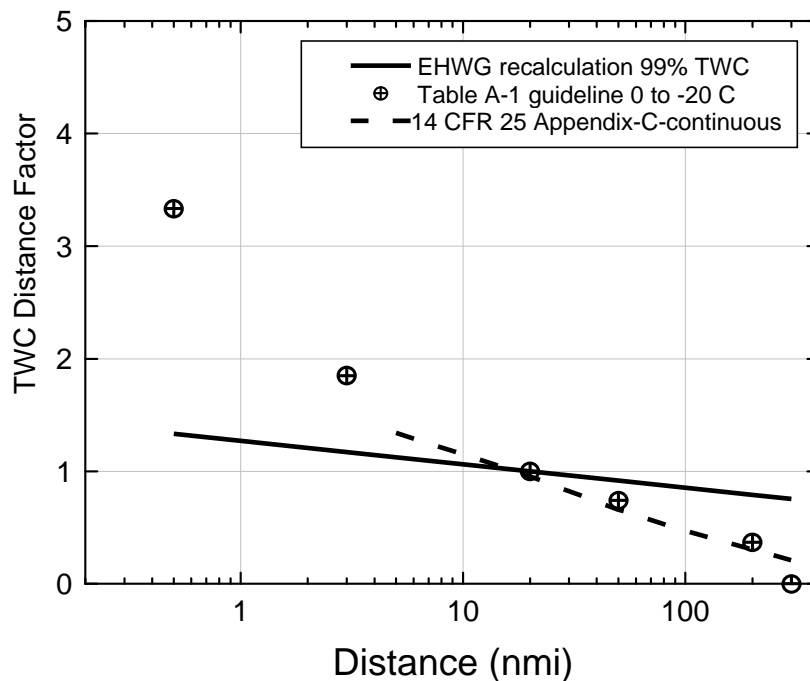


Figure 24. Reduction in TWC With Distance Normalized to 17.4 nmi

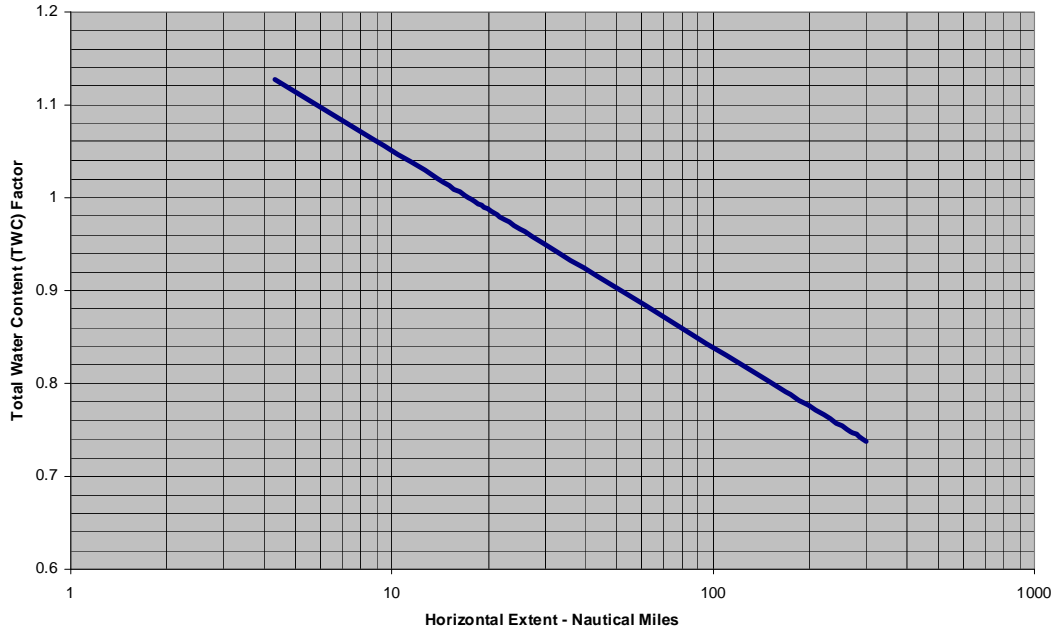


Figure 25. Exposure Length Influence on TWC

Next, the adiabatic TWC calculations are used to provide a temperature-and-altitude-sensitive estimate of maximum TWC scaled to the McNaughtan 99% observations at 17.4 nmi. The McNaughtan data set has a mean sortie altitude and temperature of about 20,000' and -9°C, respectively. The calculated adiabatic TWC for this condition is about 6.7 gm^{-3} , and the 99% McNaughtan TWC at 17.4 nmi is 4.4 gm^{-3} , a factor of 0.65 of adiabatic. The EHWG has chosen the 99% value as the prudent engine test guideline. Correspondingly, the appropriate test point for 20,000' and -9°C would be 4.4 gm^{-3} for a distance scale of 17.4 nmi. To provide test points for other temperatures and altitudes, the same scale factor of 0.65 between 99% TWC at 17.4 nmi and adiabatic TWC is assumed to apply. Figure 26 shows a reorganization of the adiabatic TWC data contained in figure 23, replotted as adiabatic TWC versus pressure altitude for a family of curves of different flight altitude temperature, where the adiabatic TWC has been scaled down by the factor of 0.65 according to the reasoning above. The curves have been truncated to the proposed Appendix D envelope. The first step in the new procedure is to pick a 0.65-scaled adiabatic TWC value from figure 26 for the desired temperature and altitude. The second and final step is to scale this value for distance using figure 25. For example, figure 26 reveals that the scaled adiabatic TWC value for -30°C and 27,500' is 4.0 gm^{-3} . If one desired a test point for 10 nmi, one would refer to figure 25 to derive the distance factor of 1.05, and the desired test point would then be the product of the scaled adiabatic TWC value (4.0 gm^{-3}) and the distance factor (1.05), or 4.2 gm^{-3} .

In the absence of any quantitative measurements on the levels of LWC in deep convective clouds, the EHWG recommends the same maximum liquid concentration guidelines as contained in table 2.

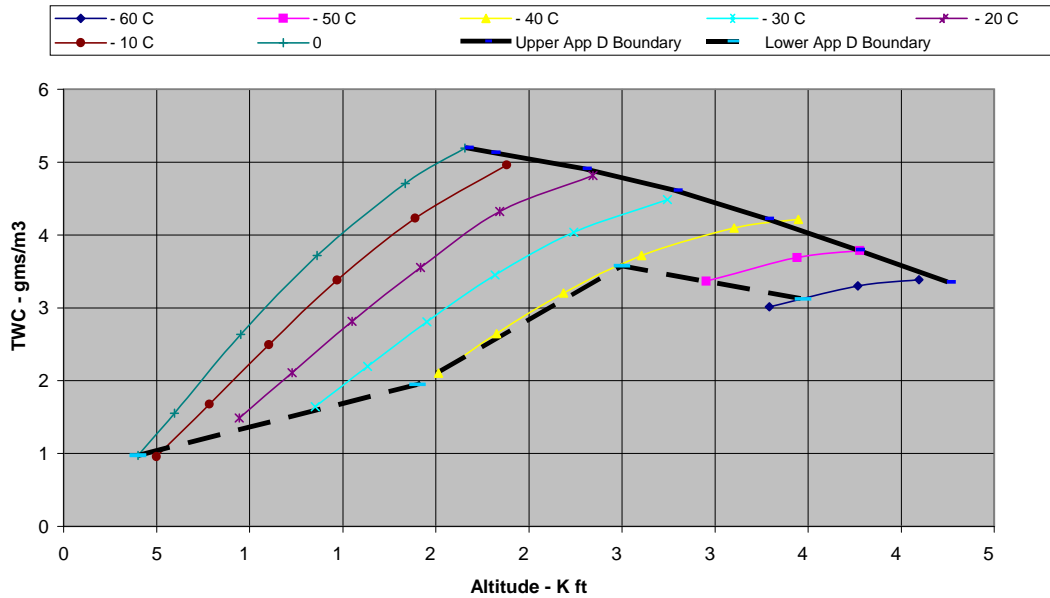


Figure 26. Total Water Content

4.7 COMPARISONS BETWEEN OLD AND NEW TWC GUIDELINES.

Comparisons between the old TWC guidelines (table 2) and the new TWC guidelines are included in table 3. The range of conditions for each category results in a range of calculations of adiabatic TWC, and thus, a range of new guideline TWCs for each category. Values outside the proposed Appendix D envelope are so noted.

Table 3. Comparisons Between Old and New TWC Guidelines

Ambient Temperature (°C)	Altitude (1000 ft)	Extent (smi/nmi)	Old Guidelines (Table 2) (gm ⁻³)	New Guidelines: Range (gm ⁻³)	New Guidelines: Middle of Range (gm ⁻³)
0 to -20	10-30	0.5/0.44	8	n/a	n/a
		3/2.6	5	n/a	n/a
		4.6		1.8-5.7	5.0
		50/44	2	1.5-4.7	4.0
		ind/161	1	1.3-4.0	3.5
-20 to -40	15-40	3/2.6	5	n/a	n/a
		4.6		2.2-5.2	4.5
		10/8.7	2	1.8-4.2	
		50/44	1	1.7-3.9	3.7
		ind/161	0.5	1.6-3.2	3.2

Table 3. Comparisons Between Old and New TWC Guidelines (Continued)

Ambient Temperature (°C)	Altitude (1000 ft)	Extent (smi/nmi)	Old Guidelines (Table 2) (gm ⁻³)	New Guidelines: Range (gm ⁻³)	New Guidelines: Middle of Range (gm ⁻³)
-40 to -60	20-45	3/2.6	2	n/a	n/a
		4.6		2.3-4.7	n/a
		10/8.7	2	1.8-3.8	n/a
		ind/161	0.5	1.6-3.3	n/a
-60 to -80	60-80	3/2.6	1	n/a	n/a
		4.6		3.4-3.8	n/a
		10/8.7	0.5	2.8-3.1	n/a
		ind/61	0.1	2.4-2.7	n/a

smi = statute miles

nmi = nautical miles

ind = indefinite

4.8 ICE PARTICLE CHARACTERISTIC SIZE.

McNaughtan's measurements [9] did not include any estimate of particle size. During the 1970s, airborne optical probes were developed to electronically measure the sizes and two-dimensional shapes of cloud particles. The interpretation of these measurements has been revealed to be quite complex, particularly for particles smaller than about 100 μm.

Using data that was collected from the optical probes in the 1980s and 1990s, a review of the microphysical properties of thunderstorms concluded that ice particle mass was concentrated in 2-mm-diameter particles [13]. However, the mass of particles smaller than about 100 μm was poorly represented in this review, and the data included characteristic size measurements derived only from particles larger than 300 μm. In the late 1990s, an industry-instrumented aircraft was used to make a limited number of measurements near thunderstorm cores [14], and in this study, not included in the former review, it was concluded that the majority of the ice particle mass was concentrated in the sub-100-μm size range. Similarly, the median-mass diameter (MMD) of ice particles observed in a high IWC region of decaying convection in a north Atlantic extra-tropical hurricane [16] was found to be about 185 μm using similar instrumentation. Due to some instrument artifacts that have recently been proposed in the literature, observations of such low MMDs remain somewhat controversial in the cloud physics community. However, there is currently a great interest in the community in the growing evidence of unexpectedly high concentrations of small ice particles near the cores of deep convection that could result in such low MMDs. The EHWG has concluded that the current evidence suggests that MMDs lower than 200 μm can be expected near deep convection, but acknowledges that further measurements are required with improved instrumentation to provide more confidence.

4.9 THE TAT ANOMALY DATA.

The EHWG database (section 2) of engine icing events shows that freezing of an aircraft's Rosemount TAT probe provides evidence of operation in an ice crystal environment. However, this TAT anomaly does not invariably occur in these conditions.

- The TAT anomaly occurs when a certain threshold of IWC is exceeded. The ambient IWC may be far in excess of the threshold, and the TAT response will be the same.
- The database includes multiple aircraft, each with differing TAT response due mainly to the location in which the probe is installed on the aircraft. Some aircraft show no propensity for TAT corruption with the same probe installed as other aircraft that do exhibit the propensity.
- A short duration exposure to TAT anomaly may mean that the TAT location on the aircraft is somewhat shielded, so that only very high concentrations can cause the anomaly.
- The EHWG database (section 2) indicates the duration of engine events in ice crystal environments is less than 100 miles. This observation is important for the collection of points for engine critical point analysis.

If the TAT anomaly occurs, its onset precedes the onset of the engine event in ice crystal environments by varying amount times. Figure 27 shows the distance flown by the aircraft from the onset of the TAT anomaly to the onset of the engine event for all events in the EHWG database for which that information is available. Database event number is shown on the horizontal axis and distance on the vertical axis.

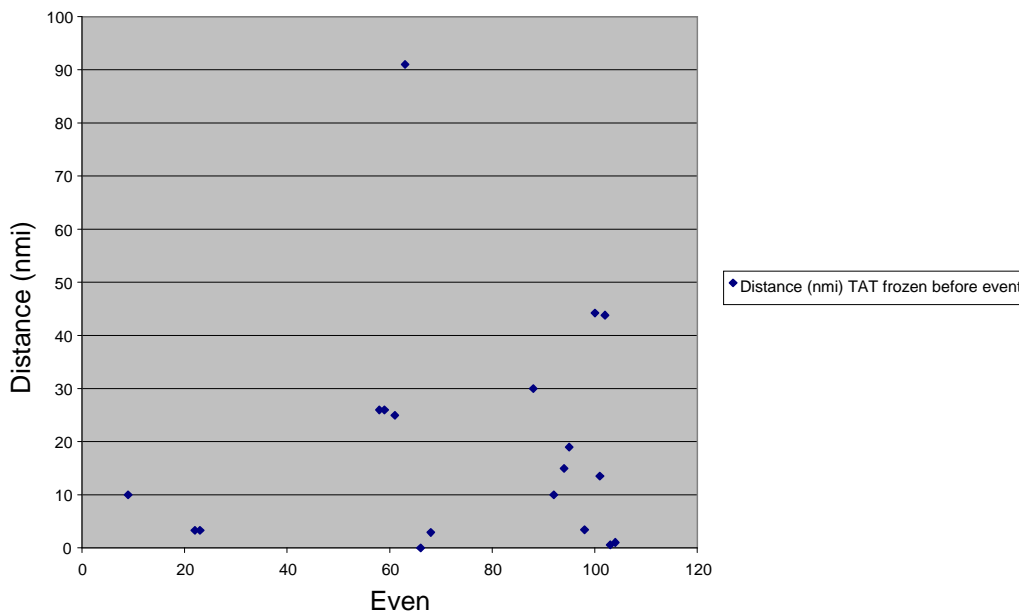


Figure 27. Distance From Onset of TAT Anomaly to Engine Event by Database Event Number

The total distance flown for the duration of the TAT anomaly (before and after the onset of the engine event) is shown in figure 28. In combination, these two figures helped to assess the cloud length of the ice crystal environment as well as to give insight into the amount of exposure necessary to precipitate an engine event in this environment.

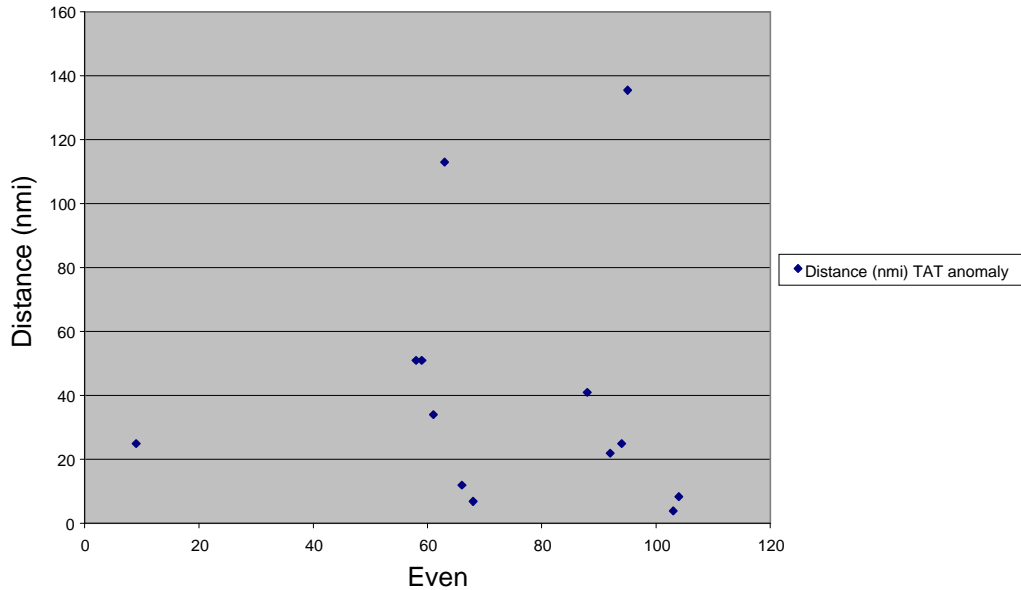


Figure 28. Total Airplane Exposure to TAT Anomaly From Engine Event Cloud Encounter by Database Event Number

5. ICE CRYSTAL TEST FACILITIES.

5.1 ICE CRYSTAL SIZE.

Simulation of supercooled liquid water flight icing encounters in an engine test facility requires accounting for differences in water droplet temperature and inlet concentration effects. Supercooled water drops are readily produced by water spray nozzles in the same size range as natural conditions. It is possible to produce ice crystals using water spray nozzles, but the ice crystals produced are typically smaller than in nature. Requirements include the characterization of ice crystal size distributions and degree of wetness from “snow” nozzles. Additionally, the freezing of the spray water droplets and subsequent coalescence into larger ice crystals takes time that may require prohibitive lengths between the spray nozzles and the engine. Consequently, ice shavers are often the preferred method for creating ice crystals for engine testing.

5.2 ICE CRYSTAL VELOCITY.

Regardless of the method for producing ice crystals, either at sea level or in an altitude test facility, it is necessary to account for differences in ice particle size and velocity relative to flight conditions. Trajectory assessments of the ice crystal velocity adjustments to surrounding air flow must also be validated. A sample of such an assessment is displayed in figure 29 but is

uncalibrated with respect to ice crystal surface area to mass ratio because the distribution of ice size and shape distribution is not yet known.

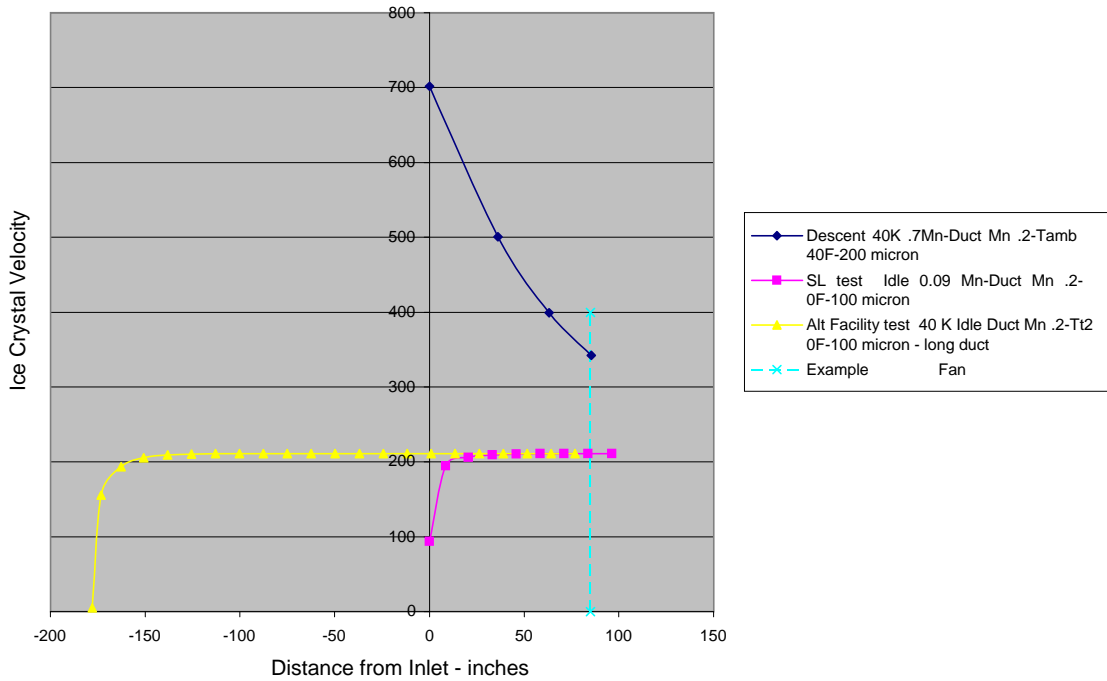


Figure 29. Potential Ice Crystal Velocity Difference From Flight Environment

5.3 TOTAL WATER CONTENT REQUIREMENTS.

The proposed Part 33 Appendix D requirements for ice crystal conditions discussed within the EHWG evolved as more information became available and more analysis was done. (Note: The discussion in this section is based upon facility simulation of an upper value of 3 gm/m³ for TWC. TWC levels as high as approximately 5 gm/m³ would need to be simulated under Part 33 Appendix D as currently proposed. Water flow rate to achieve this higher level would be proportionately higher.) Table 4 gives facility requirements for simulation of several flight conditions. A TWC simulation requirement of 3 gm/m³, when expressed as water flow requirements, equates to 500 lb/hr per square foot of inlet area.

Table 4. Comparison of Flight Conditions With Test Facility Requirements

	In Flight	Sea Level Test Facility	Altitude Test Facility
Altitude-K ft	20 to 45	0	20-45
T _{amb} -°F	-76 to -4	0 to 28	Duct static temperature: -55 to 24
T _{total} -°F	-26 to 28	0 to 28	-20 to 28
MVD-microns	<=200	>100	>100
Ice crystals Mach No.	0.6 to 0.8	0.1 (At point of generation)	0.2 to 0.6 (In duct ahead of engine)
Maximum TWC-gm/m ³	3	25	10
Maximum water flow Rate-lb/hr/ft ²	-	590 (Ahead of inlet)	500 (Within inlet duct)

T_{amb} = Ambient temperature
 T_{total} = Total temperature
 MVD = Median volume diameter

The larger value of TWC (25 gm/m³) for sea level tests compared with flight is due primarily to the concentrating effects of 200-micron ice crystals at low power in flight and the opposite effect, particularly at high power in a sea level test facility. Testing in an altitude facility that has the ice crystal source located within inlet ducting that leads to the engine needs only to reflect the flight idle concentrating effect. Due to lower engine airflow at this condition, only a maximum TWC of 10 gm/m³ is required. Figures 30 and 31 illustrate these requirements for the various conditions of the CPA.

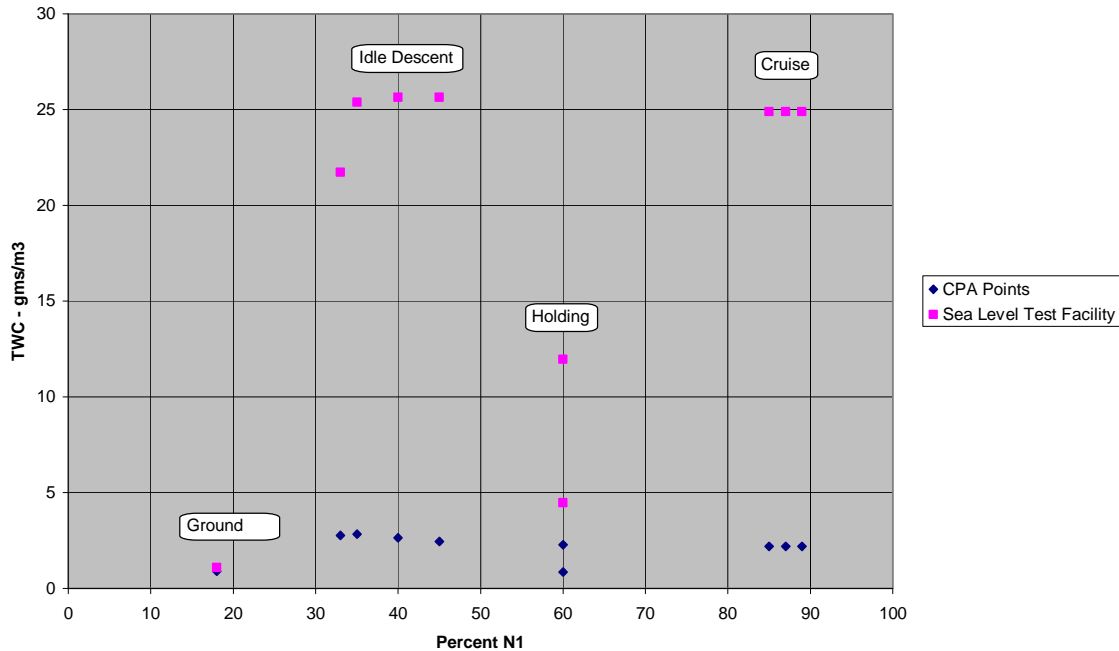


Figure 30. Total Water Content for “Free Jet” Test Setup

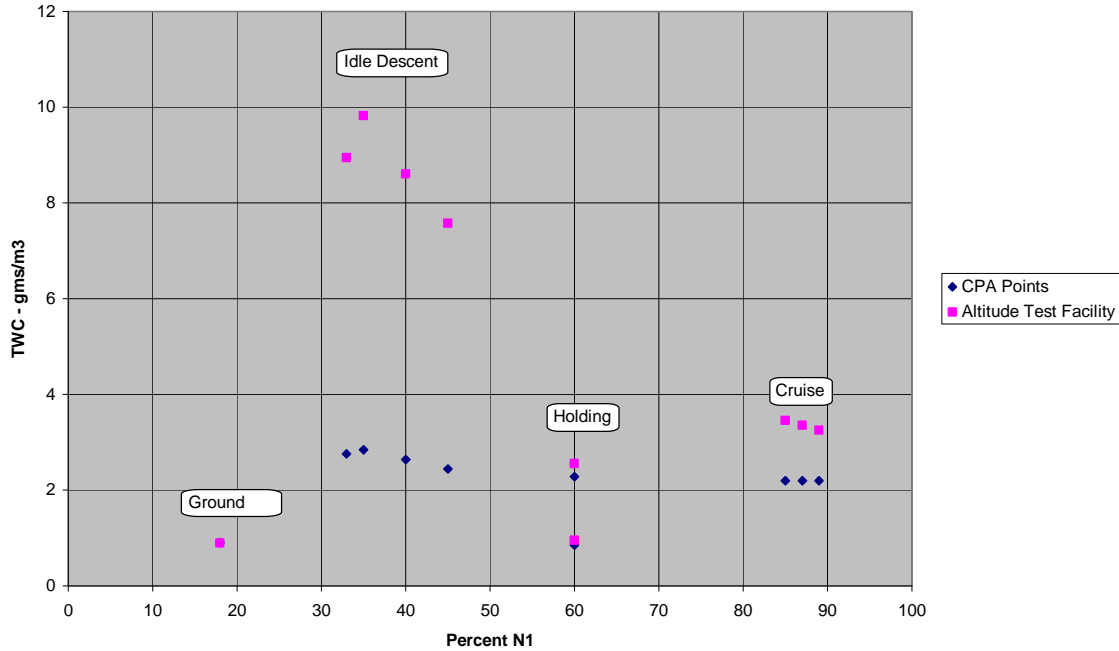


Figure 31. Total Water Content for “Direct Connect” Test Setup

As further illustration of water flow requirements, figure 32 shows the inlet water flow per unit area for CPA conditions compared to the resultant value for a sea level test facility producing an ice crystal cloud ahead of the inlet with a TWC of 25 gm/m³. With a typical “simulated cloud” approach velocity ahead of the engine inlet of 0.1 Mach number (Mn), the TWC of 25 gms/m³ requires 590 lb/hr/ft² of “cloud” frontal area. The lower value within the inlet reflects the greater ability of the engine suction to bring air into the inlet compared with the relatively large ice crystals. Note that icing associated with ice crystals is an issue for the engine core stream and not the fan bypass stream. Hence, the area of ice crystal coverage, whether in a free jet or a direct connect test facility setup, can be limited to the region from which ice crystals are drawn into the engine core.

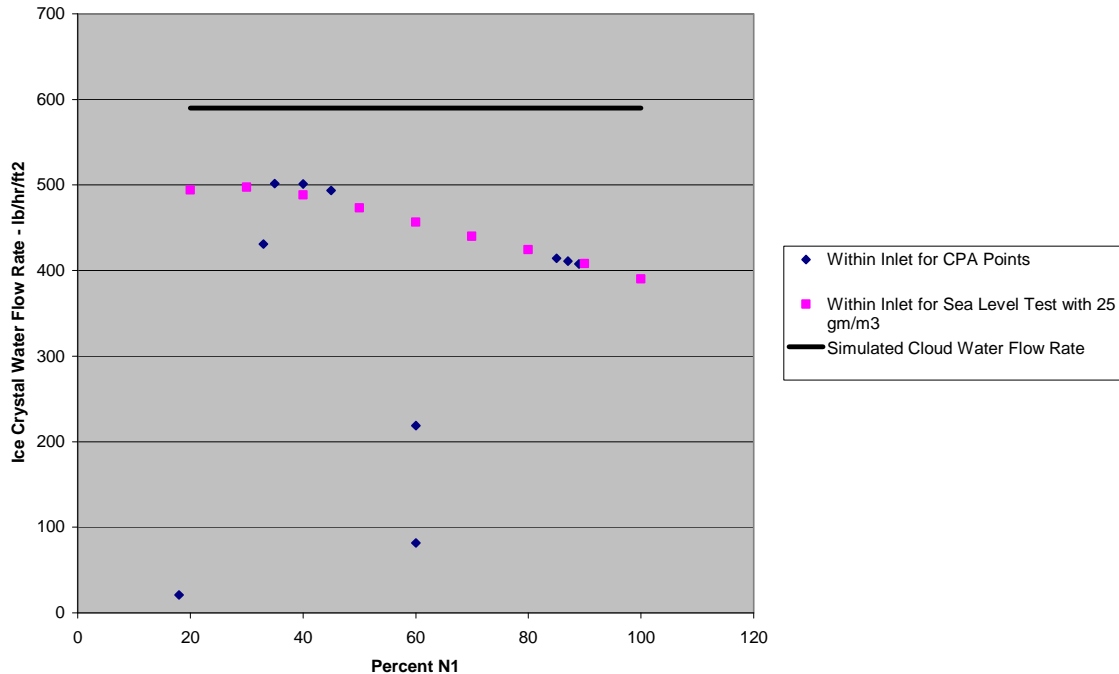


Figure 32. Water Flow Rate Requirements

5.4 COMPENSATION FOR HIGHER APPROACH AIR SPEEDS.

For free jet test arrangements with higher approach air speeds than assumed for the initial study, the required TWC should be reduced by the ratio of the approach Mach number. Since the study was based on an approach of 0.1 Mn (~65 knots = ~75 mph), the required TWC can be determined using the following relation:

$$\text{TWC} = \text{TWC (chart)} \times 75 \text{ mph/Approach Velocity (mph)}$$

6. TECHNICAL DATA AND INFORMATION RELATING TO PROPOSED CHANGES TO 14 CFR 33.77.

6.1 ICE SLAB LEGACY TESTING RESULTS.

Ice slab ingestion testing for compliance with 14 CFR 33.77 is intended to demonstrate engine tolerance to ice ingestion from a delay in nacelle anti-ice activation (nominally 2 minutes) and also to establish limits for ice released from other aircraft surfaces in 14 CFR 25 certification. The dimensions of the slab are related to engine size (defined by inlet hilite area), as depicted by the following charts. Figure 33 displays the slab thickness, and figure 34 provides the cross-sectional dimensions (slab length for a fixed width of 12 inches). Figure 33 is based on some historical compliance values, as well as calculated values, based upon scaled ice mass per unit area of the inlet. The inflection in the curve for the latter relation is due to the conscious decision to limit the ice slab thickness to 0.5 inch as a maximum potential ice accretion thickness for the two minute delay at critical icing conditions with 14 CFR 25 Appendix C and proposed Appendix X (Supercooled Large Drops).

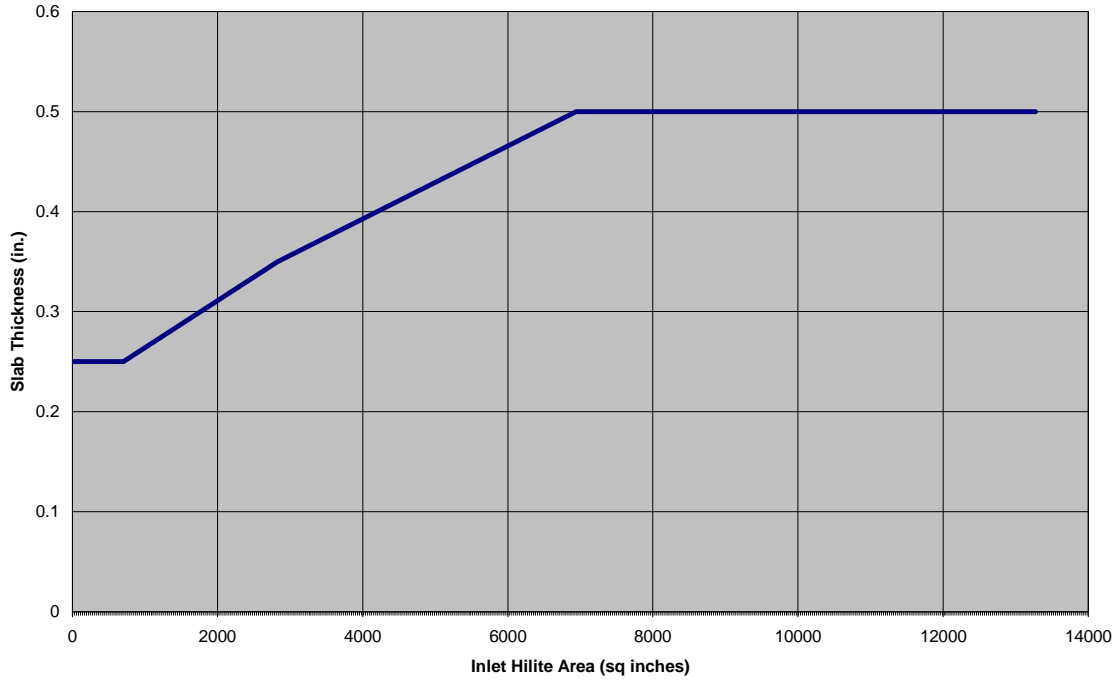


Figure 33. Slab Thickness for Range of Engine Inlet Size

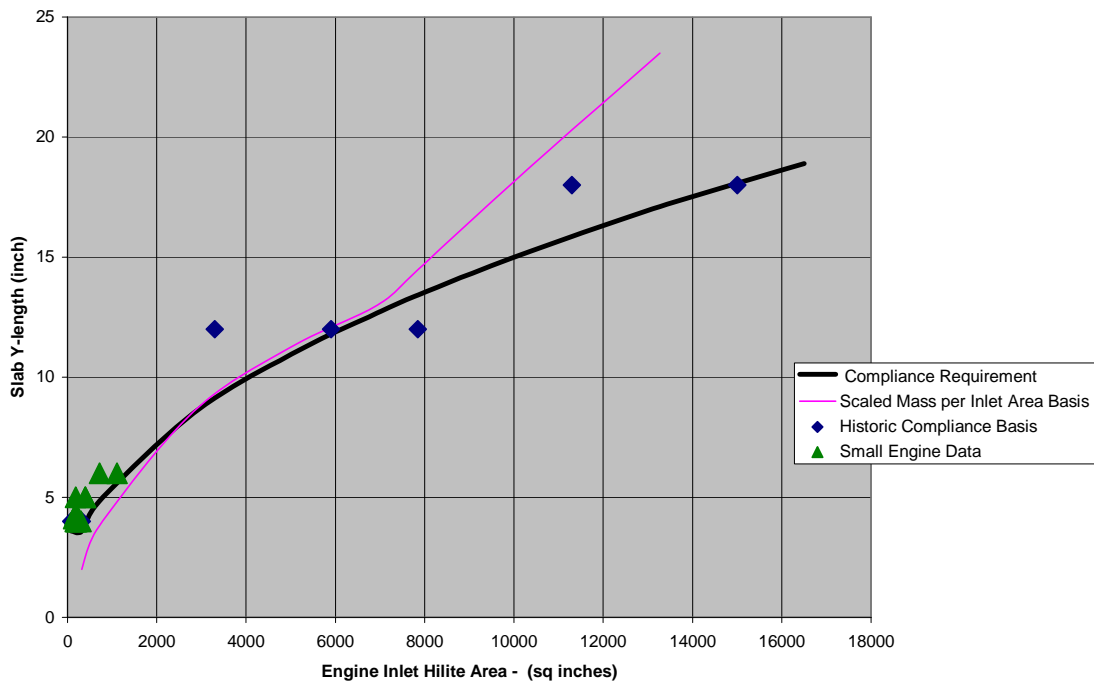


Figure 34. Slab Length With Historic Engine Data

Execution of the ice slab ingestion test typically involves targeting the slab to the air stream ahead of the fan at the outer diameter of the inlet duct. This is intended to simulate the ice release from the inlet and results in impact on the outer diameter of the fan.

6.2 ICE IMPACT KINETIC ENERGY.

The kinetic energy of ice impacting on a fan blade is key to the concept of using equivalent soft-body damage analysis as a means of complying with 14 CFR 33.77. Such an analysis must be validated by engine and/or component testing and should contain sufficient elements to show compliance, including:

- full fan blade model using latest techniques such as finite element analysis
- blade material properties for yield and/or failure, as appropriate
- dynamic/time variant capability
- thrust variance prediction, if required, to account for blade damage
- appropriate engine and/or component testing with impact in outer 1/3 span location to anchor results

The analysis of the ice slab impact on the fan must properly account for critical controlling parameters.

- Relative kinetic energy normal to the leading edge chord
- Incidence angle—relative slab speed and blade speed
- Slab dimensions and slab orientation

The following figures describe the contribution of these parameters in establishing the threat to the fan blade. Figure 35 illustrates the normal component of kinetic energy that leads to airfoil deformation. Figure 36 shows how the ice slab orientation can alter the distribution of the load of impact over varying number of airfoils, thereby potentially lessening the effect on any single airfoil.

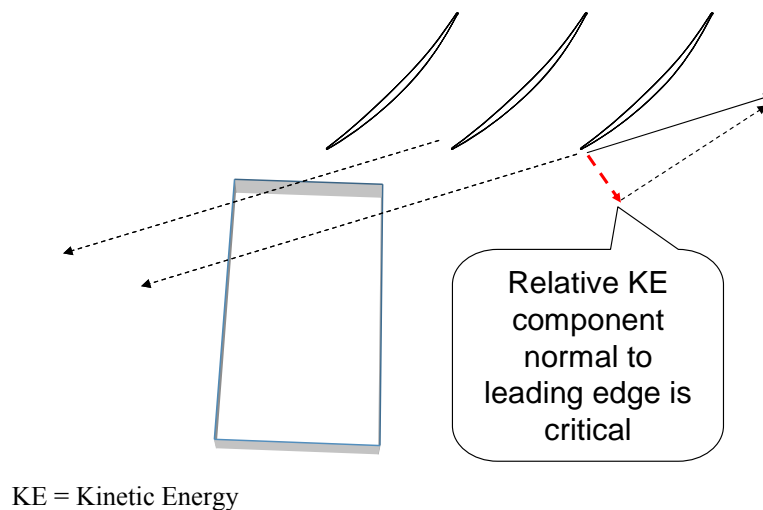


Figure 35. Normal Component of Kinetic Energy of Ice Slab

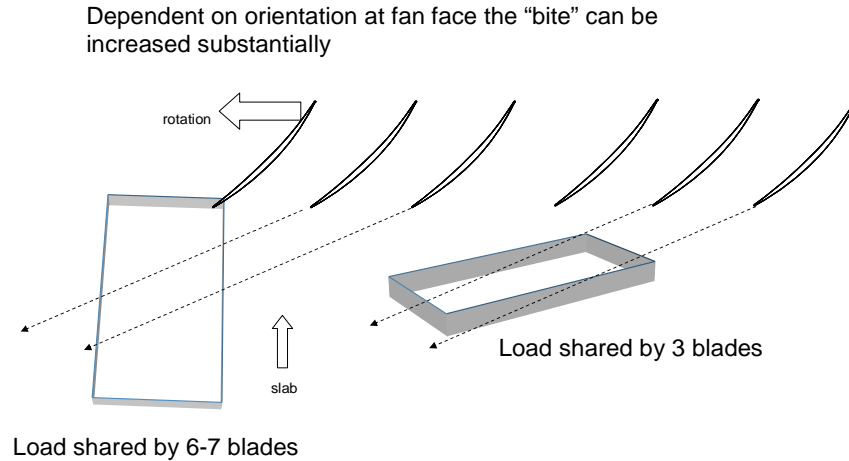


Figure 36. Ice Slab Orientation Effects

The relative kinetic energy of the ice slab depends upon the engine rotor speed and the velocity of the ice slab, which is influenced by its drag coefficient and frontal area, as well as the air stream velocity and density at the corresponding ice slab test point. An analysis of the ice slab acceleration by the air stream is included in section 7. In addition to setting the ice slab velocity, the acceleration of the air stream may also result in the ice slab breaking up into smaller segments prior to impacting the fan.

6.3 ICE SLAB BREAKUP.

Ice slab breakup can occur in the 14 CFR 33.77 certification test as the slab is accelerated when it enters the inlet air stream. In some instances, this may necessitate retesting of the engine to show compliance. The rationale for retesting is that ice slab breakup due to air loads is not predictable and should not be allowed when showing compliance. However, manufacturers' experience with ice slab breakage during 14 CFR 33.77 engine tests is included here for documentation purposes. Data included in figure 37 was derived from testing of both small and large transport engines. For this data, the largest ice piece is typically 1/3 to 1/2 the original size of the ice slab.

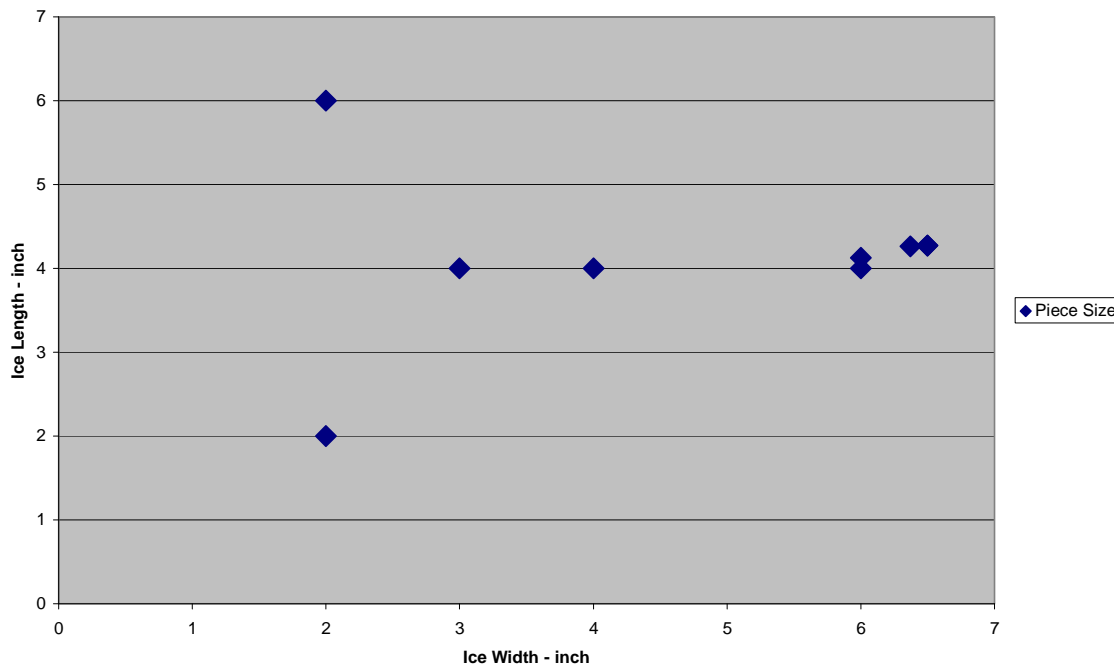


Figure 37. Available Data on Ice Slab Breakup

7. TECHNICAL DATA AND INFORMATION RELATING TO 14 CFR 25.1093.

7.1 EQUIVALENCE OF AIRCRAFT-SOURCED ICE TO 14 CFR 33.77 ICE SLAB.

The equivalence of an aircraft-sourced ice slab certified under 14 CFR 25.1093 to the ice slab used in the 14 CFR 33.77 certification test has historically been based on the physical size of the two slabs. More recently, there has been interest in developing an equivalence comparison on the basis of the relative kinetic energy of ice from the aircraft compared to that of the 14 CFR Part 33.77 ice slab. In support of discussion within the EHWG, a Microsoft[®] Excel[®] spreadsheet was prepared by The Boeing Company to calculate the energy of an ice slab. A sample of the input/output is shown below in figure 38. Key variables influencing the kinetic energy are the ice slab size, orientation and its velocity when it strikes the fan blade. The critical orientation would need to be established in conjunction with the particular engine manufacturer. The ice slab size and velocity is dependent upon its size after release from the aircraft and the trajectory after release. For this sample calculation, an orientation was chosen that imparts 80% of the maximum energy.

2005-1-20 Joe DiRusso This program is used to determine the component of kinetic energy normal to the pressure surface for the ice slab ingestion test and runback ice.
 Cells in Green require input fields

Engine Characteristics

		Comments
Fan Diameter	2.85	meters
Blade Angle	28	Degrees, includes blade twist at take-off thrust
Max Take-off N1	2400	RPM
Number of Blades	20	
Blade to Blade Spacing	14.98	

Ice Slab Ingestion Test Assumptions

Axial Velocity of Ice	50	meters per second
Impact Location (% chord)	85	70 % or greater will be targeted during ice slab ingestion test
Slab Orientation		
	Axial	0.5 inches
	Tangential	9 inches
	Radial	12 inches
Density of ice	920	kg/m ³

Ice Slab Ingestion Results

Unit	Symbol	Value		Comments
		e1 direction	e2 direction	
radius of impact location	r	1.211		meters
Fan Speed (Radians/second)	wf	251.200		radians/second
Blade Velocity	Vb	304.266	0.000	meters/second
vector normal to pressure surface	n	0.469	0.883	unit vector
Relative velocity Vector	Vr	304.266	50.000	meters/second
Speed Normal to Pressure Surface	Vn	98.624		Magnitude in meters per second, direction is parallel to unit vector n
Time between blade spacing	t_blade_passing	0.00125		seconds
Axial Length of Ice per Blade	L_impact	0.01270		meters
mass of ice ingested per fan blade	m_impact	0.81411		kg
Normal Component of Kinetic Energy	KE	3959.334431		Joules

Runback Ice Assumptions

Axial Velocity of Ice	21	meters per second
Impact Location (% chord)	100	70 % or greater will be targeted during ice slab ingestion test
Slab Orientation		
	Axial	1 inches
	Tangential	17.5 inches
	Radial	0.4 inches
Density of ice	920	kg/m ³

Runback Ice Results

Unit	Symbol	Value		Comments
		e1 direction	e2 direction	
radius of impact location	r	1.425		meters
Fan Speed (Radians/second)	wf	251.200		radians/second
Blade Velocity	Vb	357.960	0.000	meters/second
vector normal to pressure surface	n	0.469	0.883	unit vector
Relative velocity Vector	Vr	357.960	21.000	meters/second
Speed Normal to Pressure Surface	Vn	149.429		Magnitude in meters per second, direction is parallel to unit vector n
Time between blade spacing	t_blade_passing	0.00125		seconds
Axial Length of Ice per Blade	L_impact	0.02540		meters
mass of ice ingested per fan blade	m_impact	0.10553		kg
Normal Component of Kinetic Energy	KE	1178.227289		Joules

Figure 38. Sample of Ice Slab Kinetic Energy Analysis Worksheet

7.2 AIRFRAME ICE TRAJECTORY ACCELERATION.

This section compares the acceleration of an ice slab released from a pitot style inlet into a turbofan engine during a 14 CFR Part 33.77 sea level certification test to an ice slab released from an aircraft surface in flight that subsequently enters the engine inlet. The masses and velocities of the ice slabs in these two situations, together with the engine’s fan wheel speed, can be used for comparison of the relative levels of kinetic energy impacting the fan.

7.2.1 Calculation Procedure.

The calculation procedure uses a small time interval (~0.005 sec) stepping procedure to determine the drag of surrounding airflow on the ice slab and the resultant acceleration. The drag force is simply a product of a Reynolds number dependent drag coefficient (*Cd*), the relative velocity-based dynamic pressure ($q = 1/2 \rho V^2$), and the slab frontal area (*A*) relative to the airflow.

$$Drag = C_d * q * A$$

The heart of the calculation is the drag coefficient. Published data for several idealized ice slab shapes (rectangles, discs, caps, and doughnuts) are provided herein and show comparable levels of drag coefficient for the Reynolds number range of interest. The ice slab tends to tumble as it migrates from the release point to the fan. Hence, the variation of drag coefficient with slab angle relative to the airflow is provided and integrated to find a suitable average value. The calculation is also done over a range of drag coefficient to demonstrate the sensitivity to any uncertainty in its value.

This procedure is applied from the ice release location until the ice slab reaches the engine fan leading edge. At that point, the component of the ice slab velocity normal to the fan leading edge and its mass, coupled with the local fan wheel speed and the ice slab orientation, establish the impact energy. For the purpose of this study, there is no attempt to define the effect of slab orientation or fan wheel speed and slab orientation combination. That task requires knowledge of the specific fan geometry and the inlet design. Rather, the focus is on the determination of the ice slab velocity for comparison of the aircraft ice with the 14 CFR 33.77 ice slab. A simple mass-based kinetic energy level is provided using the ice slab normal velocity component and the fan tip wheel speed without regard for the ice slab orientation, but these values are just for illustrative purposes.

7.2.2 Drag Coefficients of Various Slab Shapes.

Hoerner [19] reports the similar values of drag coefficients at a Reynolds number greater than 1000 for square plates and disks. Figure 39 reproduces Figure 25 from Hoerner. The typical ice slab Reynolds number is in excess of 10,000. Additional details on the Reynolds number for the range of ice slab sizes can be found in section 7.3.

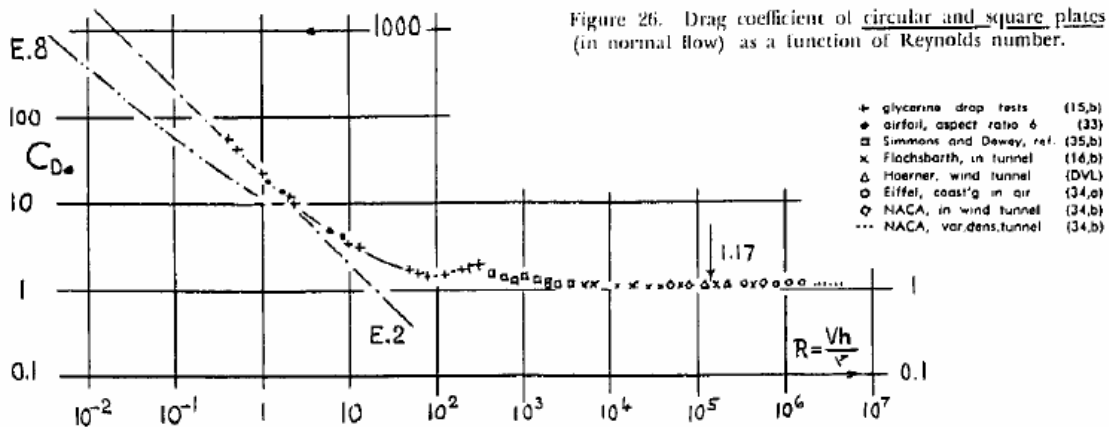


Figure 39. Drag Coefficient vs Reynolds Number

Since the 14 CFR 33.77 ice slab is typically a rectangle, it is useful to display the effect of the aspect ratio of the slab as shown in figure 40. As defined by Hoerner, the h/b ratio designates the slab width over its length. Most slabs have one dimension of 12 inches with the other dimension varying from 3 inches to 18 inches. Over this range of interest, figure 40 shows the same level of drag coefficient as a square ($h/b = 1$).

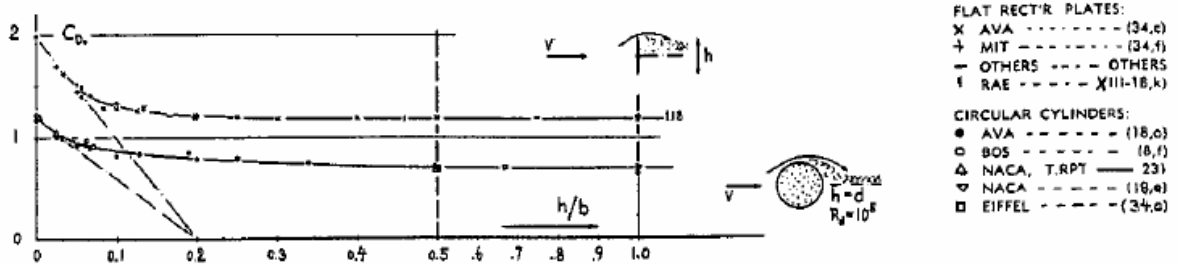


Figure 40. Drag Coefficient for Rectangles

Other shapes reported by Hoerner include annular rings (doughnuts) that show similar values for drag coefficient for a broad range of inner to outer diameter ratio, as shown in figure 41.

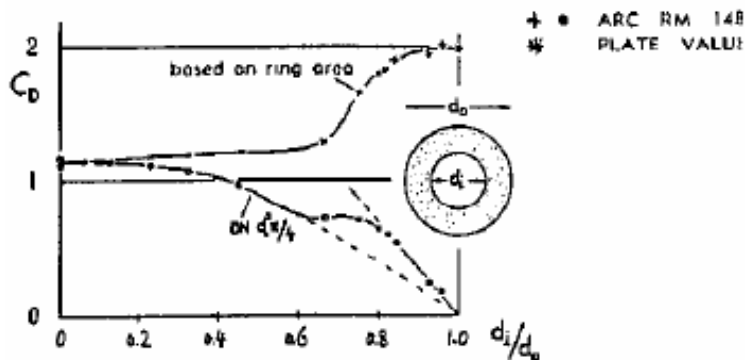


Figure 41. Drag Coefficient at Reynolds Number = 10^5 for Annular Rings

Finally, figure 42 shows data from Hoerner for caps, which may be a shape typical of ice from aircraft radomes. As noted in the figure, the drag coefficient levels are very similar to the other shapes, typically ranging from the same to no more than 20% higher in value. As shown in later results, use of lower values when comparing the impact energy of aircraft ice to the 14 CFR 33.77 ice slab is more conservative. (Higher drag coefficients tend to reduce the impact energy of airframe ice relative to the 14 CFR 33.77 ice slab due to the longer travel distance from the ice release point to the engine's fan.) Hence, the higher level of the cap shapes would be favorable in the aircraft environment.

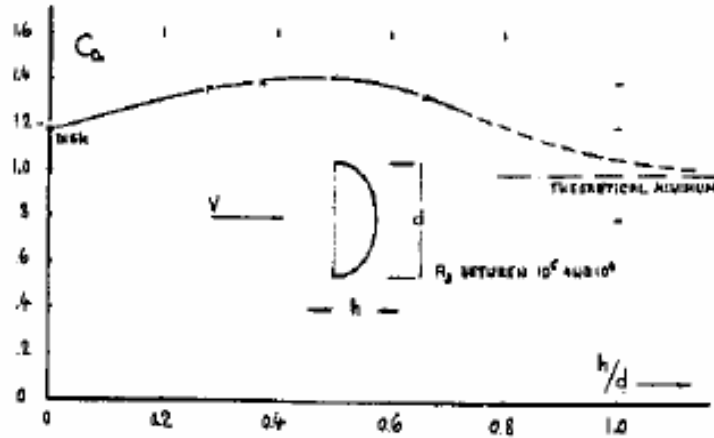


Figure 42. Drag Coefficient for Caps of Various Height Ratio

7.2.3 Effect of Ice Slab Tumbling.

As noted earlier, the ice slab tends to tumble as it is accelerated by the airflow after its release. Figure 43 shows the values of the normal force coefficient (C_{normal}) for these square plates and disks over a range of ice slab angle (α) relative to the airflow. Hoerner defined the normal force coefficient as the observed drag force normal to the plate divided by the plate planform area times the square of the air velocity. He then defined the drag coefficient from the component of the normal force aligned with the flow direction as indicated by the equation included in figure 43.

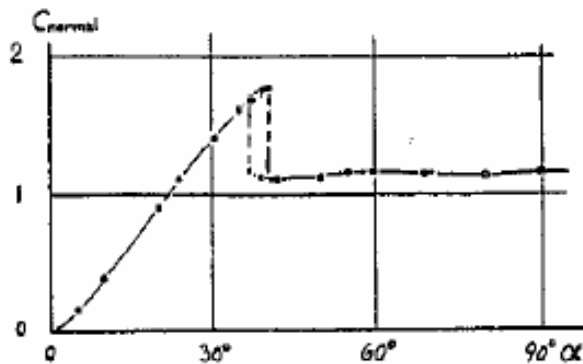
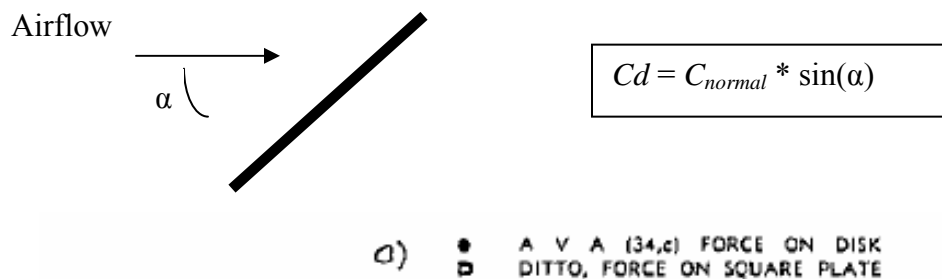


Figure 43. Normal Force Coefficient at Varying Approach Angles

For the purpose of this example, figure 43 was integrated to find the average drag coefficient value of 0.74 (assuming the slab spends same amount of time at each orientation), which will be used as the nominal value for comparison of the 14 CFR 33.77 ice slab test to ice released from the radome of an aircraft in flight.

7.2.4 Comparison of Calculation Results.

To illustrate the process, results are provided for a sea level 14 CFR 33.77 ice slab (12" x 18" x 1/2" thick) test compared to a slab of the same size assumed to be released from a large commercial transport (LCT) radome. In reality, the radome ice shape would be defined by the radome and have a nonuniform ice thickness. For the purpose of the current analysis, this equivalent ice slab to the 14 CFR 33.77 test provides some insight into the currently accepted practice of simply comparing the airframe ice size (ice volume) to determine if fan damage from aircraft-sourced ice is no worse than that from the 14 CFR 33.77 ice slab. Once the ice reaches the engine's fan, however, the details, such as maximum ice thickness and the thickness distribution, would be important for evaluating the fan's tolerance to ice impact. The sea level test results are for the engine operating at 100% N1, while the flight condition is at 95% N1 for this example. Aircraft flight speed is 440 ft/sec, while inlet airflow velocity is in excess of 650 ft/sec for both the sea level test and the aircraft situation. The ice slab in the sea level test is released 8 ft in front of the engine fan leading edge plane, while the radome ice is released 83 ft forward of the same plane.

7.2.4.1 Ice Slab Breakage.

Ice slab breakage has sometimes occurred as the slab is subjected to acceleration loads upon release during a 14 CFR 33.77 test. Likewise, an ice slab released from the aircraft is subject to deceleration loads upon initial release and also upon entry into the inlet if the inlet flow velocity differs significantly from the aircraft flight velocity. Ice slab breakage during the 14 CFR 33.77 test is often grounds for repeating the test without observed breakage to maximize the threat to the engine for certification purposes. However, the FAA does not currently allow consideration of ice breakage after its initial release from the aircraft. Consequently, ice slab breakage is not considered in this study.

7.2.4.2 Comparison of Ice Velocity and Acceleration Loads.

Figure 44 shows the ice slab velocity history for the two examples. In the case of the 14 CFR 33.77 ice slab test, the ice is initially at rest and is accelerated by the air stream entering the engine. Ice released from the airframe is initially at the flight speed and is dragged down in velocity by ambient air until it reaches the inlet, after which it is influenced by the air stream into the engine. The figures depict movement of the ice slabs from right to left; the engine fan leading edge plane establishes the "zero" location.

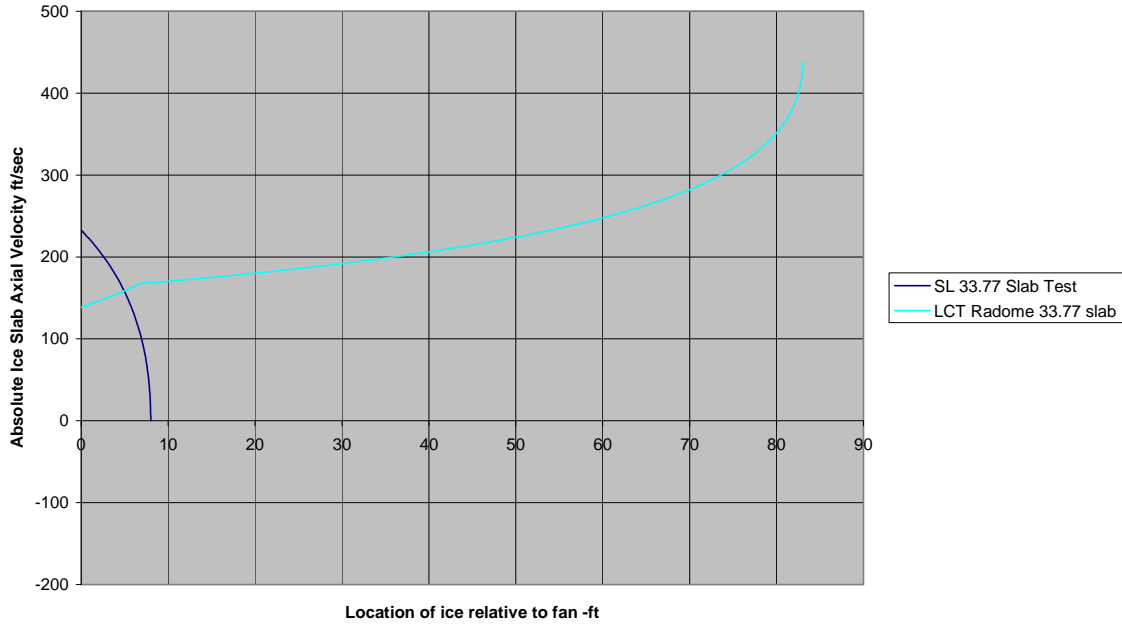


Figure 44. Ice Slab Velocity Comparison at 11,750 Feet and 0.41 Mn

Figure 45 shows the predicted acceleration (deceleration in the case of the aircraft) loads (i.e., ice mass times acceleration) for the sample calculations. In this particular case, the maximum acceleration load for the 14 CFR 33.77 test is at a higher absolute level than the example large commercial transport radome ice release. Note also that the aircraft ice release case involves two “peaks” in the deceleration, the first when released and a second when it enters the engine inlet.

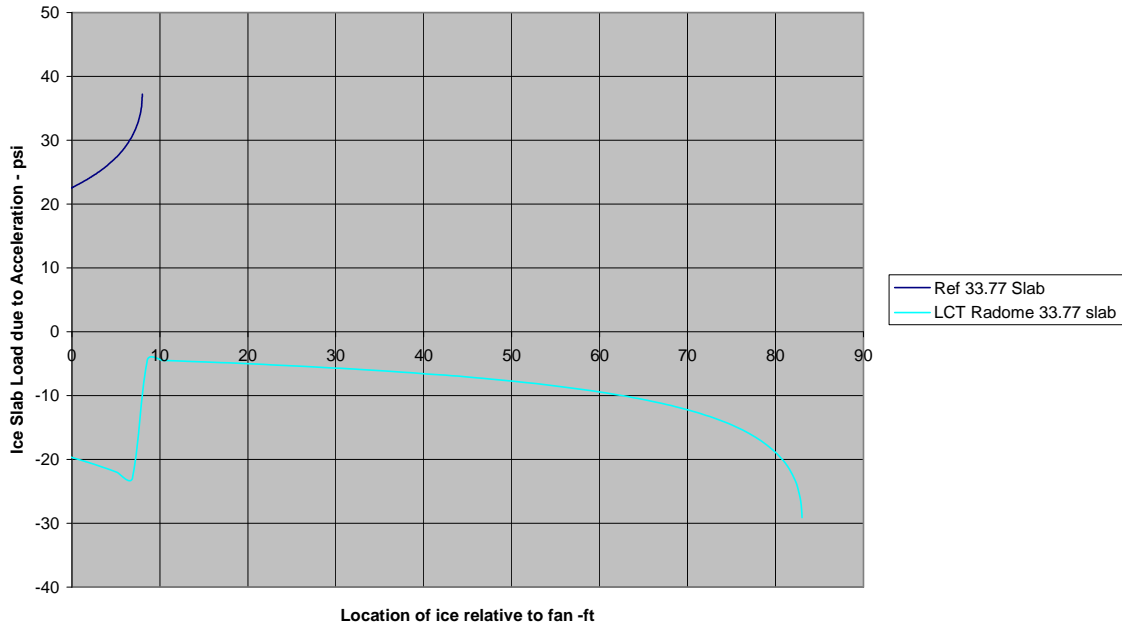


Figure 45. Ice Slab Acceleration Load at 11,750 Feet and 0.41 Mn

7.2.4.3 Comparison of Ice Slab Velocity and Impact Energy.

The next two illustrations show results for the 14 CFR 33.77 test slab and the equivalent 14 CFR 33.77 ice slab released from the aircraft in flight. Figure 46 shows the comparison of the velocity of the ice slabs relative to the engine. In the case of the 14 CFR 33.77 test, the ice slab velocity is initially zero and is accelerated to 230 ft/sec by the airflow in the engine inlet. While the aircraft ice slab is moving initially at flight speed of 440 ft/sec, it is at zero velocity relative to the engine. The 14 CFR 33.77 equivalent slab released from the large commercial transport radome arrives at the fan at a relative velocity of 300 ft/sec.

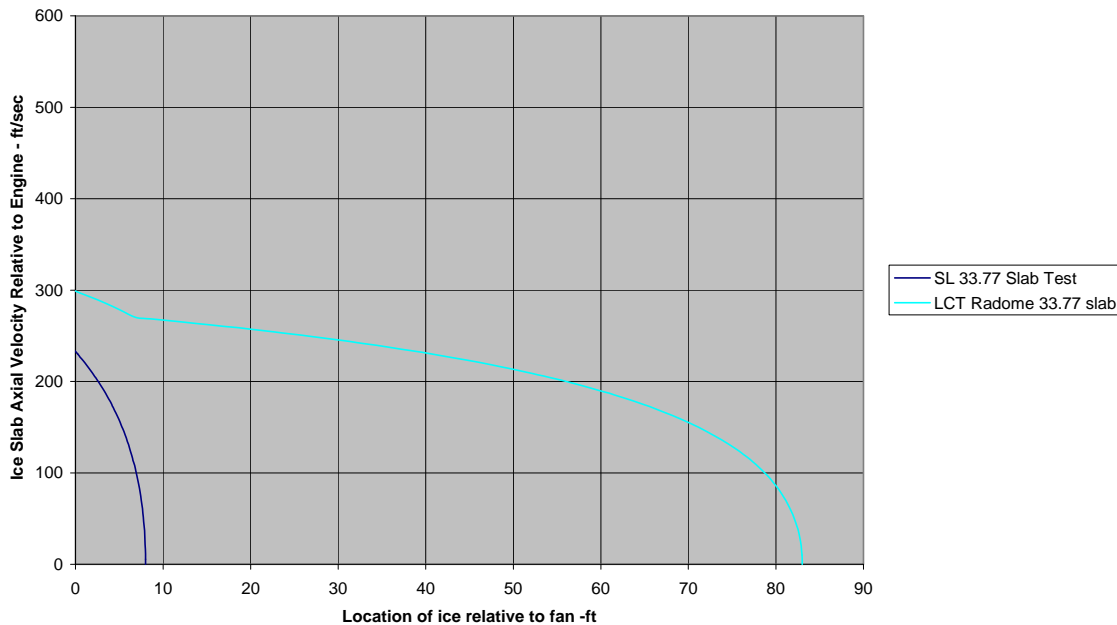


Figure 46. Ice Slab Velocity Relative to Engine at 11,750 Feet and 0.41 Mn

Although the consequence of ice impact on the fan must reflect individual fan physical properties and the ice orientation and thickness distribution, it is still useful to compare the relative levels of a simple ice mass-based kinetic energy for impact at the fan tip, as shown in figure 47. In this example, the fan leading-edge chord angle is 65 degrees from the axial flow direction. For each case, the combination of fan wheel speed and ice slab velocity determines the approach angle and velocity relative to the fan blade. From these values, the velocity component normal to the fan leading edge can be defined for the two cases to be 295 ft/sec for the sea level test and 206 ft/sec for the airframe ice release. This results in the large commercial transport radome ice slab having a lower level of kinetic energy. The 14 CFR 33.77 ice slab released from the radome in flight is shown to have 52% of the kinetic energy of the slab in the 14 CFR 33.77 sea level test. Again, for a typical pitot style inlet configuration, this result may lend support to the current practice of using equivalent ice slab size for judging the acceptability of airframe ice threats.

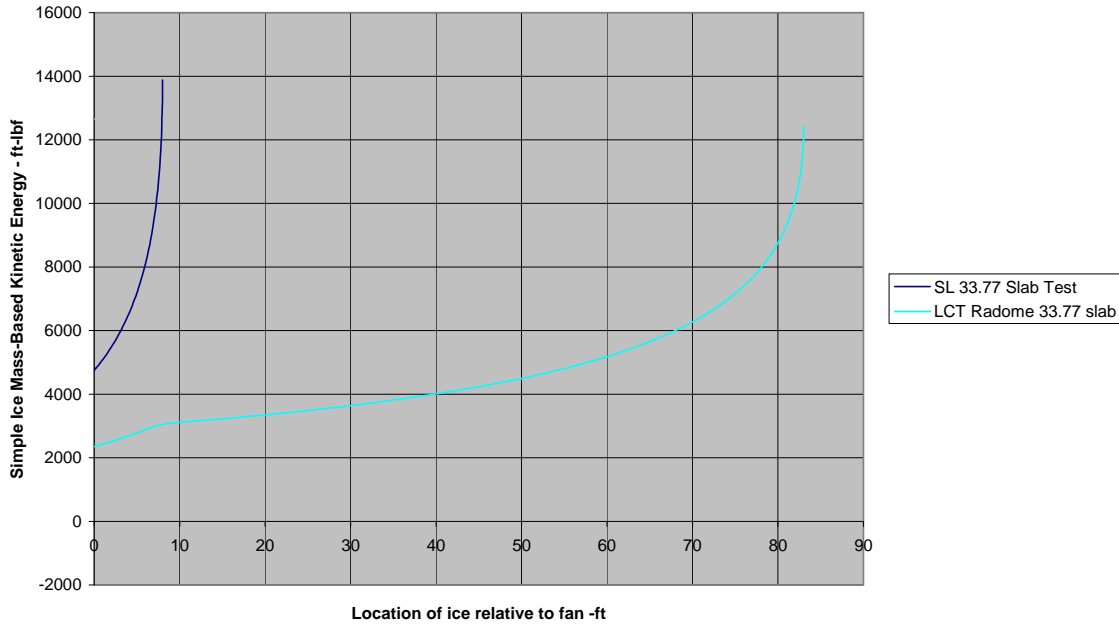


Figure 47. Comparison of Simple Ice Mass-Based Impact Kinetic Energy at 11,750 Feet and 0.41 Mn

7.2.4.4 Sensitivity to Drag Coefficient Uncertainty and Fan Rotor Speed.

It is useful to repeat the calculations for a range of drag coefficients C_d to determine the sensitivity of the results to the assumed level of C_d . Figure 48 indicates that the general conclusions reached regarding the relative levels of kinetic energy at impact are not altered for a realistic range of uncertainty in drag coefficient (0.2 to 1.0), provided it is justified to use the same drag assumptions for the inlet test and for slabs from the airframe. The question of whether this is justified is addressed in section 7.3.

Finally, a fan wheel-speed level of 1200 ft/sec was used for this study, but the conclusions do not change for a representative range of fan wheel speed, as shown in figure 49.

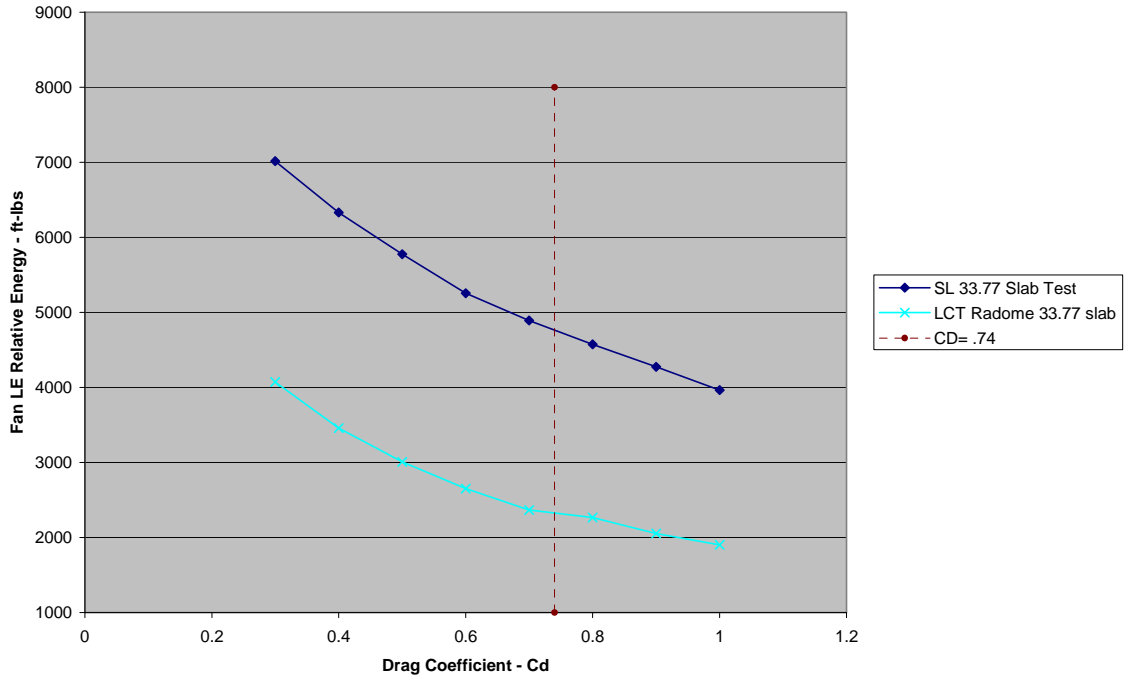


Figure 48. Sensitivity of Kinetic Energy Comparison to Drag Coefficient

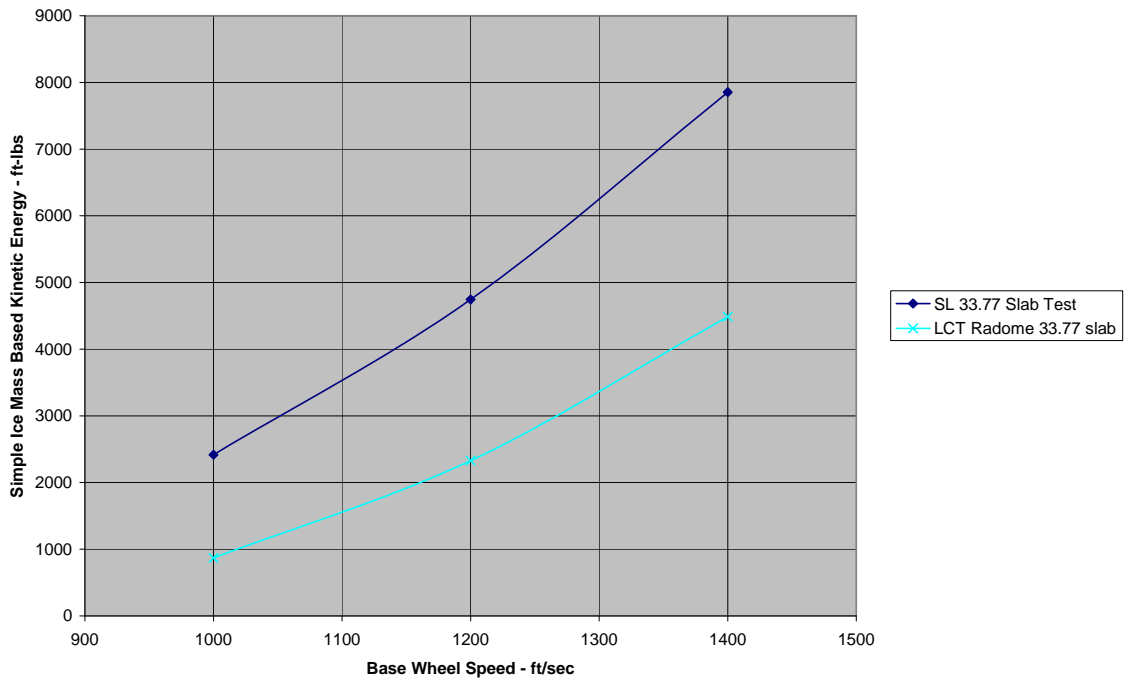


Figure 49. Influence of Fan Wheel Speed on Ice Slab Energy

7.3 ICE SLAB REYNOLDS NUMBER.

The analysis described in the last section relied on the ice slab Reynolds number being large enough to simplify the determination of drag coefficient. This section reviews the probable range of Reynolds number for different engine sizes and flight regimes. Slab Reynolds number is dependent upon the ice slab dimensions, the relative velocity between the airflow, and the slab and local values of air density and viscosity. The proposed 14 CFR 33.77 includes definition of the ice slab dimensions as a function of the inlet hilite area. The ice slab dimension used to calculate the Reynolds number is the square root of the average cross-sectional area that is exposed to the airflow. For a tumbling slab, this would be the average of length by width, length by thickness and width by thickness. Table 5 displays the proposed 14 CFR 33.77 dimensions and the calculated average for determining Reynolds number.

Table 5. The Proposed 14 CFR 33.77 Ice Slab Dimension Requirements

Inlet Hilite Area (square inch)	Thickness (inch)	Width (inch)	Length (inch)	Length by Width (square inch)	Length by Thickness (square inch)	Width by Thickness (square inch)	Average Area (square inch)	Average Length (inch)
0	0.25	0	3.6	-	-	-	-	-
80	0.25	6	3.6	21.6	0.9	1.5	13.87005	3.724252
300	0.25	12	3.6	43.2	0.9	3	27.7401	5.266887
700	0.25	12	4.8	57.6	1.2	3	36.9868	6.081678
2800	0.35	12	8.5	102	2.975	4.2	65.49746	8.09305
5000	0.43	12	11	132	4.73	5.16	84.76142	9.206597
7000	0.5	12	12.7	152.4	6.35	6	97.86092	9.892468
7900	0.5	12	13.4	160.8	6.7	6	103.2548	10.16144
9500	0.5	12	14.6	175.2	7.3	6	112.5015	10.60667
11300	0.5	12	15.9	190.8	7.95	6	112.5188	11.06882
13300	0.5	12	17.1	205.2	8.55	6	131.7655	11.47891
16500	0.5	12	18.9	226.8	9.45	6	145.6355	12.06795
20000	0.5	12	20	240	10	6	154.1117	12.41417

The relative velocity changes as the ice slab moves from the release site to the fan. Hence, the Reynolds number varies, as shown in figure 50. The values shown range from 25,000 to 132,000. Note that this example was for a large turbofan with an inlet hilite area near the highest value shown in the table. For the smallest engine inlet hilite size, the average dimension for defining the Reynolds number is approximately 32% of the value in the example. Hence, the Reynolds number would be similarly reduced. The Reynolds number for this other end of the inlet size spectrum would be from 7,900 to 42,000. Hence the drag coefficients would be appropriate for the engine sizes covered by the proposed changes to 14 CFR 33.77 (see appendix A).

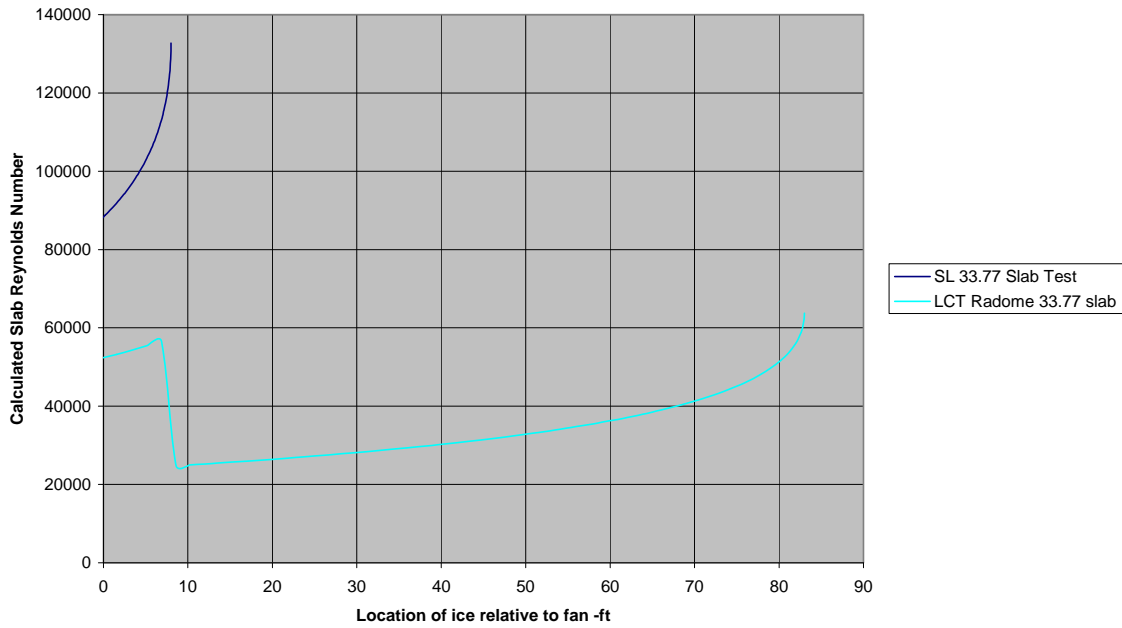


Figure 50. Ice Slab Reynolds Number for the Example Calculation at 11,750 Feet and 0.41 Mn

To be thorough in the assessment of Reynolds number range, other flight conditions can be reviewed using the initial release level of Reynolds number. Table 6 considers the 14 CFR 33.77 test at sea level, at 11,750 ft and 0.41 Mn, and at several other potential flight conditions at higher altitude.

Table 6. Reynolds Numbers for Different Inlet Highlite Areas for Specified Conditions

Altitude - ft	0	Altitude - ft	11750	20000	30000	40000
Inlet Duct Mn	0.65	Flt Mn	0.41	0.6	0.8	0.85
Tamb - deg F	70	Tamb - deg F	14	-12	-48	-69.7
Pamb - psia	14.612	Pamb - psia	9.51573125	6.746	4.283	2.8
At (sonic vel) - ft/sec	1128	At (sonic vel) - ft/sec	1067	1037	995	968
Air Visc (mu) - lb/sec ft	1.22659E-05	Air Visc (mu) - lb/sec ft	1.1216E-05	1.071E-05	9.9865E-06	9.5375E-06
rho air - lb/ft3	0.0745	rho air - lb/ft3	0.0542	0.0407	0.0281	0.0194
Velocity - ft/sec	733.2	Velocity - ft/sec	437.4	622.3	795.7	822.8

inlet hilit area							
(sq inch)							
80	Rey No.	42916	Rey No.	20386	22783	21568	16117
300	Rey No.	60692	Rey No.	28830	32221	30502	22792
700	Rey No.	70081	Rey No.	33290	37205	35221	26318
2800	Rey No.	93259	Rey No.	44300	49510	46869	35023
5000	Rey No.	106091	Rey No.	50395	56322	53318	39841
7000	Rey No.	113994	Rey No.	54149	60518	57290	42810
7900	Rey No.	117094	Rey No.	55621	62163	58847	43974
9500	Rey No.	122225	Rey No.	58059	64887	61426	45900
11300	Rey No.	127550	Rey No.	60588	67714	64102	47900
13300	Rey No.	132276	Rey No.	62833	70223	66477	49675
16500	Rey No.	139063	Rey No.	66057	73827	69889	52224
20000	Rey No.	143053	Rey No.	67952	75945	71894	53722

The Reynolds number for the highest altitude is ~80% of the values in the sample flight condition calculation. Again, the table values are the initial levels at the release point so one should ratio them down using figure 50 to find values along the ice slab trajectory. Hence, the lowest expected value of Reynolds number representing the release of the 14 CFR 33.77 ice slab from the aircraft radome would be 80% of 7900, or 6300. This minimum “worst case” level still remains above the Reynolds number of 1000 that was required to justify the values of the drag coefficients used for this study.

Therefore, the variation in Reynolds number does not appreciably affect drag coefficient, justifying the use of the same drag coefficient for the entire calculation.

7.4 SUMMARY.

A study was undertaken to assess the potential for comparing the kinetic energy of the 14 CFR 33.77 sea level test ice slab to aircraft ice slabs released in flight for the purpose of 14 CFR 25.1093 compliance. It was determined from a review of available data on drag for several representative ice slab shapes that drag coefficients are similar for a broad range of Reynolds number. For the purpose of comparing the sea level test and radome ice released in flight, an integrated average drag coefficient for a full rotation of a tumbling ice slab ($Cd = 0.74$) was selected based upon the published drag data. The results supported the current practice of using equivalent ice slab size for judging the acceptability of airframe ice threats. Moreover, it was shown that the conclusions regarding the relative level of ice impact kinetic energy are not very sensitive to the assumed drag coefficient value over a realistic range. Finally, a review of the full range of Reynolds number for the ice slabs defined in the proposed 14 CFR 33.77 showed them to be consistent with the results of this study.

8. TECHNICAL DATA AND INFORMATION RELATING TO PROPOSED CHANGES TO AC 20-147.

8.1 INLET SCOOP FACTOR.

Proposed AC 20-147 provides guidance for the execution of engine ice tests in a manner that corrects for differences between the respective icing environments of the test cell and critical flight conditions. One element of the corrections deals with the change in LWC due to the inlet “scoop factor” effect caused by any mismatch between flight speed and inlet air velocity. This section discusses available background information on the scoop factor phenomenon.

8.1.1 Inlet Scoop Effects.

At certain flight conditions, e.g., during descent at low idle, the capture stream tube area, which is far upstream of the engine inlet (or the splitter if the core ingestion is considered), is smaller than the projected area of the inlet (or the splitter). Hail stone and very large rain droplets do not follow the stream lines but rather have ballistic trajectories with the result that the mass ratio of ingested hail or water to the air flow is larger than in the free stream. On the other hand, very small droplets essentially follow the stream lines, thus preserving the water-to-air mass ratio

during ingestion at the free stream values. This phenomenon is called the Scoop Effect and should be taken into account during engine tests.

Clearly, a single scoop factor cannot be defined to cover hail, rain, and icing clouds since their trajectory behaviors are vastly different from one another. Furthermore, large droplets (normally associated with rain storms) will break up due to the local shear when the Weber number (which can be interpreted as the ratio of aerodynamic force to the surface tension force) exceeds a critical value. Supercooled liquid water drops associated with icing clouds are too small to experience further breakup. Further, while it is potentially possible that SLDs associated with freezing rain or drizzle may be subjected to large enough shear forces to promote breakup, the information from the engine database discussed in section 2 indicates this icing threat is primarily associated with a ground operation that is likely to have low shear effects. If there is a condition with significant shear to affect SLDs, however, it then would become necessary to track not only the parent droplets but the post-impact breakup droplets as well. Surface impingement and centrifuging effects also need to be included for downstream stages (see reference 22).

Computer codes for the inlet flow field and droplet trajectories are currently available and widely used in the industry. It is strongly recommended that these tools be employed to establish the correspondence between the engine inclement weather test conditions and the atmospheric flight through the appropriate cloud.

Engine cycle effects should also be included when accounting for the differences between test conditions and those required for adequate demonstration of the icing flight environment.

8.1.2 Test Evaluation of Scoop Factor.

A NACA report [20] details early experimental work done in a wind tunnel having water spray nozzles and a 31-inch-diameter engine inlet model. Results from these tests are severely limited in range, but help illustrate the scoop factor effect. Air speed in the tunnel was held constant at 156 knots (0.236 Mn) for the tests. It was possible to modulate the amount of airflow entering the inlet model independent of the wind tunnel flow level. Thus, the inlet velocity ratio could be varied to simulate different engine power/flight speed combinations. For example, a condition with a low-inlet velocity ratio with inlet spillage of excess air simulates an idle descent flight condition. Conversely, a condition with a high-inlet velocity ratio condition with the inlet “sucking” in more flow than would occur in flight simulates the engine at takeoff. Water droplet diameter was varied by adjusting the air and water pressure of the water nozzles to obtain a median droplet diameter ranging from 11.5 to 19.4 microns. The test values of inlet velocity ratio were limited in range from a minimum of 0.4 to a maximum of 1.8. However, as noted in figure 51, the data for an inlet velocity ratio higher than 1.4 is considered invalid due to the limited size of the simulated cloud in the wind tunnel.

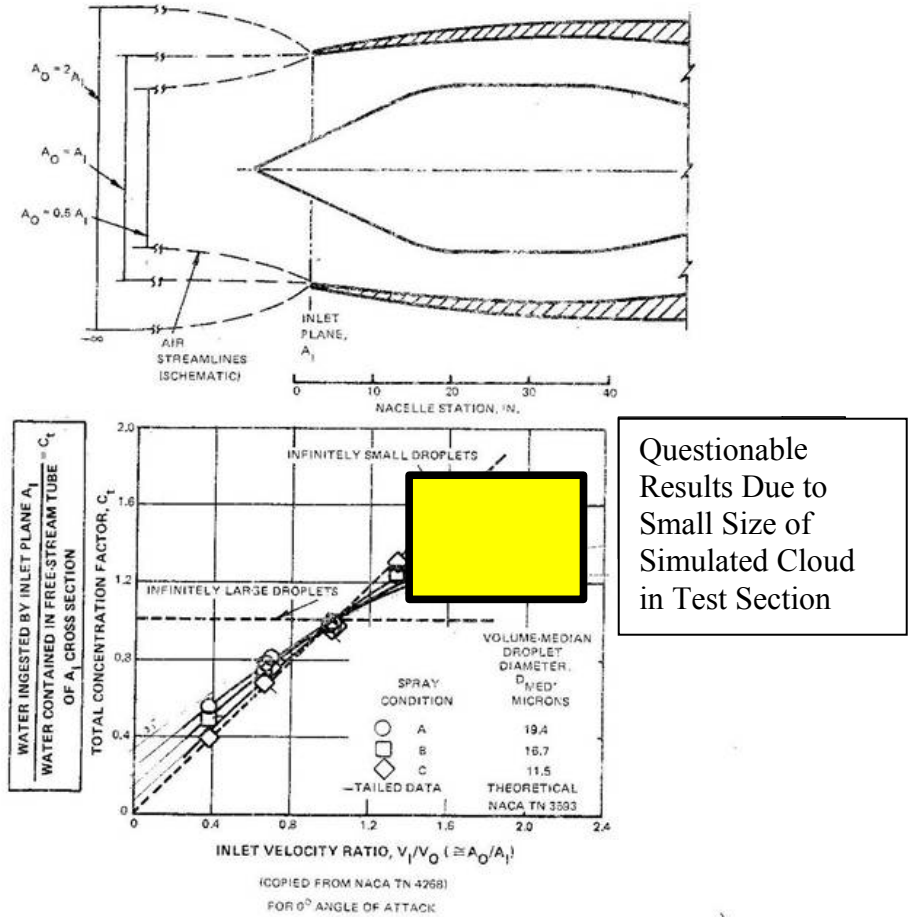


Figure 51. Background Data on Scoop Factor

8.1.3 Required Velocity Ratio Range.

As noted previously, computer codes for the inlet flow field and droplet trajectories are currently available and widely used in the industry. It is possible to use such a code to illustrate the required velocity ratio range for different engine sizes and cycle effects over the expanse of the flight envelope. Such an exhaustive study was beyond the scope of the EHWG activity, but some effort was made for this purpose using a correlating parameter for droplet response to streamline curvature, known as the modified inertia parameter, K_0 . This relationship is documented in an FAA report [21] and is based upon the momentum of droplet, air viscosity, and size scale of object (with correction for Reynolds number). It is intended for correlating the streamline effect of the “bow wave” from an object on deflecting droplets from the object. Herein, it serves to illustrate a qualitatively similar deflection due to streamlines associated with inlet spillage effects.

$$K_0 = (2 \times (d / 2) 2 \times \rho_{H_2O} x) / (9 \times Lc \times \mu)$$

where : d = droplet diameter
 ρ_{H_2O} = density of water

V_0 = droplet approach velocity
 L_c = representative dimension of object (typically diameter)
 μ = air viscosity

Figure 52 displays the limited range of the results of the NACA testing in terms of the modified inertia parameter. The required range of application can be appreciated from an inspection of figure 53. It provides the modified inertia parameter for nominal 20 micron diameter water droplets at a flight condition of 20K ft 0.6 Mn in comparison with a sea level test facility with a simulated headwind of 65 mph (<0.1 Mn). The results are provided for inlet diameters ranging from 1 to 10 ft. The NACA data from reference [20] occupies only a small region, which, as might be expected, is close to the sea level curve.

Before making use of the illustrated difference in modified inertia parameter between sea level and flight conditions, it is necessary to discuss the similar scoop factor effect at the engine's bypass splitter. Engine bypass ratio varies significantly over the flight range and is primarily influenced by engine power level and flight Mach number. The range of modified inertial parameter over the operating range of the engine is displayed for the aforementioned two icing environments in figures 54 and 55. With this information, it is now possible to proceed to calculations of the overall scoop factor for the combination of the inlet and the bypass splitter.

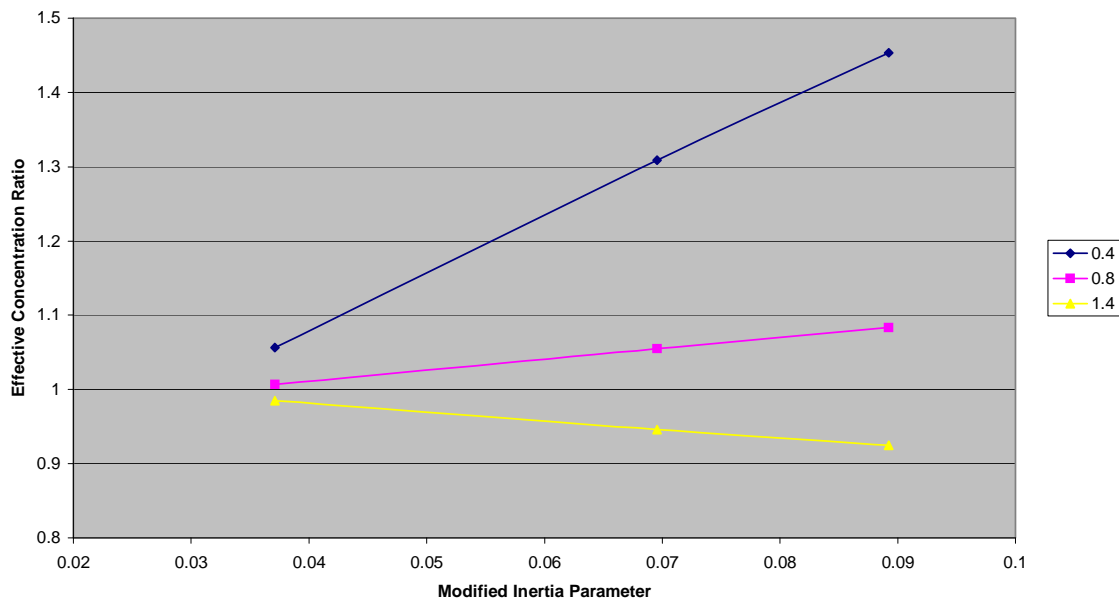


Figure 52. The NACA Test Results in Terms of Modified Inertia Parameter

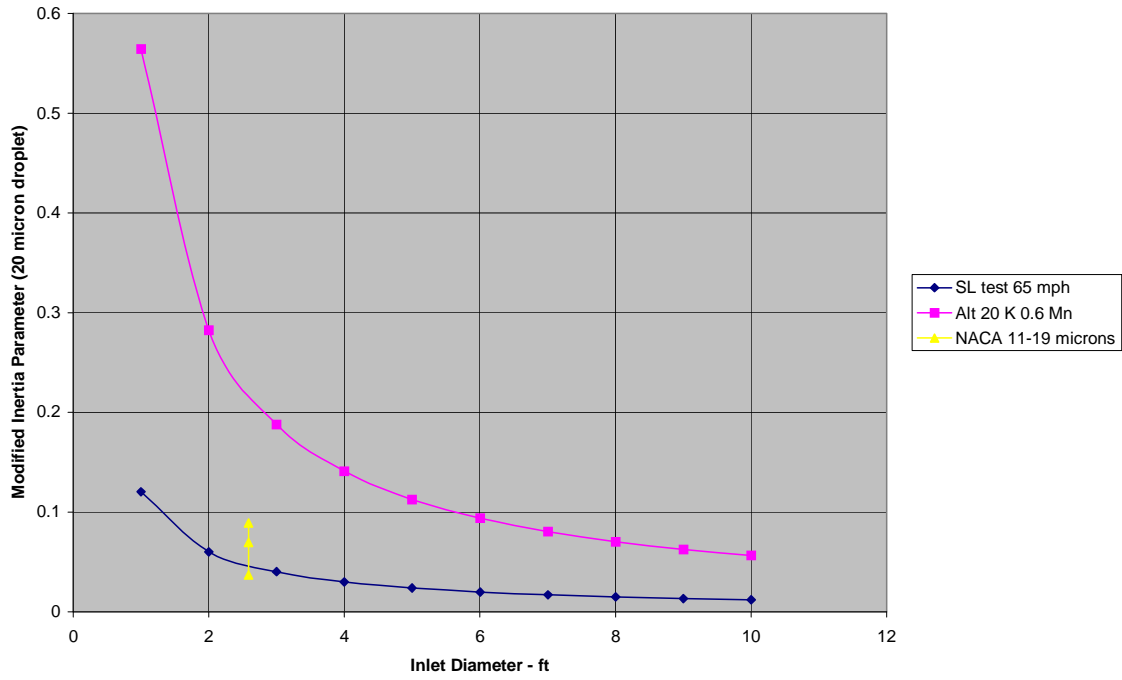


Figure 53. Required Range of Modified Inertia Parameter

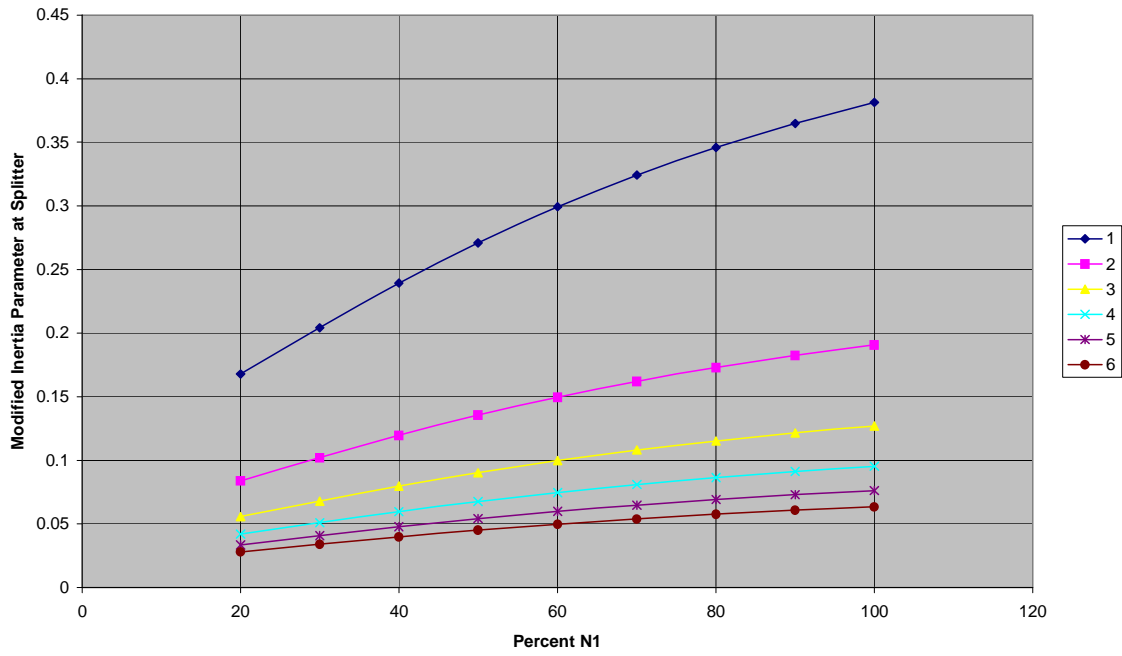


Figure 54. Splitter Modified Inertia Parameter at Sea Level

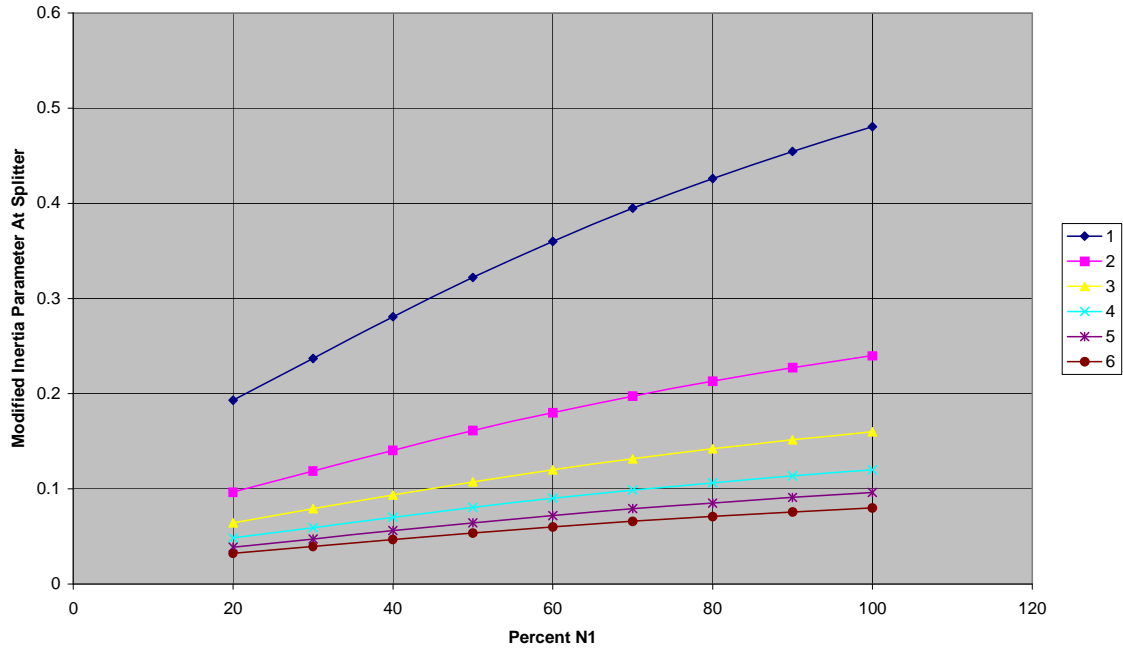


Figure 55. Splitter Modified Inertia Parameter at 20K ft 0.6 Mn

8.1.4 Illustration of Sea Level Test and Flight Scoop Factors.

The following results are intended for illustration and are not meant to replace the use of droplet trajectory codes. They are considered qualitative and meant only to serve the purpose of illustrating how the combination of engine size and flight effects on engine cycle can influence the concentration of water droplets within the engine relative to the engine test or flight environment. For this example, calculation done over a range of inlet diameters, it is assumed that the splitter diameter is a fixed ratio ($2/3$) of the inlet diameter. The assumed engine power setting is 30% N1, which would be typical of a minimum idle descent power in flight. The results shown in figure 56 give insight into the experience that various engine manufacturers may have, depending upon the test facility and the size of the engine.

The figure indicates that testing at sea level, particularly with larger engines, results in relatively little additional concentration of water above that in a simulated icing cloud. Conversely, if a manufacturer were to test an engine in an icing wind tunnel with a smaller engine, an overall scoop factor in the range of 3-4 would be evident, as it would be in the actual flight environment. From this result, it is clear that testing under certain conditions may require the addition of water to the simulated cloud ahead of the engine to achieve the correct water content in the engine.

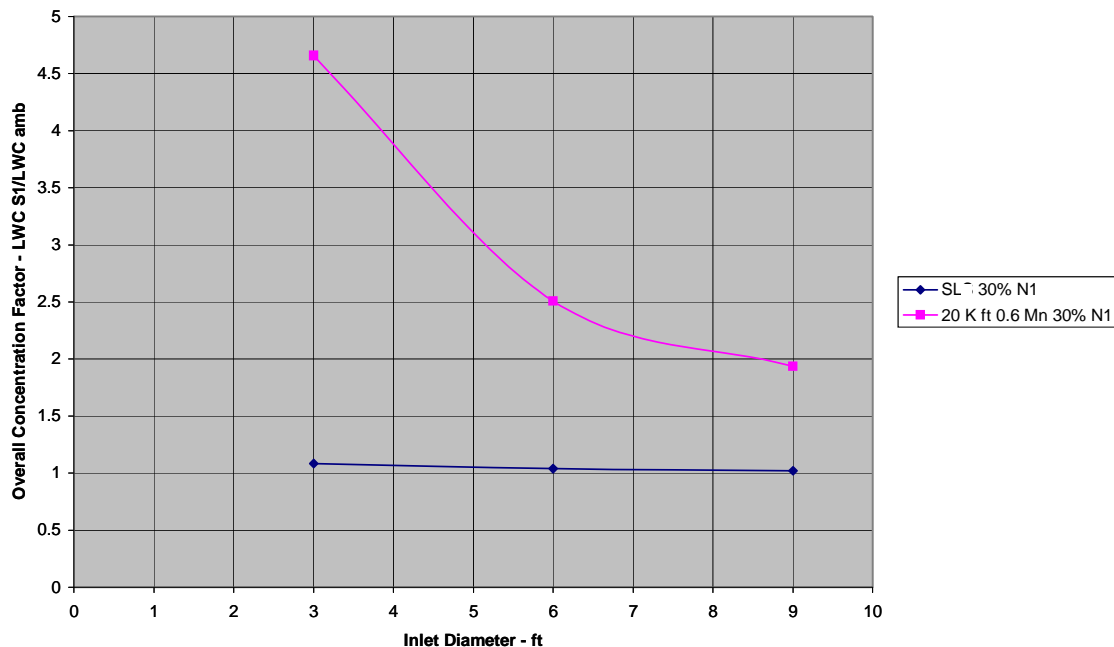


Figure 56. Illustration of Overall Scoop Factor for Two Icing Environments

8.2 SUMMARY.

The scoop factor effect on the engine’s water concentration associated with the mismatch between simulated cloud velocity and inlet air velocity needs to be factored into the requirements for ambient cloud water content. Analytical tools are available within the industry for the evaluation of droplet trajectory paths to quantify the scoop factor effect for the desired range of droplet diameters and test conditions. Use of these tools, including the accounting for altitude and air speed effects on the engine cycle, should be required to validate the testing. Failure to do so could result in the incorrect level of LWC within the engine that is required for simulating the flight icing environment.

Finally, using time as a variable for adjusting test conditions can be extremely useful for demonstrating an engine’s ice accretion tolerance if the test conditions cannot meet the corrected values required by the trajectory analysis.

9. REFERENCES.

1. TSIICE: Engine Icing Code User’s Manual, Trebor Systems, Inc., June 29, 2000.
2. Marshall, J.S. and Palmer, W.McK., “The Distribution of Raindrops With Size,” *Journal of the Atmospheric Sciences*, Vol. 5, 1948, pp. 165-166.
3. Transport Canada Deicing Report, “Winter Weather Impact on Holdover Time Table Format (1995-2004),” Report TP14375E, Nicoara Moc, APS Aviation, Inc., October 2004.

4. Stallabrass, J.R., "Snow Concentration Measurements and Correlation With Visibility," *AGARD Conference Proceedings No. 236 Icing Testing for Aircraft Engines*, April 1978.
5. Rasmussen, R.M., Vivekanandan, J., Cole, J., Myers, B., and Masters, C., "The Estimation of Snowfall Rate Using Visibility," *Journal of Applied Meteorology*, Vol. 38, 1999, pp. 1542-1563.
6. Mason, J., Strapp, W., and Chow, P., "The Ice Particle Threat to Engines in Flight," AIAA-2006-0206, January, 2006.
7. Riley, J.T., "Mixed-Phase Icing Conditions—A Review," FAA report DOT/FAA/AR-98/76, December 1998.
8. "Flight Into Ice Crystals," Aeroplanes and Rotorcraft Joint Airworthiness Committee, Paper 733, Leaflet 714Y, August 1958.
9. McNaughtan, Ian I., "The Analysis of Measurements of Free Ice and Ice/Water Concentrations in the Atmosphere of the Equatorial Zone," Royal Aircraft Establishment (Farnborough) Technical Note No: Mech. Eng. 283, 1959.
10. Bowden, D.T, Gensemer, A.E., and Speen, C.A., "Engineering Summary of Airframe Icing Technical Data," FAA technical report ADS-4, 1964.
11. Trunov, O.K., "Icing of Aircraft and the Means of Preventing IT," FTD-MT-490, August 1967.
12. Jeck, R.K., "Snow and Ice Particle Sizes and Mass Concentrations at Altitudes up to 9 Km (30,000 Ft)," FAA report DOT/FAA/AR-97/66, August 1998.
13. Lawson, R.P., Angus, L.J., and Heymsfield, A.J., "Cloud Particle Measurements in Thunderstorm Anvils and Possible Threat to Aviation," *J. Aircraft*, Vol. 35, No. 1, 1998, pp. 113-121.
14. Strapp, J.W., Chow, P., Maltby, M., Bezer, A.D., Korolev, A., Stomberg, I., and Hallett, J., "Cloud Microphysical Measurements in Thunderstorm Outflow Regions During Allied/BAe 1997 Flight Trials," *37th AIAA Aerospace Sciences Meeting and Exhibit*, Reno, Nevada, January 11-14, 1999, AIAA 99-0498.
15. McNaughtan, Ian I., "Development and Calibration of the Pitot Type Ice Concentration Meter," Royal Aircraft Establishment (Farnborough) Technical Note No: *Mechanical Engineering*, Vol. 281, February 1959.
16. Abraham, J., Strapp, J.W., Fogarty, C., and Wolde, M., "Extratropical Transition of Hurricane Michael," *Bull. Amer. Met. Soc.*, Vol. 85, 2004, pp. 1323-1339.

17. Stith, J.L., Dye, J.E., Bansemer, A., Heymsfield, A., Grainger, C., Petersen, W.W., and Berticelli, R., "Microphysical Observations of Tropical Clouds," *J. Appl. Meteor*, Vol. 41, 2002, pp. 97-117.
18. Strapp, J.W., Lilie, L.E., Emery, E.E., and Miller, D.R., "Preliminary Comparison of Ice Water Content as Measured by Hot Wire Instruments of Varying Configuration," *43rd Aerospace Sciences Meeting and Exhibit*, Reno, Nevada, 11-13 January 2005, AIAA 2005-0860.
19. Hoerner, Sighard F., *Fluid-Dynamic Drag Informaton on Aerodynamic Drag and Hydrodynamic Resistance*, published by author, 1965.
20. Gelder, T.F., "Droplet Impingement and Ingestion by Supersonic Nose Inlet in Subsonic Tunnel Conditions," NACA TN 4268, May 1, 1958.
21. Pfeifer, G.D. and Maier, G.P., "Engineering Summary of Powerplant Icing Technical Data," FAA report FAA-RD-77-76, July 1977.
22. Venkataramani, K.S. and McVey, L.J., "Scoop Effects in Inclement Weather Operation," AIAA-2006-207, 2006.

APPENDIX A—PROPOSED NEW RULES

14 CFR 33.68

Part 33 AIRWORTHINESS STANDARDS: AIRCRAFT ENGINES

Subpart E—Design and Construction; Turbine Aircraft Engines

Sec. 33.68

Induction System Icing.

Each engine, with all icing protection systems operating, must:

- A. Operate throughout its flight power range, including the minimum descent idling speeds, in icing conditions as defined in Appendix C, Appendix X of Part 25 of this chapter, and Appendix D of Part 33 of this chapter without the accumulation of ice on the engine components that:
 - 1) Adversely affects engine operation or that causes an unacceptable permanent loss of power or thrust or unacceptable increase in engine operating temperature; or
 - 2) Results in unacceptable temporary power loss or engine damage; or
 - 3) Causes a stall, surge, or flameout or loss of engine controllability (for example, rollback). The applicant must account for in-flight ram effects (for example; scoop factor amplification, water temperature, air density) in any critical point analysis or test demonstration of these flight conditions.
- B. Operate throughout its flight power range (including minimum descent idling speeds in icing) in continuous maximum and intermittent maximum icing conditions as defined in Appendix C, and Appendix X of Part 25 of this chapter. In addition,:
 - 1) It must be shown through Critical Point Analysis (CPA) that the complete ice envelope has been analyzed, and that the most critical points must be demonstrated by engine test, analysis or a combination of the two to operate acceptably. Extended flight in critical flight conditions such as hold, descent, approach, climb, and cruise, must be addressed, for these ice conditions.
 - 2) It must be demonstrated by engine test, analysis or a combination of the two that the engine can run for a duration that achieves the following compliance requirements:
 - (a) At engine powers that can sustain level flight:

A duration that achieves repetitive, stabilized operation in part 25, Appendix C and in large droplet icing conditions of part 25, Appendix X.

(b) At engine power below that which can sustain level flight:

i. Demonstration in altitude flight simulation test facility:

A duration of 10 minutes consistent with a simulated flight descent of 10000 ft (3 km) operation in Continuous Maximum icing conditions, plus 40 percent liquid water content margin, at the critical level of airspeed and air temperature, or

ii. Demonstration in ground test facility:

A duration of 3 cycles of alternating icing exposure corresponding to the LWC levels and standard cloud lengths in Intermittent Maximum and Continuous Maximum icing conditions, at the critical level of air temperature.

C. In addition to complying with paragraph B. of this section, the following conditions shown in Table 33.68-1, unless replaced by similar CPA test conditions that are more critical or produce an equivalent level of safety, must be demonstrated by engine test:

Table 33.68 - 1

Condition	Total Air Temperature	LWC (minimum)	Median Volume Droplet Diameter (+/-3 microns)	Duration
1. Glaze ice conditions	21 to 25°F (-6 to -4°C)	2 gm/m ³	25 microns	(a) 10-minutes for power below sustainable level flight (idle descent). Must show repetitive, stabilized operation for higher powers (50%, 75%, 100%MC).
2. Rime ice conditions	-10 to 0°F (-23 to -18°C)	1 gm/m ³	15 microns	(a) 10-minutes for power below sustainable level flight (idle descent). (b) Must show repetitive, stabilized operation for higher powers (50%, 75%, 100%MC).
3. Glaze ice holding conditions (Turboprop and turbofan, only)	Turbofan, only: 10 to 18°F (-12 to -8°C) ----- Turboprop, only: 2 to 10°F (-17 to -12°C)	Alternating cycle: 0.3 gm/m ³ (6 minute) 1.7 gm/m ³ (1 minute)	20 microns	Must show repetitive, stabilized operation (or 45 minutes max)

Table 33.68 - 1 (Continued)

Condition	Total Air Temperature	LWC (minimum)	Median Volume Droplet Diameter (+/-3 microns)	Duration
4. Rime ice holding conditions (Turboprop and turbofan, only)	Turbofan, only: -10 to 0°F (-23 to -18°C) ----- Turboprop, only: 2 to 10°F (-17 to -12°C)	0.25 gm/m ³	20 microns	Must show repetitive, stabilized operation (or 45 minutes max).

D. Idle for a minimum of 30-minutes on the ground in the following icing conditions shown in Table 33.68-2, with the available air bleed for icing protection at its critical condition, without adverse effect, followed by an acceleration to takeoff power or thrust. During the idle operation the engine may be run up periodically to a moderate power or thrust setting in a manner acceptable to the Administrator. The applicant must document any demonstrated run ups and minimum ambient temperature capability during the conduct of icing testing in the engine operating manual as mandatory in icing conditions. The applicant must demonstrate, with consideration of expected airport elevations, the following:

Table 33.68 - 2

Condition	Total Air Temperature	LWC (minimum)	Mean Effective Particle Diameter	Demonstration
1. Rime ice condition	0 to 15 °F (-18 to -9 °C)	Liquid - 0.3 gm/m ³	15-25 microns	By engine test
2. Glaze ice condition	20 to 30 °F (-7 to -1 °C)	Liquid - 0.3 gm/m ³	15-25 microns	By engine test
3. Snow ice condition	26 to 32 °F (-3 to 0 °C)	Ice - 0.9 gm/m ³	100 microns (minimum)	By test, analysis or combination of the two.
4. Large Droplet glaze ice condition	15 to 30 °F (-9 to -1 °C)	Liquid - 0.3 gm/m ³	100 microns (minimum) 3000 microns (maximum)	By test, analysis or combination of the two.

The applicant must demonstrate by test, analysis or combination of the two acceptable operation in ice crystals and mixed-phase icing conditions throughout the Part 33, Appendix D icing envelope throughout its flight power range, including minimum descent idling speeds.

14 CFR 33 Appendix D

14 CFR Part 33 Appendix D – Mixed Phase and Ice Crystal Icing Envelope (Deep Convective Clouds)

Ice crystal conditions associated with convective storm cloud formations exist within the 14 CFR Part 25 Appendix C Intermittent Maximum Icing envelope (including the extension to -40 deg C) and the Mil Standard 210 Hot Day envelope. This ice crystal icing envelope is depicted in the Figure D-1.

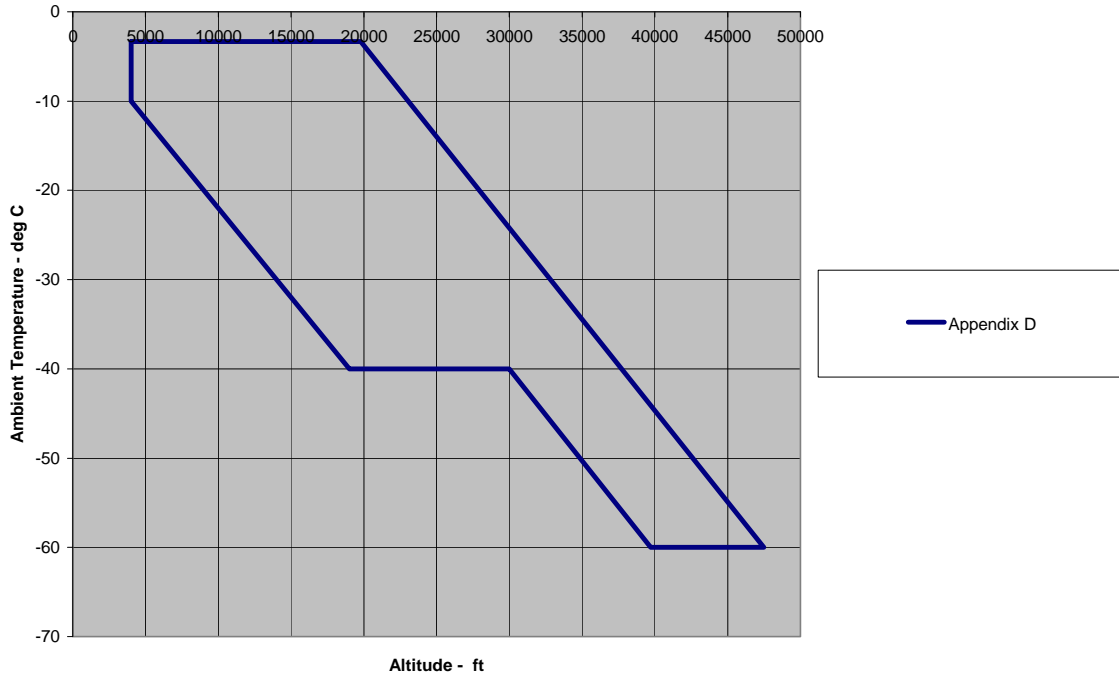


Figure D-1 Convective Cloud Ice Crystal Envelope

Within the envelope, total water content (TWC) in gms/m³ have been assessed based upon the adiabatic lapse defined by the convective rise of 90% relative humidity air from sea level to higher altitudes and scaled by a factor of 0.65 to a standard cloud length of 17.4 nautical miles. TWC is displayed for this distance over a range of ambient temperature within the boundaries of the ice crystal envelope in figure D-2.

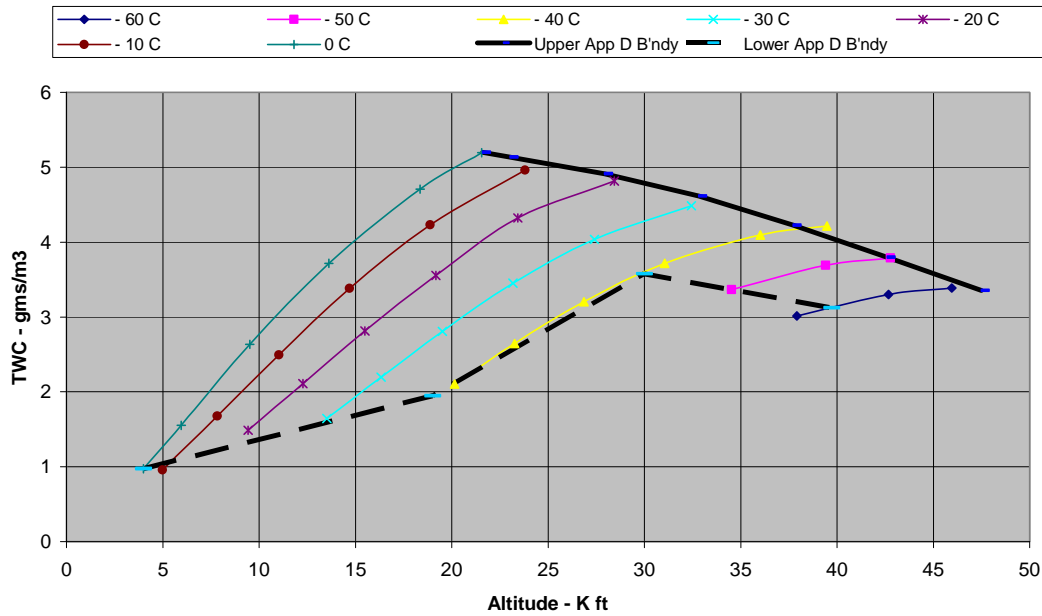


Figure D-2 Total Water Content

Ice crystal size median mass dimension (MMD) range is 50 - 200 microns (equivalent spherical size) based upon measurements near convective storm cores.

The TWC can be treated as completely glaciated except as noted in the Table D-1.

Temperature Range – deg C	Horizontal Cloud Length	LWC – gm/m3
0 to -20	</= 50 miles	</=1.0
0 to -20	Indefinite	</=0.5
< -20		0

Table D-1 Supercooled Liquid Portion of TWC

The TWC levels displayed in figure D-2 represent TWC values for a standard exposure distance (horizontal cloud length) of 17.4 nautical miles that must be adjusted with length of icing exposure. The assessment from data measurements in References 1 supports the reduction factor with exposure length shown in figure D-3.

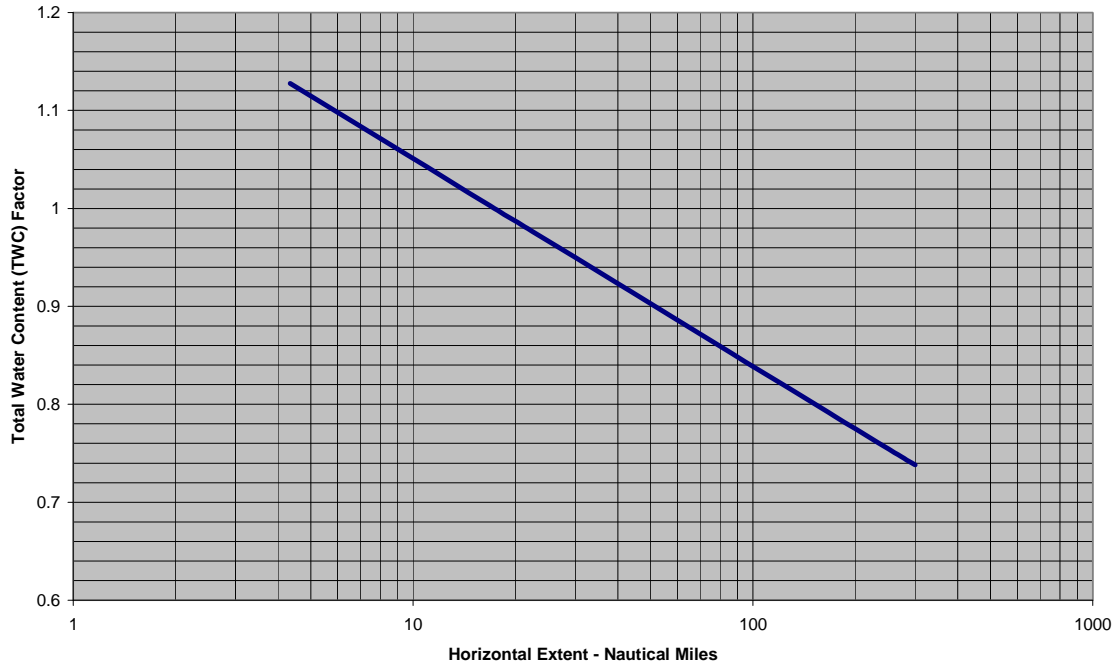


Figure D-3 Exposure Length Influence on TWC

REFERENCES

1. The Analysis of Measurements of Free Ice and Ice/Water Concentrations in the Atmosphere of the Equatorial Zone, Ian I. McNaughtan, B.Sc., Dip. R.T.C., Royal Aircraft Establishment (Farnborough) Technical Note No: Mech. Eng. 283, 1959.
2. Snow and Ice Particle Sizes and Mass Concentrations at Altitudes up to 9 km (30,000 ft), R. K. Jeck, DOT/FAA/AR-97/66, August, 1998.
3. Cloud Microphysical Measurements in Thunderstorm Outflow Regions During Allied/Bae 1997 Flight Trials, Strapp, J.W., P. Chow, M. Maltby, A.D. Bezer, A. Korolev, I. Stomberg, and J. Hallett, 37th AIAA Aerospace Sciences Meeting and Exhibit, Jan. 11-14, 1999, Reno, NV. AIAA 99-0498.

14 CFR 33.77

Part 33 AIRWORTHINESS STANDARDS: AIRCRAFT ENGINES

Subpart E – Design and Construction; Turbine Aircraft Engines

Sec. 33.77 [Foreign object ingestion--ice.]

(a) Compliance with the requirements of this paragraph shall be demonstrated by engine ice ingestion test or by validated analysis showing equivalence of other means for demonstrating soft body damage tolerance.

(b) [Reserved]

(c) Ingestion of ice under the conditions of this section may not --

- (1) Cause an immediate or ultimate unacceptable sustained power or thrust loss; or
 - (2) Require the engine to be shutdown
- (d) For an engine that incorporates a protection device, compliance with this section need not be demonstrated with respect to ice formed forward of the protection device if it is shown that--
- (1) Such ice is of a size that will not pass through the protective device;
 - (2) The protective device will withstand the impact of the ice and
 - (3) The ice stopped by the protective device will not obstruct the flow of induction air into the engine with a resultant sustained reduction in power or thrust greater than those values required by paragraph (c) of this section.
- (e) Compliance with paragraph (c) of this section may be shown by engine test under the following ingestion conditions:
- (1) The minimum ice quantity will be established by the engine size as defined in Table 1 – dimensions should be linearly interpolated based on actual hilite area
 - (2) The ingestion velocity will simulate ice being sucked into the engine from the inlet
 - (3) Engine operation will be at the maximum cruise power or thrust unless lower power is more critical

Table 1 – Minimum Ice Slab Requirements Based on Engine Inlet Size

Inlet Hilite Area (sq inch)	Thickness (inch)	Width (inch)	Length (inch)
0	0.25	0	3.6
80	0.25	6	3.6
300	0.25	12	3.6
700	0.25	12	4.8
2800	0.35	12	8.5
5000	0.43	12	11.0
7000	0.50	12	12.7
7900	0.50	12	13.4
9500	0.50	12	14.6

Table 1 – Minimum Ice Slab Requirements Based on Engine Inlet Size (Continued)

Inlet Hilite Area (sq inch)	Thickness (inch)	Width (inch)	Length (inch)
11300	0.50	12	15.9
13300	0.50	12	17.1
16500	0.5	12	18.9
20000	0.5	12	20.0

14 CFR 25.1093

Part 25

Subpart

(previous paragraphs unchanged)

Sec. 25.1093(b) Turbine engines

Induction System Icing.

Each engine, with all icing protection systems operating, must:

1. Operate throughout its flight power range, in continuous maximum and intermittent maximum icing conditions as defined in Appendix C, Appendix X of Part 25 of this chapter, and Appendix D of Part 33 of this chapter including the minimum descent idling speeds in icing, without the accumulation of ice on the engine, inlet system components or airframe components that:
 - 4) Adversely affects installed engine operation or that causes a permanent loss of power or thrust; or unacceptable increase in operating temperature; or cause an airframe/engine incompatibility.
 - 5) Results in unacceptable temporary power loss or engine damage; or
 - 6) Causes a stall, surge, or flameout or loss of engine controllability (for example, rollback).
- 2) Idle for a minimum of 30-minutes on the ground in the following icing conditions shown in Table 25.1093-1, with the available air bleed for icing protection at its critical condition, without adverse effect, followed by an acceleration to takeoff power or thrust. During the idle operation the engine may be run up periodically to a moderate power or thrust setting in a manner acceptable to the Administrator. The applicant must document any demonstrated run ups and minimum ambient temperature capability during the conduct of icing testing in the limitations section of the Aircraft Flight Manual (AFM).

Table 25.1093-1

Condition	Total Air Temperature	Water Concentration (minimum)	Mean Effective Particle Diameter	Demonstration
1. Rime ice condition	0 to 15 °F (-18 to -9 °C)	Liquid - 0.3 gm/m ³	15-25 microns	By test, analysis or combination of the two.
2. Glaze ice condition	20 to 30 °F (-7 to -1 °C)	Liquid - 0.3 gm/m ³	15-25 microns	By test, analysis or combination of the two.
3. Snow ice condition	26 to 32 °F (-3 to 0 °C)	Ice - 0.9 gm/m ³	100 microns (minimum)	By test, analysis or combination of the two.
4. Large droplet glaze ice condition	15 to 30 °F (-9 to -1 °C)	Liquid - 0.3 gm/m ³	100 microns (minimum) 3000 microns (maximum)	By test, analysis or combination of the two.

14 CFR 25.903

REVISED REGULATION: Part 25, section 25.903

(a) * * *

(3) Each turbine engine must comply with one of the following:

- (i) Section 33.68 of this chapter in effect on [insert effective date of final rule], or as subsequently amended; or
- (ii) Comply with § 33.68 of this chapter in effect on February 23, 1984, or as subsequently amended before [insert effective date of final rule], unless that engine's ice accumulation service history has resulted in an unsafe condition; or
- (iii) Comply with § 33.68 of this chapter in effect on October 1, 1974, or as subsequently amended prior to February 23, 1984, unless that engine's ice accumulation service history has resulted in an unsafe condition; or
- (iv) Be shown to have an ice accumulation service history in similar installation locations which has not resulted in any unsafe conditions.